

2010

Fabrication of polymeric hollow fiber membrane for the production of safe drinking water

Latifa Obeid Hamad Al-Nuaimi

Follow this and additional works at: https://scholarworks.uaeu.ac.ae/all_theses

Part of the [Engineering Commons](#)

Recommended Citation

Hamad Al-Nuaimi, Latifa Obeid, "Fabrication of polymeric hollow fiber membrane for the production of safe drinking water" (2010). *Theses*. 309.

https://scholarworks.uaeu.ac.ae/all_theses/309

This Thesis is brought to you for free and open access by the Electronic Theses and Dissertations at Scholarworks@UAEU. It has been accepted for inclusion in Theses by an authorized administrator of Scholarworks@UAEU. For more information, please contact fadl.musa@uaeu.ac.ae.



United Arab Emirates University

Faculty of Engineering

M.Sc. Program in Petroleum Science & Engineering

**FABRICATION OF POLYMERIC HOLLOW FIBER
MEMBRANE FOR THE PRODUCTION OF SAFE
DRINKING WATER**

By

Latifa Obeid Hamad Al- Nuaimi

Submitted to

United Arab Emirates University

In Partial Fulfillment of the Requirements for the Degree of M.Sc
in Petroleum Science & Engineering

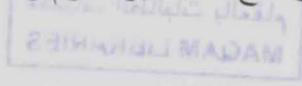
2010/2011



جامعة الإمارات العربية المتحدة

كلية الهندسة

برنامج ماجستير علوم وهندسة البترول



تصنيع الألياف البوليمرية للحصول على المياه الصالحة للشرب

رسالة مقدمة من الطالبة

لطيفه عبيد حمد النعيمي

إلى

جامعة الإمارات العربية المتحدة

استكمالاً لمتطلبات الحصول على درجة الماجستير في علوم وهندسة البترول

2010/2011

United Arab Emirates University

Faculty of Engineering

M.Sc. Program in Petroleum Science & Engineering

Thesis Title

Fabrication of polymeric hollow fiber membrane for the production of safe drinking water

Author Name

Latifa Obeid Hamad Al- Nuaimi

Supervisors

No.	Name	Position
1	Dr. Nayef Ghasem	Associate Professor of Chemical Engineering
2	Dr. Mohamed Al-Marzouqi	Chairman, Chemical and Petroleum Eng. Dept.

2010/2011

Thesis of Latifa Obeid Hamad Al-Nuaimi

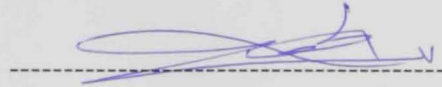
Title: Fabrication of polymeric hollow fiber membrane for production of safe drinking water

Submitted in Partial Fulfillment for the Degree of
Master of Petroleum Science and Engineering (Chemical Engineering)

Chair of Examination Committee
Dr. Nayef Ghasem
Chemical & Petroleum Engineering Department
United Arab Emirates University



Internal Examiner
Dr. Yaser E. Greish
College of Science
United Arab Emirates University



Program Director
Prof. Abdulrazag Y. Zekri
Master of Petroleum Sci. & Eng.



Ali Hassan

Dr. Ali Al-Marzouqi

Associate Dean for Research and Graduate Studies
United Arab Emirates University

20010/2011

Acknowledgements

At the beginning and before everything I would thank my god, because my success is due to Allah. I express my deepest gratitude to all whose help in various ways enabled me to complete my thesis research.

I would like to thank Dr. Nayef and Dr. Mohamed Al-Marzouqi for all their support through all the times. Their enthusiasm and drive kept me motivated to keep striving forward towards completion of the degree.

I would like to thank my committee members Dr. Yasser E. Greish and Dr. Li-Ping Zhu for their time.

I would like to express my deep gratitude and appreciation to Dr Ali Dawaidar and Eng Hasan Kamel for their help during my thesis research work.

Thanks to my mother for her help and moral support, from my first day in the primary school. I am grateful to my father for his financial support, during the many years of my continued education. I prayed to god to grant them forgiveness and paradise. I am especially indebted to my brothers and my sisters for their love, support and encouragement through all the years.

Finally, thanks to my friends for everything.

Abstract

Production of safe drinking water by using micro-filtration and ultra filtration technology become more interesting. Water purification or filtration by using membrane began attracting much attention worldwide, because of its good characteristics such as: high efficiency in removing solid particles, viruses and germs and their low cost. This new technology is useful in industrial water treatment. The current studies in this field of polymer membrane manufacturing try to improve the characteristics, water flow rate and remove unwanted particles from water.

The recent project's aimed is to manufacture cellulose acetate hollow fibers. They were prepared by the Non Solvent Induced Phase Separation (NIPS) method at different spinning conditions and discussed the effect of rheology of cellulose acetate at different concentrations and temperatures. Thesis research has been assessed to study several variables during manufacture of hollow membranes, to attempt, clarify and clearly the variables and factors will be effect on the efficiency of hollow fiber membranes. Thesis project was divided into several sections as follows:

- Study the rheology of cellulose acetate at different concentrations and temperatures. Hershed-Balkley (H-B) model were used to test polymer solution behaviors.
- Determine how much the cellulose acetate concentration in solvent and polymer solution flow rate during spinning will be effect on the characterizations of hollow fiber membrane.

- Examine the effect of changing bore fluid flow rate on the properties of hollow fiber. Water was as inner coagulation at different flow rates; 8, 10, 12, 13, and 16 g/min.
- Change the distance between the spinneret and external coagulation (water) at different distances (5.5, 7, 9 and 10 cm) in order to study the structure and performance on hollow fiber.
- Check if the internal coagulation type and composition will be effect on the characterizations of hollow fiber and solids rejection or not. Study the effect of ethanol at different concentration in internal coagulation (Ethanol/Water), while ethanol concentrations in water are 18, 25, 35 and 50%.

Table of Contents

Acknowledgements	V
Abstract.....	VI
Table of Contents	VIII
List of Tables	XI
List of Figures.....	XIII
Chapter One: Introduction	2
1.1. Water Pollution	2
1.1.1. Water Chemical Pollution.....	3
1.1.2. Water Microbiological Pollution	4
1.1.3. Radiological Water Pollution.....	5
1.2. Water Purification	6
1.2.1. Water Purification Techniques	6
1.3. Water Filtration	8
1.3.1 Membrane Process	9
1.3.2. Microfiltration.....	12
1.3.3. Ultra filtration	13
1.3.4. Nanofiltration	14
1.3.5. Reverse Osmosis.....	14
1.4. Methods of Making Hollow Fibers and Its Application	15
1.4.1. Thermally Induced Phase Separation (TIPS).....	16
1.4.2. Dry Jet Wet Spinning Process.....	17
1.4.3. Non Solvent Induced Phase Separation (NIPS).....	18
1.4.4. Wet Phase Inversion Process	19
1.5. Cellulose Acetate Hollow Fibers (Background and Literature Review).....	19
1.5.1. Characterization of Cellulose Acetate (CA)	19
1.5.2. Background and Literature Review	22
Chapter Two: Thesis Background	29
2.1. Objectives.....	29
2.2. Thesis Review	30
Chapter Three: Materials and Methods.....	33
3.1. Materials.....	33

3.1.1.	Cellulose Acetate Solution.....	33
3.1.2.	Bovine Serum Albumin	33
3.2.	Methods.....	34
3.2.1.	Hollow Fibers Preparation	34
3.3.	Characterization	35
3.3.1.	Membrane Morphology	35
3.3.2.	Permeability Measurements.....	36
3.3.3.	Solid Rejection.....	37
3.3.4.	Water Contact Angle.....	37
3.3.5.	Mechanical Properties.....	37
3.3.6.	Rheological Measurements.....	38
3.3.7.	Measuring Fibers Bore Diameter.....	38
3.4.	Operating Parameters	38
3.4.1.	Effects of CA Concentration and Dope Solution Flow Rate	38
3.4.2.	Effect of Bore Fluid Flow Rate.....	40
3.4.3.	Effect of Air Gap	41
3.4.4.	Effect of Bore Fluid Concentration.....	42
Chapter four: Effect of Temperature, Composition and Shear Rate on Cellulose Acetate / Dimethyl-acetamide Solution Viscosity		44
4.1.	Introduction	44
4.2.	Results and Discussions	45
4.3.	Conclusions	60
Chapter Five: Effect of Cellulose Acetate Concentration and Dope Solution Flow Rate.....		61
5.1.	Introduction	61
5.2.	SEM Micrographs	62
5.3.	Water Permeability and Rejection.....	75
5.4.	Contact Angle and Inner Diameter Measurements	79
5.5.	Strength of Fabricated Fibers	82
5.6.	Conclusions	84
Chapter Six: Effect of Bore Fluid Flow Rate		85
6.1.	SEM Micrographs	85
6.2.	Water Permeability and Rejection.....	91
6.3.	Contact Angle and Diameter Measurements.....	93
6.4.	Strength of Fabricated Fibers	94
6.5.	Conclusions	95

Chapter Seven: Effect of Air Gap	96
7.1. Introduction	96
7.2. SEM Micrographs	97
7.3. Water Permeability and Rejection.....	102
7.4. Contact Angle and Diameter Measurements.....	104
7.5. Strength of Fabricated Fibers	105
7.6. Conclusions	106
Chapter Eight: Effect of Bore Fluid Concentration.....	107
8.1. Introduction	107
8.2. SEM Micrographs	107
8.3. Water Permeability and Rejection.....	113
8.4. Contact Angle and Diameter Measurements.....	114
8.5. Strength of Fabricated Fibers	115
8.6. Conclusions	116
Chapter Nine: Conclusions and Recommendations	118
9.1. Conclusions	118
9.2. Recommendations	119
References	121
ملخص الأطروحة	137

List of Tables

Chapter 1

Table 1.1: Classification of Membrane Processes	10
Table 1.2: Experimental parameters used in LCST membrane fabrication.....	23
Table 1.3: Experimental parameters used in UF (CA/PVP 360 K/NMP/water) membrane fabrication.....	24
Table 1.4: Experimental parameters used in study of effect of take up speed membrane fabrication.....	25
Table 1.5: Experimental parameters used in nano-filtration hollow fiber membranes for forward osmosis processes.....	26

Chapter 3

Table 3.1: Spinning parameters for CA/DMAc hollow fibers with different CA concentration and dope Solution flow rate.....	39
Table 3.2: Spinning parameters for CA/DMAc hollow fibers with different pore flow.	40
Table 3.3: Spinning parameters for CA/DMAc hollow fibers by changing air gap length.	41
Table 3.4: Spinning parameters for CA/DMAc hollow fibers with different pore concentration.....	42

Chapter 4

Table 4.1: Parameters of Herschel Bulkley model for cellulose acetate prepared at different temperatures.....	56
---	----

Chapter 5

Table 5.1: Rejection ratio of BSA at different CA concentrations.....	76
Table 5.2: Contact angle and inner diameter measurements of 15% CA with different dope flow rates.....	79

Table 5.3: Contact angle and inner diameter measurements of 18% CA with different dope flow rates.....	80
Table 5.4: Contact angle and inner diameter measurements of 21% CA with different dope flow rates.....	80
Table 5.5: Contact angle and inner diameter measurements of 24% CA with different dope flow rates.....	81

Chapter 6

Table 6.1: Rejection ratio of BSA at different bore flow rates.....	92
Table 6.2: Contact Angle and diameter measurements cellulose acetate at different bore flow rates.....	93

Chapter 7

Table 7.1: Rejection ratio of BSA at different air gap lengths.....	103
Table 7.2: Contact Angle and diameter measurements cellulose acetate at different air gap distance.....	104

Chapter 8

Table 8.1: Rejection % of BSA at different concentrations of bore fluid.....	113
Table 8.2: Contact Angle and inner diameter measurements for different concentrations of bore fluid.....	114

List of Figures

Chapter 1

Figure 1.1: Cellulose Acetate Preparation Steps	20
---	----

Chapter 3

Figure 3.1: Schematic diagram of the spinning system.	35
Figure 3.2: Schematic diagram of ultra-filtration.	36

Chapter 4

Figure 4.1: Viscosity as a function of shear rate at different CA mass fractions at $T = 25^{\circ}\text{C}$.47	
Figure 4.2: Viscosity as a function of shear rate at different CA mass fractions at $T = 35^{\circ}\text{C}$.48	
Figure 4.3: Viscosity as a function of shear rate at different CA mass fractions at $T = 45^{\circ}\text{C}$.48	
Figure 4.4: Viscosity as a function of shear rate at different CA mass fractions at $T = 55^{\circ}\text{C}$.49	
Figure 4.5: Viscosity as a function of shear rate at different CA concentrations at $T = 65^{\circ}\text{C}$.49	
Figure 4.6: Viscosity as a function of shear rate at different CA concentrations at $T = 75^{\circ}\text{C}$.50	
Figure 4.7: Viscosity as a function of shear rate at different CA concentrations at $T = 85^{\circ}\text{C}$.50	
Figure 4.8: Flow curves of CA solution fitted to the Herschel Bulkley model at $T = 25^{\circ}\text{C}$... 52	
Figure 4.9: Flow curves of CA solution fitted to the Herschel Bulkley model at $T = 35^{\circ}\text{C}$... 52	
Figure 4.10: Flow curves of CA solution fitted to the Herschel Bulkley model at $T = 45^{\circ}\text{C}$. 53	
Figure 4.11: Flow curves of CA solution fitted to the Herschel Bulkley model at $T = 55^{\circ}\text{C}$. 54	
Figure 4.12: Flow curves of CA solution fitted to the Herschel Bulkley model at $T = 65^{\circ}\text{C}$. 54	
Figure 4.13: Flow curves of CA solution fitted to the Herschel Bulkley model at $T = 75^{\circ}\text{C}$. 55	
Figure 4.14: Flow curves of CA solution fitted to the Herschel Bulkley model at $T = 85^{\circ}\text{C}$.55	
Figure 4.15: Flow curves of cellulose acetate at different temperatures with 0.15 CA..... 57	
Figure 4.16: Flow curves of cellulose acetate at different temperatures with 0.18 CA..... 58	
Figure 4.17: Flow curves of cellulose acetate at different temperatures with 0.21 CA..... 58	
Figure 4.18: Flow curves of cellulose acetate at different temperatures with 0.24 CA..... 59	

List of Figures

Chapter 1

Figure 1.1: Cellulose Acetate Preparation Steps 20

Chapter 3

Figure 3.1: Schematic diagram of the spinning system. 35

Figure 3.2: Schematic diagram of ultra-filtration. 36

Chapter 4

Figure 4.1: Viscosity as a function of shear rate at different CA mass fractions at $T = 25^{\circ}\text{C}$.47

Figure 4.2: Viscosity as a function of shear rate at different CA mass fractions at $T = 35^{\circ}\text{C}$.48

Figure 4.3: Viscosity as a function of shear rate at different CA mass fractions at $T = 45^{\circ}\text{C}$.48

Figure 4.4: Viscosity as a function of shear rate at different CA mass fractions at $T = 55^{\circ}\text{C}$.49

Figure 4.5: Viscosity as a function of shear rate at different CA concentrations at $T = 65^{\circ}\text{C}$.49

Figure 4.6: Viscosity as a function of shear rate at different CA concentrations at $T = 75^{\circ}\text{C}$.50

Figure 4.7: Viscosity as a function of shear rate at different CA concentrations at $T = 85^{\circ}\text{C}$.50

Figure 4.8: Flow curves of CA solution fitted to the Herschel Bulkley model at $T = 25^{\circ}\text{C}$... 52

Figure 4.9: Flow curves of CA solution fitted to the Herschel Bulkley model at $T = 35^{\circ}\text{C}$... 52

Figure 4.10: Flow curves of CA solution fitted to the Herschel Bulkley model at $T = 45^{\circ}\text{C}$. 53

Figure 4.11: Flow curves of CA solution fitted to the Herschel Bulkley model at $T = 55^{\circ}\text{C}$. 54

Figure 4.12: Flow curves of CA solution fitted to the Herschel Bulkley model at $T = 65^{\circ}\text{C}$. 54

Figure 4.13: Flow curves of CA solution fitted to the Herschel Bulkley model at $T = 75^{\circ}\text{C}$. 55

Figure 4.14: Flow curves of CA solution fitted to the Herschel Bulkley model at $T = 85^{\circ}\text{C}$.55

Figure 4.15: Flow curves of cellulose acetate at different temperatures with 0.15 CA..... 57

Figure 4.16: Flow curves of cellulose acetate at different temperatures with 0.18 CA..... 58

Figure 4.17: Flow curves of cellulose acetate at different temperatures with 0.21 CA..... 58

Figure 4.18: Flow curves of cellulose acetate at different temperatures with 0.24 CA..... 59

List of Figures

Chapter 1

Figure 1.1: Cellulose Acetate Preparation Steps	20
---	----

Chapter 3

Figure 3.1: Schematic diagram of the spinning system.	35
Figure 3.2: Schematic diagram of ultra-filtration.	36

Chapter 4

Figure 4.1: Viscosity as a function of shear rate at different CA mass fractions at $T = 25^{\circ}\text{C}$.47	
Figure 4.2: Viscosity as a function of shear rate at different CA mass fractions at $T = 35^{\circ}\text{C}$.48	
Figure 4.3: Viscosity as a function of shear rate at different CA mass fractions at $T = 45^{\circ}\text{C}$.48	
Figure 4.4: Viscosity as a function of shear rate at different CA mass fractions at $T = 55^{\circ}\text{C}$.49	
Figure 4.5: Viscosity as a function of shear rate at different CA concentrations at $T = 65^{\circ}\text{C}$.49	
Figure 4.6: Viscosity as a function of shear rate at different CA concentrations at $T = 75^{\circ}\text{C}$.50	
Figure 4.7: Viscosity as a function of shear rate at different CA concentrations at $T = 85^{\circ}\text{C}$.50	
Figure 4.8: Flow curves of CA solution fitted to the Herschel Bulkley model at $T = 25^{\circ}\text{C}$... 52	
Figure 4.9: Flow curves of CA solution fitted to the Herschel Bulkley model at $T = 35^{\circ}\text{C}$... 52	
Figure 4.10: Flow curves of CA solution fitted to the Herschel Bulkley model at $T = 45^{\circ}\text{C}$. 53	
Figure 4.11: Flow curves of CA solution fitted to the Herschel Bulkley model at $T = 55^{\circ}\text{C}$. 54	
Figure 4.12: Flow curves of CA solution fitted to the Herschel Bulkley model at $T = 65^{\circ}\text{C}$. 54	
Figure 4.13: Flow curves of CA solution fitted to the Herschel Bulkley model at $T = 75^{\circ}\text{C}$. 55	
Figure 4.14: .Flow curves of CA solution fitted to the Herschel Bulkley model at $T = 85^{\circ}\text{C}$.55	
Figure 4.15: Flow curves of cellulose acetate at different temperatures with 0.15 CA..... 57	
Figure 4.16: Flow curves of cellulose acetate at different temperatures with 0.18 CA..... 58	
Figure 4.17: Flow curves of cellulose acetate at different temperatures with 0.21 CA..... 58	
Figure 4.18: Flow curves of cellulose acetate at different temperatures with 0.24 CA..... 59	

List of Figures

Chapter 1

Figure 1.1: Cellulose Acetate Preparation Steps	20
---	----

Chapter 3

Figure 3.1: Schematic diagram of the spinning system.	35
Figure 3.2: Schematic diagram of ultra-filtration.	36

Chapter 4

Figure 4.1: Viscosity as a function of shear rate at different CA mass fractions at $T = 25^{\circ}\text{C}$.47	
Figure 4.2: Viscosity as a function of shear rate at different CA mass fractions at $T = 35^{\circ}\text{C}$.48	
Figure 4.3: Viscosity as a function of shear rate at different CA mass fractions at $T = 45^{\circ}\text{C}$.48	
Figure 4.4: Viscosity as a function of shear rate at different CA mass fractions at $T = 55^{\circ}\text{C}$.49	
Figure 4.5: Viscosity as a function of shear rate at different CA concentrations at $T = 65^{\circ}\text{C}$.49	
Figure 4.6: Viscosity as a function of shear rate at different CA concentrations at $T = 75^{\circ}\text{C}$.50	
Figure 4.7: Viscosity as a function of shear rate at different CA concentrations at $T = 85^{\circ}\text{C}$.50	
Figure 4.8: Flow curves of CA solution fitted to the Herschel Bulkley model at $T = 25^{\circ}\text{C}$... 52	
Figure 4.9: Flow curves of CA solution fitted to the Herschel Bulkley model at $T = 35^{\circ}\text{C}$... 52	
Figure 4.10: Flow curves of CA solution fitted to the Herschel Bulkley model at $T = 45^{\circ}\text{C}$. 53	
Figure 4.11: Flow curves of CA solution fitted to the Herschel Bulkley model at $T = 55^{\circ}\text{C}$. 54	
Figure 4.12: Flow curves of CA solution fitted to the Herschel Bulkley model at $T = 65^{\circ}\text{C}$. 54	
Figure 4.13: Flow curves of CA solution fitted to the Herschel Bulkley model at $T = 75^{\circ}\text{C}$. 55	
Figure 4.14: .Flow curves of CA solution fitted to the Herschel Bulkley model at $T = 85^{\circ}\text{C}$.55	
Figure 4.15: Flow curves of cellulose acetate at different temperatures with 0.15 CA..... 57	
Figure 4.16: Flow curves of cellulose acetate at different temperatures with 0.18 CA..... 58	
Figure 4.17: Flow curves of cellulose acetate at different temperatures with 0.21 CA..... 58	
Figure 4.18: Flow curves of cellulose acetate at different temperatures with 0.24 CA..... 59	

Chapter 5

Figure 5.1: SEM micrographs of 15% CA fiber at dope solution flow rate = 6 (g/min)	63
Figure 5.2: SEM micrographs of 15% CA fiber at dope solution flow rate = 7.5 (g/min)	63
Figure 5.3: SEM micrographs of 15% CA fiber at dope solution flow rate = 9 (g/min)	64
Figure 5.4: SEM micrographs of 15% CA fiber at dope solution flow rate = 10.5 (g/min) ...	64
Figure 5.5: SEM micrographs of 18% CA fiber at dope solution flow rate = 6 (g/min)	65
Figure 5.6: SEM micrographs of 18% CA fiber at dope solution flow rate = 7.5 (g/min)	65
Figure 5.7: SEM micrographs of 18% CA fiber at dope solution flow rate = 9 (g/min)	65
Figure 5.8: SEM micrographs of 18% CA fiber at dope solution flow rate = 10.5 (g/min) ...	66
Figure 5.9: SEM micrographs of 21% CA fiber at dope solution flow rate = 6 (g/min)	67
Figure 5.10: SEM micrographs of 21% CA fiber at dope solution flow rate = 7.5 (g/min) ...	68
Figure 5.11: SEM micrographs of 21% CA fiber at dope solution flow rate = 9 (g/min)	69
Figure 5.12: SEM micrographs of 21% CA fiber at dope solution flow rate = 10.5 (g/min) .	70
Figure 5.13: SEM micrographs of 24% CA fiber at dope solution flow rate = 6 (g/min)	71
Figure 5.14: SEM micrographs of 24% CA fiber at dope solution flow rate = 7.5 (g/min) ...	71
Figure 5.15: SEM micrographs of 24% CA fiber at dope solution flow rate = 9 (g/min)	73
Figure 5.16: SEM micrographs of 24% CA fiber at dope solution flow rate = 10.5 (g/min) .	74
Figure 5.17: Filtration time of water permeability for 15% CA/DMAc hollow fiber.	77
Figure 5.18: Filtration time of water permeability for 18% CA/DMAc hollow fiber.	77
Figure 5.19: Filtration time of water permeability for 21% CA/DMAc hollow fiber.	78
Figure 5.20: Filtration time of water permeability for 24% CA/DMAc hollow fiber.	78
Figure 5.21: Effect of polymer concentration on the stress of cellulose acetate hollow fibers.	82
Figure 5.22: Effect of polymer concentration on the strain of cellulose acetate hollow fibers.	83

Chapter 6

Figure 6.1: SEM images of 21% cellulose acetate at bore flow rate = 8 (g/min)	86
Figure 6.2: SEM images of 21% cellulose acetate at bore flow rate = 10 (g/min)	87
Figure 6.3: SEM images of 21% cellulose acetate at bore flow rate = 12 (g/min)	88

Figure 6.4: SEM images of 21% cellulose acetate at bore flow rate = 13 (g/min).....	89
Figure 6.5: SEM images of 21% cellulose acetate at bore flow rate = 16 (g/min).....	90
Figure 6.6: Filtration time of water permeability at different bore flow rate.	91
Figure 6.7: Effect of bore fluid flow rate on the stress of cellulose acetate hollow fibers.	94
Figure 6.8: Effect of bore fluid flow rate on the strain of cellulose acetate hollow fibers.	95

Chapter 7

Figure 7.1: SEM images of 21%CA at air gap = 5.5cm.	98
Figure 7.2: SEM images of 21%CA at air gap = 7cm.	99
Figure 7.3: SEM images of 21% CA at air gap = 9cm.	100
Figure 7.4: SEM images of 21% CA at air gap = 10 cm.	101
Figure 7.5: Filtration time of water permeability at different air gap distance.	102
Figure 7.6: Effect of air gap distance on the stress of fibers fabricated from 21% CA.	105
Figure 7.7: Effect of air gap distance on the strain of cellulose acetate hollow fibers.	106

Chapter 8

Figure 8.1: SEM micrographs of 24% CA at bore fluid concentration 0% Ethanol/H ₂ O.	108
Figure 8.2: SEM micrographs of 24% CA at bore fluid concentration 18% Ethanol/H ₂ O. .	109
Figure 8.3: SEM micrographs of 24% CA at bore fluid concentration 25% Ethanol/H ₂ O. .	110
Figure 8.4: SEM micrographs of 24% CA at bore fluid concentration 35% Ethanol/H ₂ O. .	111
Figure 8.5: SEM micrographs of 24% CA at bore fluid concentration 50% Ethanol/H ₂ O. .	112
Figure 8.6: Filtration time of water permeability for different concentration of bore fluid. .	113
Figure 8.7: Effect of % ethanol in the bore fluid on the fibers stress.	115
Figure 8.8: Effect of % ethanol in the bore fluid on the fibers strain.	116

Introduction

Chapter One: Introduction

In this chapter, literature has been explored. The use of hollow fiber membranes in water pollution, water purification, water filtration and methods of fabricating polymeric hollow fibers, primarily cellulose acetate hollow fibers and its application were searched and presented in the following sections.

1.1. Water Pollution

Water is very important to the lives of all living organisms on the earth. It is present as 71% of the Earth's surface, and it is presented in the following forms: oceans, rivers, seas and groundwater. Water is also a main compound in the biological processes, agriculture application and industrial processes. Organism whatever kind or size can't live without water and plants also need water in order to grow. For all these reasons water pollution is important for all researchers in order to keep the water clean and healthy to continue the life on the earth.

Industrial production is a major cause of water pollution. It has environmental impact on water and air, and has led to soil degradation, acid rain, global warming, and ozone depletion; all these phenomena have indirectly affected the water quality (1). Water pollution may occur due to discharge of industrial waste in the sea. This waste may contain toxic substances that affect the marine life and the physical and chemical characteristics of sea water (2). Five major problems arise from the discharge of waste water like sewage into sea; these are associated with disease, deoxygenate enrichment, toxicity and aesthetics (3).

1. Introduction

Human activities are another reason of water pollution which has affected the water system in numerous ways. For example, through deforestation, urbanization, agricultural development, land drainage, pollutant discharge, and flow regulation (4). The polluted water may contain harmful chemicals or toxic biological elements or radioactive elements.

1.1.1. Water Chemical Pollution

The chemical pollution of water was associated with chemical water quality index, which employs dissolved oxygen, ammonium and biochemical oxygen demand (BOD) (5). In chemical water pollution concentration of Total Nitrogen (TN), Ammonia (N) Silica (Si), Calcium (Ca), Magnesium (Mg), and total Phosphorus (TP) were tabulated to compare the level of pollution (6).

The total dissolved solids (TDS) can be classified as chemical pollutants, it is generally defined as material that can pass through a 2 μ m filter, can be as high as 170,000mg/L. The recommended TDS for potable water is less than 500mg/L and 1000–2000mg/L for other beneficial uses such as stock ponds or irrigation. By comparison, average sea water has a TDS of 35,000mg/L (7). The high total dissolved solids (TDS) can be removed from produced water by reverse osmosis (8).

The present of toxic chemical elements in low concentration in water could be causes to carcinogenic, mutagenic, teratogenic and bioaccumulated, such as phosphorus, nitrogen and pesticides, these elements come from agriculture sources. Water pollution may result from the presence of some elements in high concentrations, such as Copper, zinc, manganese, boron and phosphorus. These

1. Introduction

elements may be toxic to humans and marine life if their concentrations exceed certain levels, in spite of the availability of low concentration help to preserve the balance in the aquatic life (9).

Fluoride is another example; high rate of fluoride in water could lead to mottling of teeth and in severe cases, crippling skeletal fluorosis. In addition the exposure to arsenic in drinking water may result in a risk of cancer and skin lesions. Chemical compounds containing uranium and selenium, may cause cancer if they more than the specified percentage (10).

1.1.2. Water Microbiological Pollution

Water pollution could be biological when it contains biological pollutants. Microorganisms are introduced into aquatic environments mainly by discharges of non-treated wastewater and sewage that are the main sources of pollution in natural aquatic environments (11). The greatest microbial risks are associated with intake of water that is contaminated with human or animal wastes. It can be a source of pathogenic bacteria, viruses, protozoa and helminthes (12). *E. coli*, *Shigella*, *Salmonella typhimurium*, *S. enteritidis*, *S. typhosa*, *V. cholerae*, *Streptococcus fecalis*, *Proteus*, *Klebsiella*, *Enterobacter*, and *P. aeruginosa* are famous examples of bacterial pathogens (13).

Cyan bacteria produces a variety of toxins, known as cyan toxins. In contrast to pathogenic bacteria, cyan bacteria do not grow within the human body after uptake. They grow only in the aquatic environment before intake (14). Cyantoxins can be dangerous to animals and humans. Cyantoxins such as, anatoxin-

1. Introduction

a, anatoxin-as aplysiatoxin, cylindrospermopsin, and domoic acid. These toxins may also break through filtration systems (15).

Some microorganisms will grow as bio-films on surfaces in contact with water, such as Legionella. Most of these organisms do not cause illness for healthy persons, but they can cause nuisance through generation of tastes and odors or discoloration of drinking-water supplies (14).

1.1.3. Radiological Water Pollution

Radioactive elements are found in nature and water, but the pollution of water may occur if the concentration of the radioactive materials are exceeded the permitted levels. Radiological water pollution was raised by the military uses of nuclear energy as fuel or navigation and the passage of submarines and aircraft carriers. Moreover, radiological pollution may result from medical, oil and industrial applications.

When radioactive materials are released into the environment, Radio-nuclides will be moved into the body by inhalation and ingestion, which causes internal exposure. Drinking water is an ingestion pathway. Radio-nuclides release large amounts of energy to a tissue directly, causing DNA damage, other cell damage and a cancer risk (16). The Increased levels of ^{60}Co , ^{90}Sr , ^{137}Cs , ^3H , ^{90}Sr , ^{137}Cs and $^{239+240}\text{Pu}$ isotopes in water cause radiological water pollution by calculated radioactivity and radiation dose rate (17).

1.2. Water Purification

There are several ways and processes are used to water desalination and treatment. In order to reduce water pollution, for example multistage flash (MSF), seawater reverse osmosis (SWRO) processes and membrane technologies. In the current research, fabrication of polymeric hollow fiber membranes for the production of safety drinking water will be used.

Water purification is the process of removing unwanted chemicals, materials and biological contaminants from raw water to achieve water fit in specific standard (18). It is effective to remove large particles such as sand, minerals (Ca, Si and Mg) and toxic metals and the method is used to purify the water depends on the size of the contaminants involved (19).

There are many methods and technologies that used for water purification. The coming paragraphs will give a clear idea about the latest and the most popular technologies for water purification specially the technology which regard to water purification by using membrane methods.

1.2.1. Water Purification Techniques

Water purification techniques can be categorized into six groups; the adsorption, biotechnology, catalytic processes, membrane processes, ionizing radiation processes and magnetically assisted processes (20).

2.2.1.1 Chemical Water Purification

Photocatalytic process in several situations cases a complete degradation of organic pollutants in very small and harmless species without apply any chemicals.

1. Introduction

This process is based on excitation of a molecule or solid caused by light absorption. Ultra Visible (UV) light could be used, that drastically alters its ability to lose or gain electrons and promote decomposition of pollutants to harmless by products (21). Lately the photocatalytic reactors were linked to membrane process to get high degree of effectiveness. The membrane was selected because it has good environmental properties, low cost and high separation process. There are a lot of articles described the connected of photo-catalytic reactor with membrane. Some papers state about membrane filtration reactor fixed with novel photocatalytic oxidation slurry reactor to conserve catalyst for purification control (22), utilized of TiO_2 photo catalyst in a photo catalytic connected with polypropylene membrane reactor (23) and photo catalyst membrane reactor with catalyst suspended in feed solution (24). Photo catalytic process is possible to include a catalytic, membrane and radiation technique.

Magnetic separation is a process for the separation of elements on the basis of their magnetic properties. on the other hand, it was shown that non magnetic water pollutants could be removed with the combination of magnetic seeding techniques. Magnetic technique has provided an evidence that metal ions can be removed from liquids by means of hydroxide flocs, these flocs combined with magnetic seeds can be separated from water body by means of magnetic separation. Magnetic seeding combined magnetic separation techniques were used for heavy metal ions removal from waste water since the 1970s (25). The water purification by magnetic could be a combined with biological process (26).

1. Introduction

1.2.1.1. *Microbiological Water Purification*

The purpose of using this technique is removing all waterborne pathogens without use any chemicals disinfectants or external power requirement. One of the studies discussed this topic by using portable water filtration units, these units were challenged with test organisms with taking into account the PH and turbidity. And the results led to the geometric average removal exceeded 99.9999% for bacteria, 99.99% for viruses, and 99.9% for *Cryptosporidium parvum* oocysts (27).

The second example about the Microbiological water purification is using Bio-films where it was formed inside the filter. This method investigates the microbiological performance of a point of use domestic water filter that consisted of a micro filter membrane layer and an activated carbon filter. The filter tested in the present study showed high purification capability of removing the turbidity and total hardness from the tap water and absorbing some suspended solids (28).

1.3. **Water Filtration**

The focus in this section will be on water filtration by using membrane because the use of membrane in water treatment is the main objective of the project, while the knowledge of water filtration is wide, so it is not easy to study thoroughly this technology. For this reason, the focus will be on membrane process.

Water filtration is removal of heavy metals and suspended solids from water. It is necessary to keep the water and marine environment clean because the heavy metals and suspended solids accumulate toxic components in the bottom of the sea and lack (29). Currently, membrane filtration becomes a new technology in

1. Introduction

1.2.1.1. *Microbiological Water Purification*

The purpose of using this technique is removing all waterborne pathogens without use any chemicals disinfectants or external power requirement. One of the studies discussed this topic by using portable water filtration units, these units were challenged with test organisms with taking into account the PH and turbidity. And the results led to the geometric average removal exceeded 99.9999% for bacteria, 99.99% for viruses, and 99.9% for *Cryptosporidium parvum* oocysts (27).

The second example about the Microbiological water purification is using Bio-films where it was formed inside the filter. This method investigates the microbiological performance of a point of use domestic water filter that consisted of a micro filter membrane layer and an activated carbon filter. The filter tested in the present study showed high purification capability of removing the turbidity and total hardness from the tap water and absorbing some suspended solids (28).

1.3. **Water Filtration**

The focus in this section will be on water filtration by using membrane because the use of membrane in water treatment is the main objective of the project, while the knowledge of water filtration is wide, so it is not easy to study thoroughly this technology. For this reason, the focus will be on membrane process.

Water filtration is removal of heavy metals and suspended solids from water. It is necessary to keep the water and marine environment clean because the heavy metals and suspended solids accumulate toxic components in the bottom of the sea and lack (29). Currently, membrane filtration becomes a new technology in

1. Introduction

water treatment. Moreover, membrane processes also is a better choice over the traditional separation methods due to their unique properties, such as no phase change, no chemical addition, and simple operation. Although it has a good efficiency of water recycles to meet water reusable request in foodstuff, leather, textile, and electronic industry (30).

1.3.1. Membrane Process

Sidney Loeb was developed in the early sixties as functional synthetic reverse osmosis membrane from cellulose acetate polymer. The membrane was capable of rejecting salt and passing water at moderate flow rates and pressures. Membrane filters were ranged from nano-filtration (partial desalination) through ultra-filtration (virus removal) to microfiltration (suspended solids removal). For every application a specific membrane and filtration principle should be developed. For ultra and micro filtration the cross flow principle is being used, where the suspension to be filtered has to be pumped along the membrane surface in order to avoid fouling and allowing only a small part to pass through the membrane. Filtration membranes for water treatment and applications for the food, beverage, bioreactors and pharmaceutical industry are currently fast developing with ever increasing market figures (31). Table 1.1 shows the classification of membrane process with common examples according to pore size.

1. Introduction

Table 1. 1: Classification of Membrane Processes (32).

Size	Molecular Weight	Example	Membrane Process
100 μm		Pollen	
		Starch	
10 μm		Blood Cells	Micro-filtration
		Typical Bacteria	
1 μm		Smallest Bacteria	
1000 A°		DNA, Viruses	
	100000		
100 A°	10000	Albumin	Ultra-filtration
	1000	Vitamin B ₁₂	
10 A°		Glucose	
		Water	Reverse Osmosis
1 A°		Na ⁺ Cl ⁻	

In this project membrane was used for water treatment. Application of membranes to drinking water treatment has become the focus of a lot of water desalination in the world, when the drinking water industry began to utilize membrane filtration; water sources that required minimal treatment are commonly used. As a result of efforts to expand the application of membrane technology, coagulation pre treatment for membrane filtration is now becoming more common (33). In addition to the previously reported for the classification of membrane according to size, T. Wintgens et al (2005); was mentioned in his article Water and

1. Introduction

wastewater treatment membranes are typically classified in order of decreasing pore size as microfiltration (MF), ultrafiltration (UF), nanofiltration (NF) and reverse osmosis (RO). As a general rule, MF is suitable for the removal of suspended solids, including larger microorganisms like protozoa and bacteria. UF is required for the removal of viruses and organic macromolecules down to a size of around 20 nm. Smaller organics and multivalent ions may be removed by NF while RO is even suitable for the removal of all dissolved species (34).

Microfiltration (MF) and ultrafiltration (UF) are Low pressure processes (0.1-2 bar for MF, and 2-10 bars for UF) that effectively remove microorganisms and suspended solids (MF) and colloids (UF). Nanofiltration (NF) and reverse osmosis (RO) work at high pressures (8-20 bars for NF and 10-80 bar for RO). Nanofiltration is a relatively young membrane process which is effective for water softening through the removal of magnesium and calcium ions and for removing some simple organic compounds. The application of RO for desalting brackish water and seawater is well known, but this process can be also used for the removal of low molecular weight organic compounds either of natural or synthetic origin from water. Nevertheless a wider diffusion of membrane processes is still limited mainly by technological and economical factors. From an economical point of view the cost of some types of membrane especially those based on ceramic materials is still high and the costs increase as the desired water quality increases. MF and UF are cheaper than NF and RO even though, over the last few years, the cost of a RO plant has decreased due to a greater diffusion of this technology for water desalination (35).

1. Introduction

The use of membrane filtration processes such as microfiltration, ultrafiltration, nanofiltration and reverse osmosis offer many advantages for the treatment of produced water:

1. The technology is more widely applicable across a range of industries
2. The membrane is a positive barrier to rejected components, thus the variation in feed water quality will have a minimal impact on permeate quality.
3. No addition of chemicals is required.
4. Membranes can be used in process to allow recycling of selected waste streams.
5. Membrane equipment has a smaller footprint, energy costs are often lower and the plant can be highly automated (36).

Note: two parameters can be modified to enhance the flux: membrane permeability and temperature on the water flux (37).

1.3.2. Microfiltration

Microfiltration systems can be operated in one of two configurations, dead-end and cross-flow mode. In dead-end operation, the feed flow is perpendicular to the filter surface and only clean water leaves the filter housing. Particles that are retained on the membrane continue to accumulate, causing a filter-cake to buildup.

In dead-end filtration, clogging of membrane pores generally occurs in a short time and is thus not suitable for continuously run applications, while In cross-flow mode, the feed solution is passed parallel to the filter surface and two streams leave the membrane module: permeate and retentate. The major advantage of cross-

flow filtration is the reduction in cake buildup on the membrane surface, thereby reducing pore clogging (38).

1.3.3. Ultra filtration

In ultra filtration processes, the commercial modules often used are hollow fiber and spiral-wound. Hollow-fiber modules are constituted of tiny polymer cylinders disposed in the tube and shell arrangement. The modules contain about 50-3000 fibers and can be operated in two different ways as the mention below:

1. The feed solution enter inside the fibers, whereas, the permeate is collected on the outside of the fibers.
2. The feed solution is introduced on the shell side and the permeate passes into the fibers.

The main advantage of hollow-fiber modules in ultra filtration processes is the high packing density followed by easiness in the operation and maintenance and low energy consumption. The performance of this process depends on the characteristics of the module and the operating conditions. The characteristics of the module are the nature of the polymeric material, the structure of the fibers, the porosity and pore size distribution, the diameter, thickness, length of the fibers, and the packing density. The operational parameters are the following:

1. The characteristics of the solution which depend on the chemical nature of the solute, the solvent and solute concentration; physical properties as density, viscosity and osmotic pressure
2. Feed flow and trans-membrane pressure drop (39).

1.3.4. Nanofiltration

Nanofiltration can be successfully applied in drinking water production, textile industry, food industry and other industries (40). and so on the nanofiltration (NF) membrane was found to be successful in removal of turbidity, removal of hardness and in lowering of the seawater total dissolved solid (TDS) (41). Nanofiltration membranes are intermediate between ultrafiltration membranes and reverse osmosis membranes (42). that mean NF has many advantages for example lower osmotic pressure difference, higher permeate flux, higher retention of multivalent salts and molecular weight compounds with more than 300, low investment and low operation and maintenance costs (43).

1.3.5. Reverse Osmosis

The idea of desalination of sea and brackish water by reverse osmosis (RO) was seriously proposed 50 years ago (44). It is one of the commercially viable processes available for water desalination for both domestic and industrial purposes. But recently RO is also being used for the separation of impurities from industrial effluent. There are three common types of module configuration that available in the market. These are tubular, spiral-wound and hollow-fiber configurations. Among these the hollow fiber module offers the highest surface area per unit volume of module (45).

Treatment by RO reduces high levels of dissolved salts but has severe limitations when it comes to the removal of organics from industrial chemical effluents. Relatively little is known about the effect of RO osmosis in the removal

of organic compounds of low molecular weight, although some studies have shown that the rejection may be very low, depending on the molecular weight, polarity and structure of the molecule and on the physicochemical properties of the membrane (46).

1.4. Methods of Making Hollow Fibers and Its Application

There are two basic configurations of membrane: flat sheet and hollow fiber (47). In addition, there are many methods and techniques used in the manufacture of the hollow fibers. They are used in various fields. Wet casting, thermally induced phase separation (TIPS) (48) Immersion precipitation method (49), Dry jet wet spinning process (50) and Non solvent induced phase separation (NIPS) (51) are famous examples of making hollow fiber membrane.

Because the manufacture of membrane has become a revolution in the world of research and industry, consequently each field contains a membrane as a part of them. In medicine membrane technology is important. It is used in drug delivery, artificial organs, tissue regeneration, diagnostic devices, as coatings for medical devices, bio-separations (52). Membrane processes in petroleum industry is used for the removal of acid gases from natural gas (53). In water treatment technology membrane is used in water desalination (54) especially in current time. Hollow fiber membranes are used in industry for carbon dioxide absorption (55).

Membrane separation processes have many advantages in terms of less energy needed, less environmental impacts, capital investments and processes are simple and easy to operate. Membrane separation is given a high quality water,

1. Introduction

removal or recovery of toxic or valuable components from industries applications and used in food and pharmaceutical industries (56).

Noteworthy, it is complex to simulate the hollow fiber spinning process by depending on the process conditions developed for flat membranes. The parameters factors for hollow fiber morphology are completely different from flat membranes. There are two coagulations taking place in hollow fiber spinning which are internal and external surfaces while there is only one major coagulation surface for flat sheet membrane (57).

In the next pages in this section will be about simple descriptions of the process were being given. The processes are Dry jet wet spinning process, Wet phase inversion process, Non Solvent Induced Phase Separation (NIPS) and Thermally Induced Phase Separation (TIPS). These processes are widely used in membrane fabrication.

1.4.1. Thermally Induced Phase Separation (TIPS)

Thermally induced phase separation (TIPS) is one of the most useful techniques for the preparation of polymeric porous membranes by controlling phase separation. It was divided into processes; Solid-liquid (S-L) separation and liquid-liquid (L-L) separation (58).

Thermally induced phase separation has a possibility to fabricate isotropic micro-porous membranes from semi crystalline thermoplastics (59). Semi crystalline polymers have high thermal resistances to conventional solvent cast membrane (60). The solution which was used in thermally induced phase is a homogeneous solution of polymer. It is prepared at high temperature by blending

1. Introduction

the polymer with diluents of high boiling point. After that, the mixture is cooled to solid-liquid (S-L) or liquid-liquid (L-L) phase separation (61).

Xun Yao Fu et al. (2006) during their research, they were observed thermally induced phase separation is used to create membrane with acceptable thermal, rheological and mechanical properties (62). TIPS fabrication process has an Attention since 1980s because of the ability to control the membrane structure and it has a range of applications in polymer industries (63).

The TIPS included five main steps. The first step come when the polymer is mixed at superior temperature with a high boiling point, low molecular weight liquid, then the hot polymer solution is emit onto preferred shape. The casting solution is cooled to induce phase separation. After that, the diluents are trapped in the polymer matrix during phase separation and solidification is removed to produce a micro-porous structure. Finally, the process ended with post-treatment processing (64).

1.4.2. Dry Jet Wet Spinning Process

Dry jet wet spinning process enables to obtain lyocell fibers with good physical properties and good mechanical properties (65). Spinning is the transformation of a liquid material into a solid fiber. There are three major methods for spinning fiber; melt spinning, dry spinning and wet spinning. Dry and wet spinning can be linked together to form dry jet wet spinning process. In this method Polymer dissolved in a suitable solvent, and then the solution will be extruded into a gap before entering a coagulation bath. A Coagulation bath is containing a coagulant that is miscible with the solvent but not with the polymer. A phase

1. Introduction

inversion process takes place to produce a solid fiber. The bath could be containing a mixture of solvent and non solvent (66).

Dry jet wet spinning method, the dry stage for solvent evaporation and wet stage for exchange of solvent with non-solvent. It was fabricated membranes with different structure, and the final membrane structure will effected according to dry stage (67).

1.4.3. Non Solvent Induced Phase Separation (NIPS)

Phase inversion is accepted way for preparing polymeric membranes. This method is used to fabricate fibers by evaporation of the solvent, thermal precipitation, immersion precipitation and vapor precipitation. By using a typical immersion precipitation technique a homogeneous polymer solution consisting of a polymer and solvent with or without an additive is extruded through a die then is immersed in a non-solvent bath (68). The membranes that made by phase inversion process are suitable for micro-filtration and ultra-filtration membranes by giving higher flux (69).

Non-solvent induced phase inversion technology has been a known technique to prepare polymeric membranes from a homogeneous polymer solution (70). Amides, polysulfones and cellulose acetates membranes are examples of the fabricated polymers created by this technique (71).

In non solvent induced phase separation, the polymer was dissolved in a solvent and optionally with some non solvent with pore formers to make homogenous solution. This homogenous solution is called blend, and the porous structure is formed when the solution is immersed in non solvent, such as water

1. Introduction

(72). By materials and methods, this process will be explained in details. In addition, this technique was used in the present report.

1.4.4. Wet Phase Inversion Process

In this process, the dope solution and the bore fluid are transported into the spinneret by applying gear pumps. Tube in orifice spinneret with different dimensions, inner diameter of the hollow needle, inner slit diameter and outer slit diameter are used.

The dope was directly extruded into the coagulation medium at the bottom of the bath, and the formed hollow fiber was continuously drawn out of the coagulation bath with a specific flow rate. The hollow fiber was washed and reeled up on rolls. Finally, the collected fibers were washed for long time with water (73).

1.5. Cellulose Acetate Hollow Fibers (Background and Literature Review)

1.5.1. Characterization of Cellulose Acetate (CA)

Cellulose was found in cotton 94% and 50% in wood page. It is obtained by the reacting cellulose with acetic acid or acetic anhydride (74).

Cellulose is one of the most ideal membrane materials since it is a kind of most available organic resource, naturally degradable, biology compatible, hydrophilic, foul resistant and it has good resistance to acid and organic solvents. Cellulose and its derivatives are widely used in the manufacture of membranes. The

1. Introduction

most common commercial cellulose esters are cellulose acetate (CA), cellulose acetate propionate (CAP) and cellulose acetate butyrate (CAB) (75).

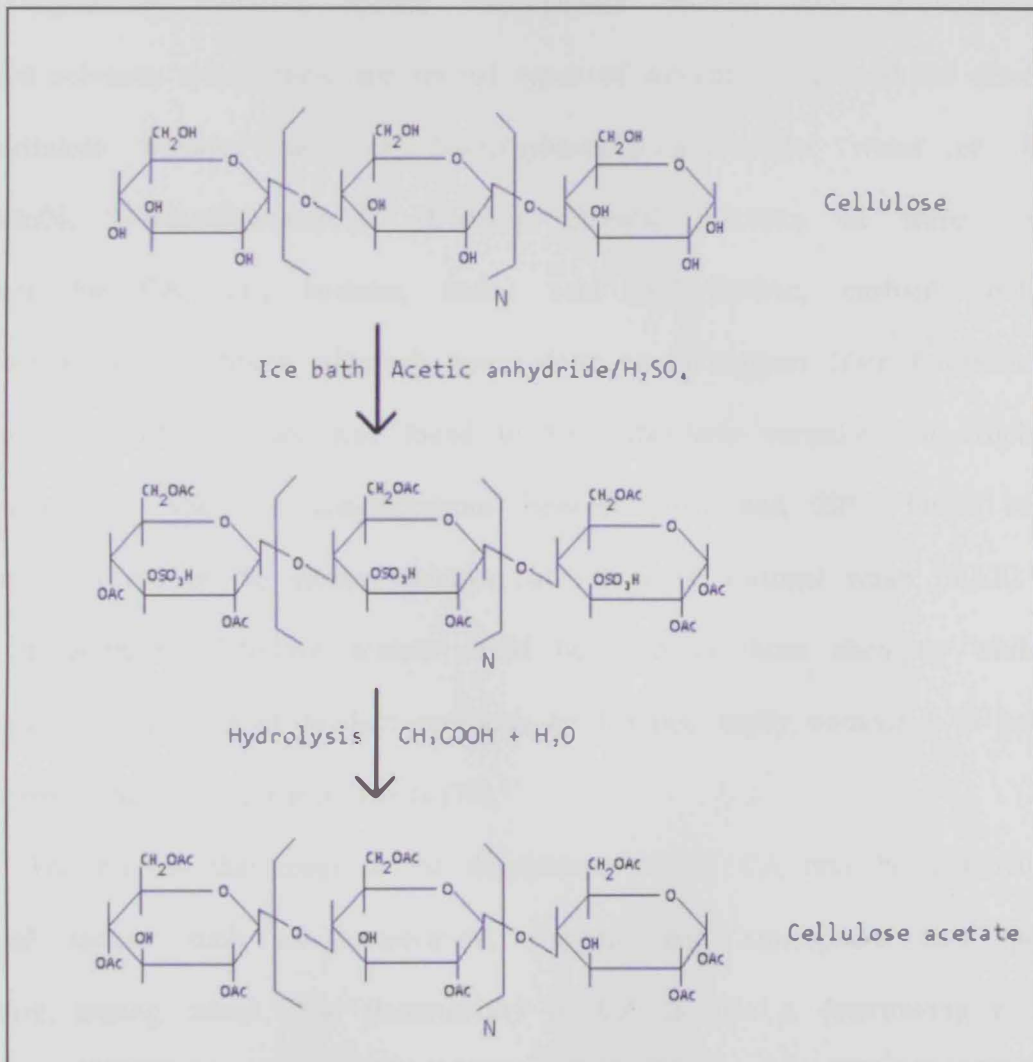


Figure 1. 1: Cellulose Acetate Preparation Steps (76).

Cellulose acetate is one of the first polymer membranes that have been used for aqueous based separation for example, reverse osmosis and ultra-filtration (UF) techniques. A hydrophilic property of cellulose acetate offers a good fouling

1. Introduction

resistance. However, cellulose acetate is not suitable for more aggressive cleaning, has low oxidation and chemical resistances and poor mechanical strength and hence the modification of cellulose acetate importance (77).

Sometimes cellulose acetate was chosen because of its solubility in selected solvents, which there are special types of solvents were used for dissolution of cellulose acetate, such as N-methylmorpholine-N-oxide/ water or lithium chloride/N, N-dimethylacetamide (DMAc). Several mixtures of three common solvents for CA, i.e., acetone, acetic acid and DMAc, enabled continuous electrospinning into fibers, although none alone could support fiber formation. The 2:1 acetone/DMAc mixture was found to be particularly versatile and efficient in generating CA fibers at concentrations between 10% and 20%. Other reported solvents involved in the electro spinning of CA were acetone/ water (80:20, w/w) (78). In addition, Cellulose acetate could be used in these attempts, while this polymer is a commercial product and can be handled easily compared to cellulose or to most of the other natural polymers (79).

The process that leads to the degradation of the CA may be a function of external factors such as temperature, oxygen, and atmosphere and radiation exposure, among others. The flammability of CA is also a determining factor in many applications, considering the increasing usage of its products in daily life. CA degradation products in cigarette filters are a major problem as an additional risk to smokers' health because of the high flammability of the polymer (80). Although cellulose acetate fibers have weak thermal chemical stability, but the Characteristic

1. Introduction

of CA membrane could be improved by mixing it with additives to have new requirements and new membrane properties (81).

1.5.2. Background and Literature Review

There are a many applications and fabrication methods for Cellulose acetate hollow fiber. Cellulose acetate hollow fibers for ultra low pressure (0 to 25 kg/cm²) reverse osmosis applications. Hollow fiber was fabricated by the dry wet spinning system. The dope solution of Cellulose acetate dissolved in solvent and was extruded through 3C-shaped spinneret of three or six holes. The thin of hollow fiber come out from process is 200 μ m. The hollow fiber display a higher flux of 4-6.5 gfd and salt rejection of 60-85% for tap water at 8 kg/cm². In addition the flux and salt rejection were increased with increasing the operation pressure (82).

Cellulose acetate was used to get adsorptive fibers for biomedical and environmental applications. Cellulose acetate and Chitosan were utilize as a dope mixture to spun by wet spinning process, that after the dope solution was dried at 65 °C to remove moisture. The stainless steel spinneret used has the following dimensions; outer diameter is 1.3 mm and inner diameter is 0.5 mm. NaOH solution with 3% concentration with water was used as both the external and internal coagulant. The fabricated fibers were immersed in 1-propanol and 1-heptane multi step solvent exchange and then dried at room temperature to avoid the pore collapse during drying. Cellulose acetate and Chitosan show an acceptable tensile stress and the tensile stress drop with increase the concentration of Chitosan in dope solution. By contrasting between Cellulose acetate fibers and Cellulose acetate with Chitosan, the fibers from Chitosan have better adsorption (83).

1. Introduction

Cellulose acetate ultra-filtration hollow fiber is used in the applications of separation and purification technologies by using LCST method. LCST refer to lower critical solution temperature that means the solubility decrease with increasing the temperature. LCST membrane was prepared by the dry wet spinning method from cellulose acetate/poly (vinyl pyrrolidone) (PVP 360K)/N-methyl-2-pyrrolidone (NMP)/1, 2-propanediol.

Table 1. 2: Experimental parameters used in LCST membrane fabrication

Parameters	Values
Take-up speed (m/min)	0.14
Pore flow rate (cm ³ /min)	2
Dope solution flow rate(g/min)	0.28
Coagulation composition	Water
Coagulation temperature (°C)	25
Dope solution composition	CA/NMP/PVP360K/1,2-propanediol (24%, 62.6%, 5% and .8.4%)
Air gap (cm)	51

According to current conditions, water flux was decreased with increased the cellulose acetate concentration in blended fibers. That because the skin layer became denser with increasing polymer concentration. The fibers produced according to the parameters in table 1.2 have good separation performance of bovine serum albumin (BSA) (84).

Moreover cellulose acetate mixed with other chemicals to obtain a new property of blending membrane. Hollow fiber ultra-filtration (UF) have been formed from 19% cellulose

1. Introduction

acetate/5% poly (vinyl pyrrolidone) (PVP 360 K)/74.8% N-methyl-2-pyrrolidone (NMP)/1.2% water by a dry jet wet spinning process.

Table 1. 3 Experimental parameters used in UF (CA/PVP 360 K/NMP/water) membrane fabrication.

Parameters	Values
Spinneret dimension, ID/OD (mm)	0.6/1.0
Take-up speed (m/min)	0.71
Pore flow rate (cm ³ /min)	0.85
Dope solution flow rate(g/min)	0.29
Coagulation composition	Water
Coagulation temperature (°C)	30
Dope solution composition	CA/NMP/PVP 360 K/water
Air gap (cm)	55, 88

The results illustrate that water flux of a membrane decreased while the retention increases with increasing air gap. PVP additive in the dope would favor the suppression of macrovoids and the thickness of inner skin increases with increasing air gap (85).

Tai-Shung Chung et al. (85) investigated the effect of air gap distance on the fabrication of hollow fiber membranes. An equation was developed to explain the velocity profile of nascent hollow fiber during formation in the air gap region and to predict fiber dimension as a function of air gap distance. Their idea is derived the essential equations related to velocity profile of a nascent hollow fiber in the air gap region, where this velocity is an a function of

1. Introduction

gravity, mass transfer, surface tension, drag forces, spinning stress, and rheological parameters of spinning solutions (86). The research on the effect of air gap length on hollow fiber still continues (87), (88), (89) and (90).

Chou and Yang (90) demonstrated that effect of take up speed on physical properties and permeation performance of cellulose acetate hollow fibers. Cellulose acetate was mixed with N-dimethylformamide (DMF) to obtain fiber by using dry wet technique. The table below shows the spinning conditions.

Table 1.4 Experimental parameters used in study of effect of take up speed membrane fabrication.

Parameters	Values
Spinneret dimension, ID/OD (mm)	0.4/0.6
Take-up speed (m/min)	35-75
Pore flow rate (g/min)	8
Dope solution flow rate(g/min)	9
Coagulation composition	Water
Coagulation temperature (°C)	40
Dope solution composition	25% CA/DMF
Air gap (cm)	20

The conclusions come from this experiment are:

Inner and outer diameters of the fiber decreased with the increase of take up roll speed, tensile stress increased and the breaking elongation decreased with the increase of take-up

1. Introduction

speed and permeability increased and the retention decreased slightly with the increase of the take up speed (91).

There are a number of researches about the successful utilize of cellulose acetate hollow fiber for water treatment. Jincai Su et al. (91) state that cellulose acetate nano-filtration hollow fiber membranes were prepared for forward osmosis processes by dry jet wet spinning method. Acetone and formamide are mixture was used as the solvent where cellulose acetate dissolved in solvent solution. A mixture of N-methyl-2-pyrrolidone (NMP) and deionized (DI) water was used as the bore fluid for spinning. The cellulose acetate blending solutions were 25%, 45% and 30% of total weight. Just for remind the bore fluid composition by weight is NMP/water (90:10).

Table 1.5 Experimental parameters used in nano-filtration hollow fiber membranes for forward osmosis processes.

Parameters	Values
Spinneret dimension, ID/OD (mm)	1.05/1.6
Take-up speed (m/min)	9.4
Pore flow rate (mL/min)	1
Dope solution flow rate(mL/min)	2
Coagulation composition	Water
Coagulation temperature (°C)	26± 1
Dope solution composition	25,30, 45% CA
Air gap (cm)	15

1. Introduction

The rejection percentage is 90.17% for NaCl and 96.67% for MgCl₂. The water flux and the salt leakage of the Cellulose acetate nano-filtration hollow fiber are measured in the forward osmosis processes by using NaCl or MgCl₂ draw solutions also with increasing the draw solution concentration, the water flux increases (92).

In the present work, cellulose acetate polymeric hollow fiber membranes were fabricated using non solvent induced phase separation method. The effect of bore fluid concentration, dope solution concentration, air gap and dope solution flow rate were studied. The hollow fiber membranes were characterized by measuring membrane strength, membrane water contact angle, water permeability and solute rejection. Scanning electron microscope (SEM) was used to test the membrane morphology.

Thesis Background

Chapter Two: Thesis Background

2.1. Objectives

There are two main objectives in this study. First one is the fabrication of cellulose acetate fibers at different cases, each case has specific parameters and conditions to manufacture the fibers, which have good selectivity and permeability for producing safe drinking water by using non-solvent induced phase separation (NIPS) technology. The second objective is examining the structure-property relationships between cellulose acetate and N, N-Dimethylacetamide as solvent. This objective was achieved by studying the rheology of the polymer mixtures at different concentrations and temperatures.

Producing safe drinking water using microfiltration and ultrafiltration has been becoming an interesting method. These membrane processes have been attracting much attention throughout the world due to their highly efficient removal properties of particulates, viruses, and bacteria. To be useful in industrial water treatment, membranes with high flux, high rejection, high mechanical stability, and good chemical resistance must be developed.

Non-solvent induced phase separation (NIPS) was used as the selected technology to achieve the objective of the present study. The non-solvent induced phase separation (NIPS) or immersion precipitation method is one of the major phase-separation methods that are mostly used to produce commercial porous polymeric membranes. In the membrane preparation process via NIPS, a polymer is dissolved in the solvent, and the homogeneous polymer solution is cast on a support

2. Thesis Background

or is extruded through a spinneret and subsequently immersed in a non solvent coagulant bath.

2.2. Thesis Review

In this study, the following outlines are presented:

Chapter one is a general introduction about the main classifications of water pollution (chemical, biological and radioactive). It presents the newest water purification knowledge; in addition, it previews a brief description about the membrane process and advanced methods of making hollow fibers, specially, the methods of making cellulose acetate hollow fibers for water treatment.

Chapter two presents the goals of project explain the main reasons of idea of the project and important objectives which the researcher tried to achieved during the research, thesis report overview also was present for the recent project.

Chapter three indicates all the materials were used through the study. Also in this chapter the method used to prepare the fibers (non-solvent induced phase separation method) was described in details. The last section in chapter three presents the main characterizations that were used to study the hollow fibers methodology.

Chapter four presents rheology of cellulose acetate solutions by using different concentration in N, N-Dimethylacetamind. They were examined by varying the temperatures of solution. In addition, Hershend-Balkley (H-B) model was used to test fluid behaviors.

2. Thesis Background

Chapter Five consists of study the morphology of cellulose acetate hollow fibers which were fabricated at different polymer concentrations and flow rates.

Chapter six discussed how the pore fluid flow rate could be effect on the properties and characterization of hollow fibers.

Chapter seven is about the how the air gap length could be an important parameter during the fabrication of hollow fibers.

Chapter eight shows the effect of pore solution on the performance of hollow fibers at different concentrations of ethanol in water.

Chapter nine consists of general conclusions and last chapter is recommendation for future studies about cellulose acetate hollow fibers.

Materials and Methods

Chapter Three: Materials and Methods

In this chapter chemicals used in the preparation of the cellulose acetate hollow fiber membranes are presented. Methods used to measure the dope solution viscosity; membrane properties such as water contact angle, membrane strength, water permeability and membrane morphology were considered.

3.1. Materials

3.1.1. Cellulose Acetate Solution Cellulose acetate was purchased from ALDRICH Chemistry in solid form from USA. It has an average molecular weight of 50,000 with 39.7% of acetyl content. N,N-Dimethylacetamide (DMAc) is a good solvent for CA and dissolves CA forming homogenous solutions at high concentrations (93). DMAc was purchased from SIGMA ALDRICH, Germany.

3.1.2. Bovine Serum Albumin

Bovine Serum Albumin (BSA) is a model protein that was selected in order to evaluate membrane fouling. It was purchased from SIGMA Life Science Company. It was stored at 2-8°C. The protein was used to measure the rejection factor of the fabricated fibers.

3.2. Methods

In the present section, the method of fabrication of hollow fiber was explained. In addition techniques used to study the membrane characteristics.

3.2.1. Hollow Fibers Preparation

Hollow fiber membranes were prepared via non-solvent induced phase separation (NIPS) method by a batch extruder. Membranes were prepared from CA/DMAc mixtures of 15%, 18%, 21% and 24% by dissolving a predefined quantity of Cellulose acetate in DMAc for 24 hours until each solution was completely homogeneous. The prepared dope solutions were transferred to the dope mixing tank and remained for 2 hours for degassing so that no bubbles remained in the solution. After 2 hours of degassing the process was started.

Predefined operating conditions were set; such as the dope solution flow rate, pore fluid flow type, pore fluid flow rate, air gap, fibers take up speed and coagulation bath temperature. The experimental setup used in the cellulose acetate hollow fiber fabrication is shown in Figure 3.1. Bore fluid was supplied from a pressurized tank and metered to the spinning process. The pressure was monitored using a pressure gage on a nitrogen (N₂) cylinder. The dope and bore fluids were filtered by a metal filter (25 μm) and were degassed before spinning to remove the particles and gas bubbles that may exist in the dope. The formed fibers were dropped into a coagulation water bath as a roll of fibers where they were wrapped multiple times around a take up roller with controlled speed. Finally, fibers were collected at the bottom of the hollow fibers collected vessels

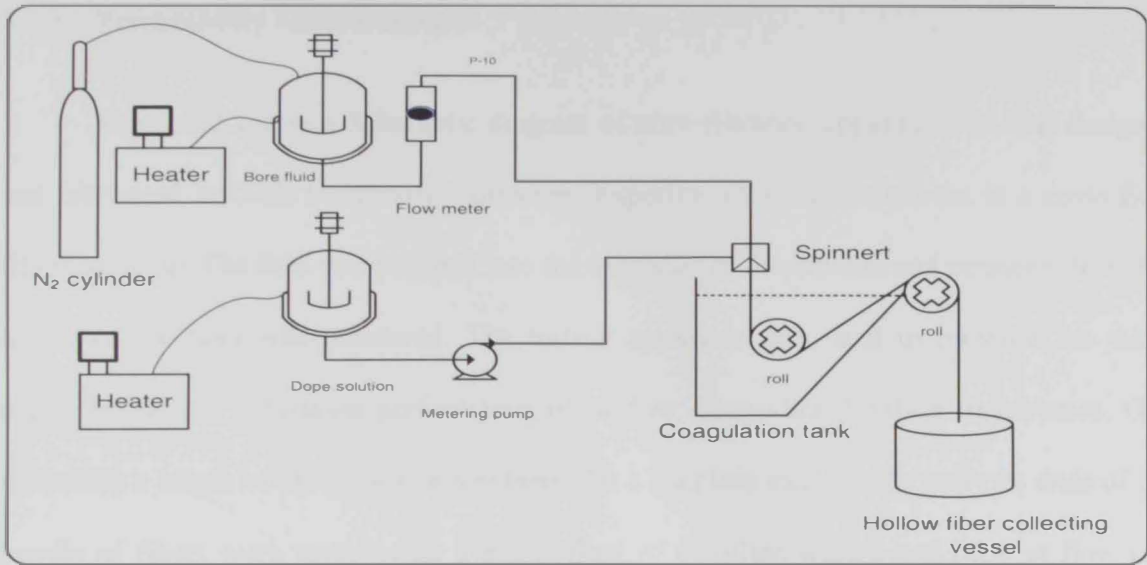


Figure 3. 1: Schematic diagram of the spinning system.

3.3. Characterization

Different techniques were used throughout the current study to characterize the fabricated membrane hollow fibers made at different concentrations and operating conditions.

3.3.1. Membrane Morphology

Membrane morphology (whole cross-section, enlargement cross-section, inner and outer surfaces) were observed by a Scanning Electron Microscope (SEM) with an accelerating voltage of (10) kV. The membrane samples were dried in a freeze dryer (EYELA Freeze Dryer mark of Tokyo Rikakikai Co.Ltd) for about 3 h to avoid structure shrinkage. The freeze dried hollow fiber membranes were fractured in liquid nitrogen to get clean and tidy break.

3. Materials and Methods

3.3.2. Permeability Measurements

Figure 3.2 shows a Schematic diagram of ultra-filtration apparatus that was designed and fabricated in UAE University workshop. Experiments were carried out in a cross flow filtration setup. The feed was pumped into the tube side of the module and permeate from the lumen of the fiber was measured. The testing apparatus was used to measure the water permeability and separation performance of hollow fiber ultra-filtration membranes. One fiber with a length of 30 cm was assembled into a stainless steel needle and two ends of the bundle of fibers were sealed with a pump flow of distillate water and BSA at flow rate 8ml/min to make a test module. The trans-membrane pressure could be applied adjusting the pressure valve close to the release side, and the average of the readings of the two pressure gauges was taken as the feed pressure.

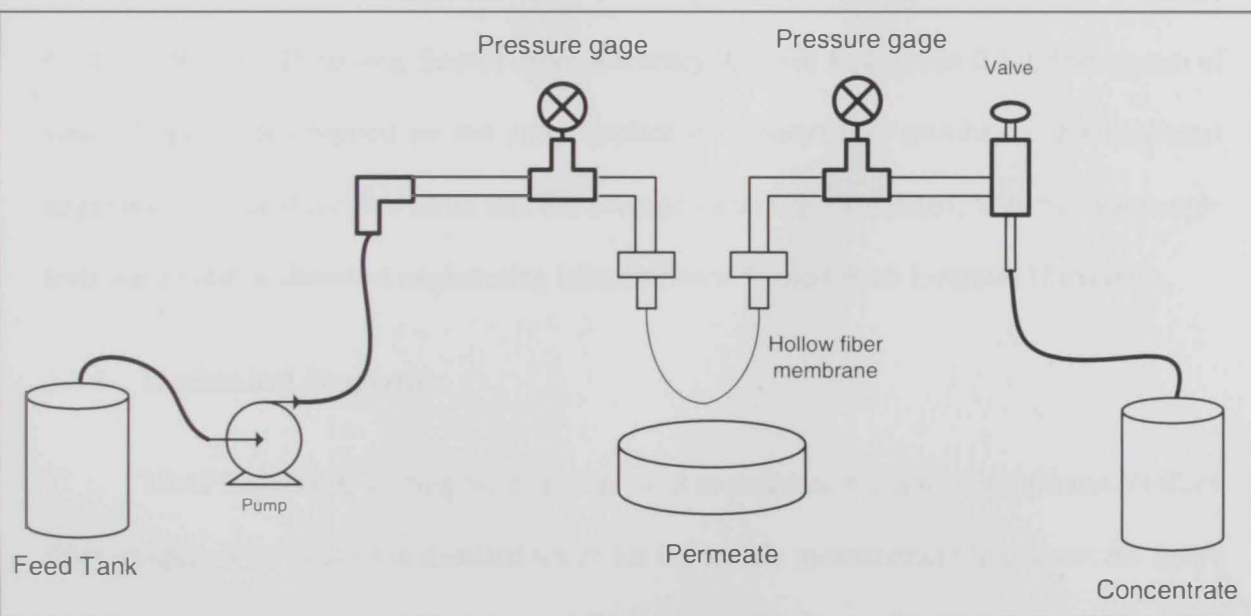


Figure 3. 2: Schematic diagram of ultra-filtration.

3. Materials and Methods

3.3.3. Solid Rejection

The concentration of BSA in permeate was measured by a UV-Spectrophotometer at a wavelength of 278 nm. The fiber rejection percentage was measured by using the following equation (94);

$$R\% = \left(1 - \frac{C_p}{C_f} \right) \times 100 \quad (1)$$

Where C_f and C_p represent the solute concentration in feed and permeate solution, respectively.

3.3.4. Water Contact Angle

Water contact angle measurement was performed to observe the degree of membrane hydrophilicity by a contact angle meter (contact angle meter from KYOWA interface science Co;LTD. With CCD camera, Sessile drop, Accuracy 0.2° and Resolution 0.1°). Microgram of water droplet was dropped on the outer surface of hollow fiber membrane. Each contact angle was measured for five times and the average value was calculated. Water contact angle tests were done in chemical engineering laboratories at United Arab Emirates University.

3.3.5. Mechanical Properties

TRAPEZIUM-X Testing System was used to measure the tensile properties. Hollow fiber samples were soaked in distilled water for the tensile measurement to prevent the fibers from drying. The test conditions were as follows:

- Number of test specimens 3 for each sample.
- Sample length between the two grips is 8 cm.

3. Materials and Methods

Break stress and break strain were automatically calculated by the TRAPEZIUM-X Software for each of the fibers. TRAPEZIUM-X Software enables to easily and quickly execute test operations.

3.3.6. Rheological Measurements

The rheological measurements were carried out to study the effect of concentration of CA and temperature using a cylinder viscometer. Viscosity in general was related to the polymer molecular weight. It was determined at different concentrations (15% CA, 18% CA, 21% CA, and 24% CA) and temperatures (25°C, 35 °C, 45 °C, 55 °C, 65 °C, 75 °C and 85 °C).

3.3.7. Measuring Fibers Bore Diameter

The internal diameters of hollow fibers were measured by microscope from Motic Microscopes Company. This microscope is suitable to measure internal diameter of fabricated fibers.

3.4. Operating Parameters

The effect of Cellulose Acetate concentrations, effect of dope solution flow rate, effect of pore fluid flow rate, pore fluid concentration, and the effect of air gap length on the properties of fabricated fibers are briefly mentioned in the following sections and discussed in more details in chapter 4.

3.4.1. Effects of CA Concentration and Dope Solution Flow Rate

One of the objectives of this study was investigating the morphology of the membranes at different concentration of dope solution while fixing all other conditions.

3. Materials and Methods

Different weights of CA were dissolved in N, N-Dimethylacetamide (DMAc) at 25 °C, with constant stirring for 1-2 days. Table 3.1 shows the concentrations used in the spinning process (15, 18, 21 and 24% CA). In addition this table shows the effect of dope solution flow rates on the hollow fiber membrane characteristics that was investigated for dope mass flow rates of 6, 7.5, 9 and 10.5 g/min while fixing other operating conditions.

Table 3. 1: Spinning parameters for CA/DMAc hollow fibers with different CA concentration and dope Solution flow rate.

Spinning parameters	Values
Spinneret dimension (mm)	1.7, 0.98, 0.35
Take-up speed (m/min)	9.4
Pore flow rate (g/min)	15
Temperature of dope solution (°C)	25
Temperature of bore fluid (°C)	25
Pressure gauge (bar)	0.18
Dope solution flow rate(g/min)	6, 7.5, 9 & 10.5
Coagulation composition	Water/water
Coagulation temperature (°C)	25
Dope solution composition	15%, 18%, 21% & 24% CA
Air gap (cm)	7

3. Materials and Methods

3.4.2. Effect of Bore Fluid Flow Rate

Table 3.2 shows the change in bore fluid flow mass rate while fixing other conditions. The bore fluid flow rate was changed from 8 to 16 g/min.

Table 3. 2: Spinning parameters for CA/DMAc hollow fibers with different pore flow.

Spinning parameters	Values
Spinneret dimension (mm)	1.7, 0.98, 0.35
Take-up speed (m/min)	9.4
Pore flow rate (g/min)	8, 10, 12, 13 & 16
Temperature of dope solution (°C)	25
Temperature of bore fluid (°C)	25
Pressure gauge (bar)	0.18
Dope solution flow rate(g/min)	6
Coagulation composition	Water
Coagulation temperature (°C)	25
Dope solution composition	21% CA
Air gap (cm)	7

3. Materials and Methods

3.4.3. Effect of Air Gap

The fabricated membranes were prepared by change the air gap length. Air gap length is the space between the spinneret and the coagulation bath. The effect of changing air gap distance on the fabricated membranes were studied at 5.5 cm, 7 cm, 9 cm and 10 cm with concentration of dope solution of 21% CA/DMAc. Table 3.3 shows the conditions of spinning.

Table 3. 3: Spinning parameters for CA/DMAc hollow fibers by changing air gap length.

Spinning parameters	Values
Spinneret dimension (mm)	1.7, 0.98, 0.35
Take-up speed (m/min)	9.4
Pore flow rate (g/min)	15
Temperature of dope solution (°C)	25
Temperature of bore fluid (°C)	25
Pressure gauge (bar)	0.18
Dope solution flow rate (g/min)	6
Coagulation composition	Water
Coagulation temperature (°C)	25
Dope solution composition	21% CA
Air gap (cm)	5.5, 7, 9 & 10

3. Materials and Methods

3.4.4. Effect of Bore Fluid Concentration

The effect of ethanol/water concentration as a bore was investigated for ethanol concentrations of 0, 18, 25, 35 and 50 wt% ethanol/water while fixing other operating conditions as shown in Table 3.4.

Table3.4: Spinning parameters for CA/DMAc hollow fibers with different pore concentration.

Spinning parameters	Values
Spinneret dimension (mm)	1.7, 0.98, 0.35
Take-up speed (m/min)	9.4
Pore flow rate (g/min)	15
Temperature of dope solution (°C)	25
Temperature of bore fluid (°C)	25
Pressure gauge (bar)	0.18
Dope solution flow rate(g/min)	6
Coagulation composition	0, 18, 25, 35 and 50% ethanol/water
Coagulation temperature (°C)	25
Dope solution composition	24% CA
Air gap (cm)	7

Results and Discussions

Chapter four: Effect of Temperature, Composition and Shear Rate on Cellulose Acetate / Dimethyl-acetamide Solution Viscosity

Cellulose acetate fibers are used for textiles and clothing by many designers in the world. This is attributed to the fact that is comfortable, breathable and biodegradable. Viscosity required for casting or spinning dope polymeric solution plays an essential role in the formulation of cellulose acetate fibers. In this study, the effects of temperature, polymer mass fraction, and shear rates on the viscosity of cellulose acetate polymer in DMAc solvent were experimentally investigated. The dope polymer was used in the fabrication of polymeric hollow fiber membranes engaged in building membrane contactors for water treatment. Data were obtained for (0.15, 0.18, 0.20, and 0.24) mass fraction of cellulose acetate in DMAc solvent at temperatures of 25, 35, 45, 55, 65, 75 and 85°C. The predicted values by the correlation were in good agreement with the experimental data. Its rheological behavior can be closely approximated by a Herschel Bulkley model which describes well the rheology of cellulose acetate in DMAc.

4.1. Introduction

Rheology is the study of material flow or deformation under stress. For mixed solutions, rheological parameters help to describe the ease with which it can be used in the fresh state, including workability, placcability, compactability, finishability, flowability, pumpability and extrudability. Different applications require different rheological characteristics. Thus rheology (particularly the study of the viscous flow of polymers) is very important in processing and proved useful as a quality control tool (95).

4. Effect of Temperature, Composition and Shear Rate on CA /DMAc Solution Viscosity

They are mainly features effect on the rheological and properties of polymer solution such as molecular weight, type of solvent and temperature of formation (96).

In addition, the properties of hollow fiber membranes have been affected by flow conditions during extrusion due to molecular orientation. Shear flow and elongation flow in the air gap region lead to molecular orientation in the fiber structure, that mean the molecular orientation will be effected on the rheological behavior of the polymer solution (97). The objective of this work was to study the effect of polymer concentration and temperature on the rheological behavior cellulose acetate dope solutions and its viability to fiber fabrications. The viscosity of the dope solution was investigated for four cellulose acetate mass fractions (0.15, 0.18, 0.21, 0.24) at temperatures 25 to 85 °C,

4.2. Results and Discussions

Over quite a wide range of shear rates, cellulose acetate rheological behavior can be closely approximated by a Herschel Bulkley model. Herschel Bulkley is a simple shear flow equation (98), that describes the rheology of cellulose acetate in DMAc. Herschel Bulkley fluids are a class of Non-Newtonian fluids, some examples of fluids behaving in this manner includes paint, food products, plastics, slurries, pharmaceutical products, polymeric solutions, paper pulp and semisolid materials (99). Non-Newtonian fluid is a function of temperature, pressure and shear rate.

The standard procedure for the estimation of the three rheological parameters for Herschel Bulkley mixture, with rheological equation,

$$\tau = \tau_o + m\dot{\gamma}^n \quad (2)$$

4. Effect of Temperature, Composition and Shear Rate on CA /DMAc Solution Viscosity

Where τ is the shear stress, $\dot{\gamma}$ is the shear rate, τ_0 is the yield stress, n is the flow behavior index and m is the consistency coefficient. This is done by using a numerical package, minimizing the sum of error squares and judging the goodness of fit through the value of the correlation coefficient R^2 . Equation (2) was linearized as shown below (100).

$$\ln(\tau - \tau_0) = \ln(m) + n \ln(\dot{\gamma}) \quad (3)$$

Pierre Saramito (101) was said that, if the value of n is greater than zero and n is the power index. When $n = 1$ the model reduces to the Bingham model. The shear thinning behavior is associated with $0 < n < 1$ and the unusual shear thickening behavior at $n > 1$. Diego Gomez (102) mentioned that the index k is a strong function of the concentration of the solution and the temperature, whereas n does not have a strong dependence on the concentration and temperature of the polymeric solution. Figures 1-7 show the apparent viscosity of cellulose acetate as a function of shear rate measured at different concentrations. These Figures show that the type of fluid is pseudoplastic fluid, this fluid illustrate a decrease in viscosity with increasing shear rate and hence referred to as shear thinning fluids (102) & (103) . These Figures show that the cellulose acetate solution at different concentrations exhibited a typical shear thinning behavior, where the apparent viscosity decreased with shear rate. The phenomenon of shear thickening was not observed in the current system.

Viscosity is proportional to concentration where as the concentration was increased the viscosity was increased, that was clear to be observed at 0.21 CA and 0.24 CA. This is appropriate to the fact that the increase in molecular weight number results from the dissolution of cellulose acetate in DMAc solvent. Mark Houwink Sakurada (MHS) equation investigated the viscosity as a function of molecular weight (104);

$$\eta = KM_v^a \quad (4)$$

4. Effect of Temperature, Composition and Shear Rate on CA /DMAc Solution Viscosity

Where η is the intrinsic viscosity, M_v is the viscosity average molecular weight, and K and A are viscometric constants for given solute solvent system and temperature.

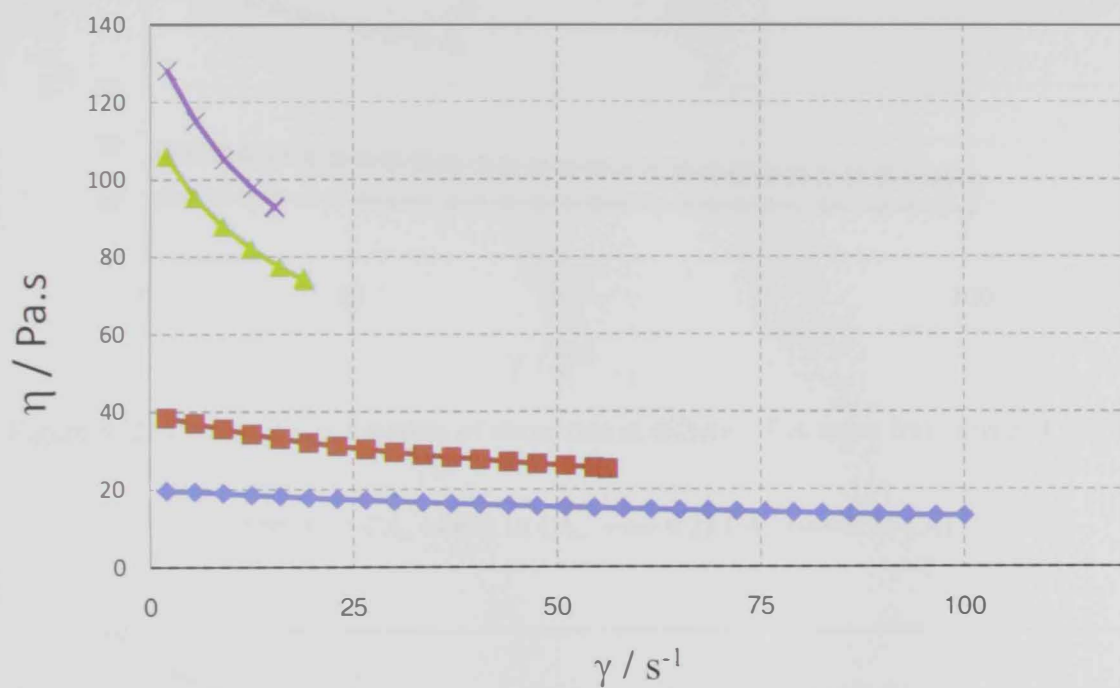


Figure 4. 1: Viscosity as a function of shear rate at different CA mass fractions at $T = 25^{\circ}C$.

(— 0.15 CA, —+ 0.18 CA, —▲ 0.21 CA, —× 0.24 CA)

4. Effect of Temperature, Composition and Shear Rate on CA /DMAc Solution Viscosity

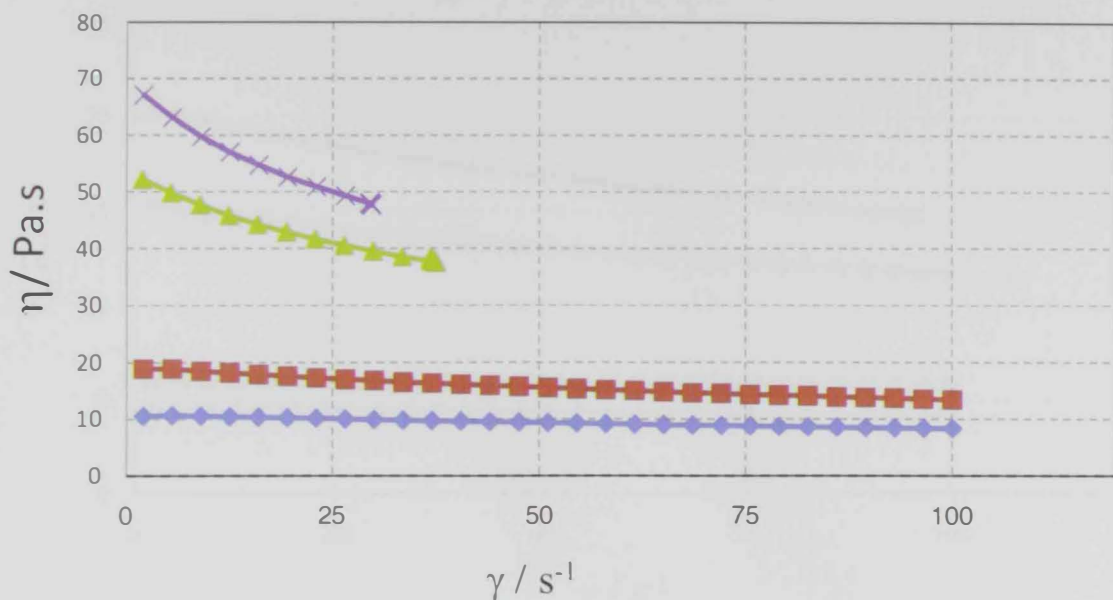


Figure 4. 2: Viscosity as a function of shear rate at different CA mass fractions at T = 35°C.

(— 0.15 CA, — 0.18 CA, — 0.21 CA, — 0.24 CA)

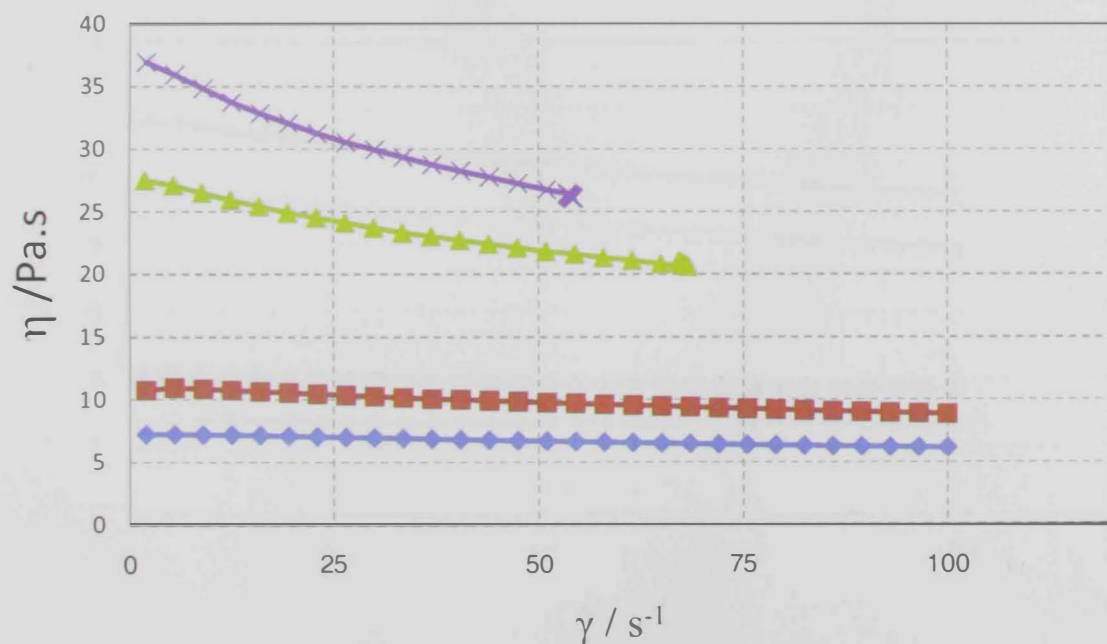


Figure 4. 3: Viscosity as a function of shear rate at different CA mass fractions at T = 45°C.

(— 0.15 CA, — 0.18 CA, — 0.21 CA, — 0.24 CA)

4. Effect of Temperature, Composition and Shear Rate on CA /DMAc Solution Viscosity

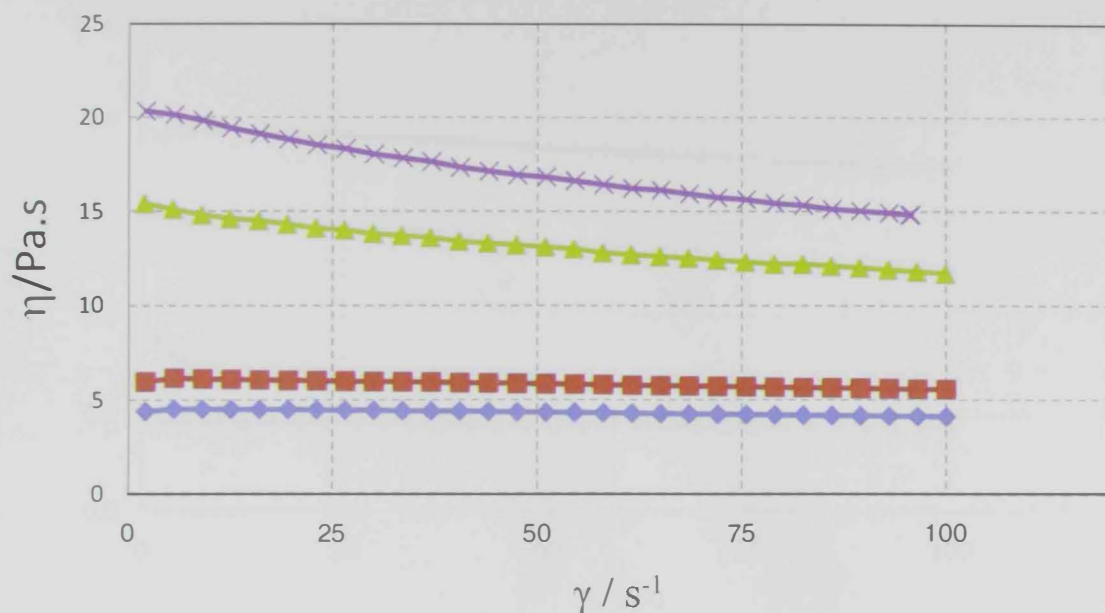


Figure 4. 4: Viscosity as a function of shear rate at different CA mass fractions at $T = 55^{\circ}C$.

(— 0.15 CA, — 0.18 CA, — 0.21 CA, — 0.24 CA)

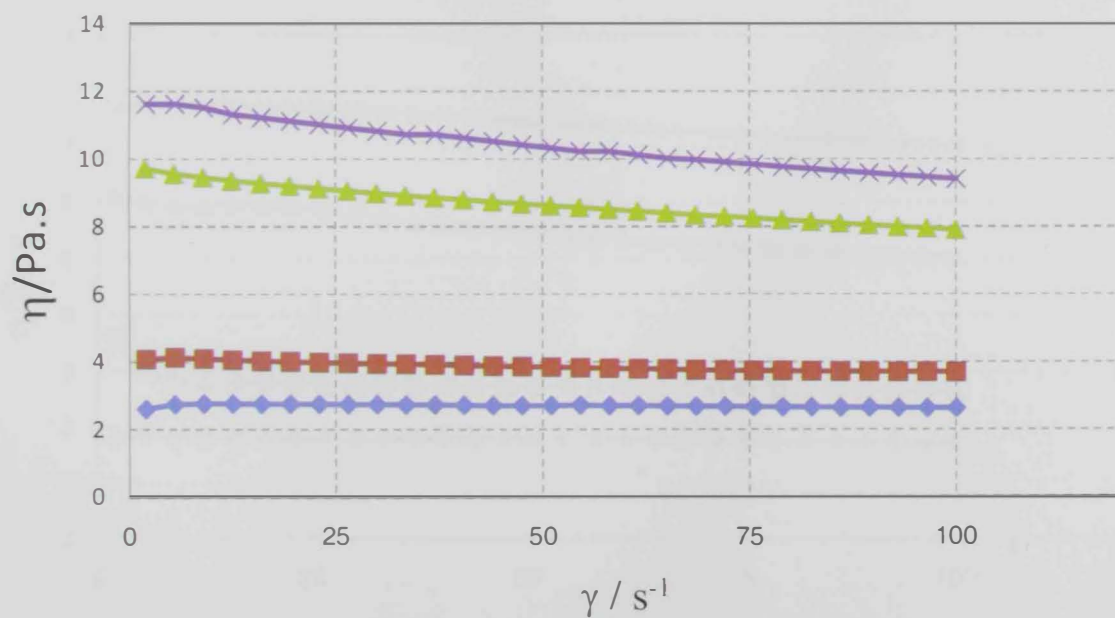


Figure 4. 5: Viscosity as a function of shear rate at different CA concentrations at $T = 65^{\circ}C$.

(— 0.15 CA, — 0.18 CA, — 0.21 CA, — 0.24 CA)

4. Effect of Temperature, Composition and Shear Rate on CA /DMAc Solution Viscosity

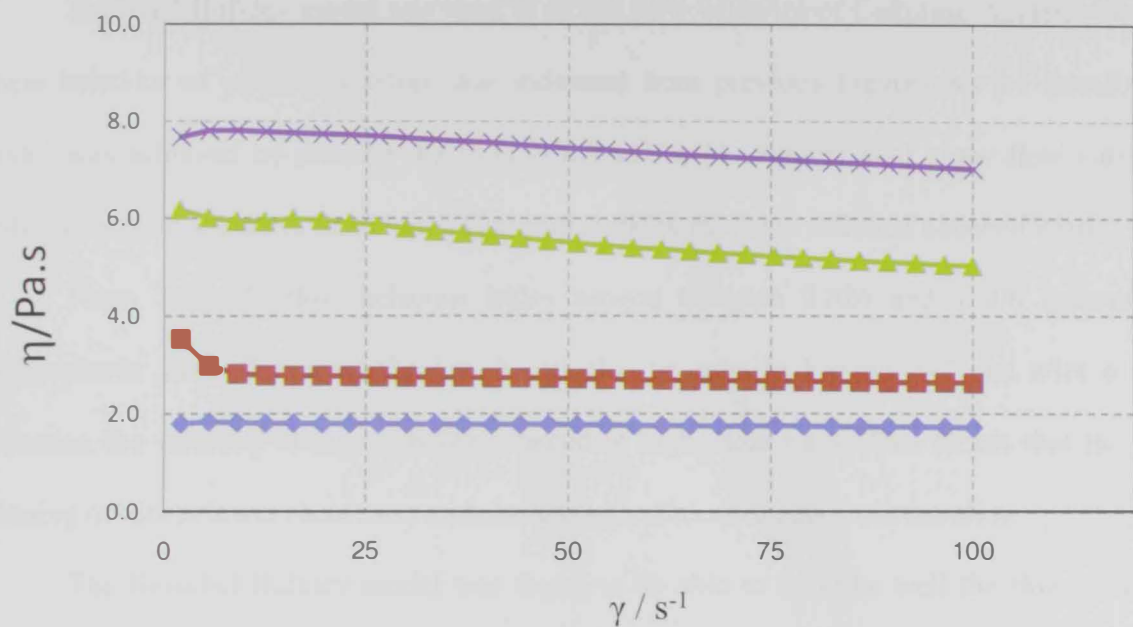


Figure 4. 6: Viscosity as a function of shear rate at different CA concentrations at T = 75°C.

(— 0.15 CA, — 0.18 CA, — 0.21 CA, — 0.24 CA)

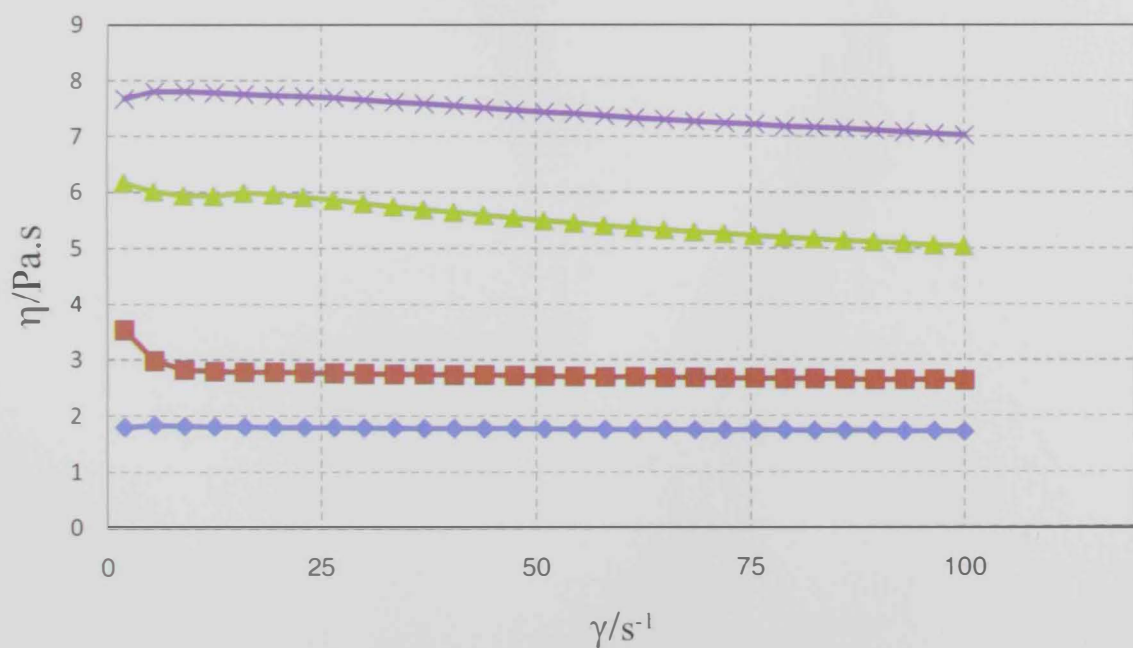


Figure 4. 7: Viscosity as a function of shear rate at different CA concentrations at T = 85°C.

(— 0.15 CA, — 0.18 CA, — 0.21 CA, — 0.24 CA)

4. Effect of Temperature, Composition and Shear Rate on CA /DMAc Solution Viscosity

Herschel Bulkley model was used to fit the flow behavior of Cellulose Acetate. The non linear behavior of polymer mixture was indicated from previous Figures, so the linearization model was achieved by plotting the $\ln(\tau - \tau_0)$ vs. $\ln(\dot{\gamma})$. Figures 8-13 show flow curves of cellulose acetate solutions fitted to the Herschel Bulkley model at different concentrations.

From Table 1, flow behavior index ranged between 0.826 and 1.008 indicating a pseudoplastic shear thinning behavior. It can also be seen in Figures 1-7 that after a sharp reduction the viscosity change was smoothed at high shear rates. This means that the shear thinning occurs at lower shear rates with increasing cellulose acetate concentration.

The Herschel Bulkley model was found to be able to describe well the flow curves of cellulose acetate solutions. The obtained Herschel Bulkley model parameters showed a high dependence of the yield stress on cellulose acetate concentration for a given concentration and more dependence on temperature of the solution.

4. Effect of Temperature, Composition and Shear Rate on CA /DMAc Solution Viscosity

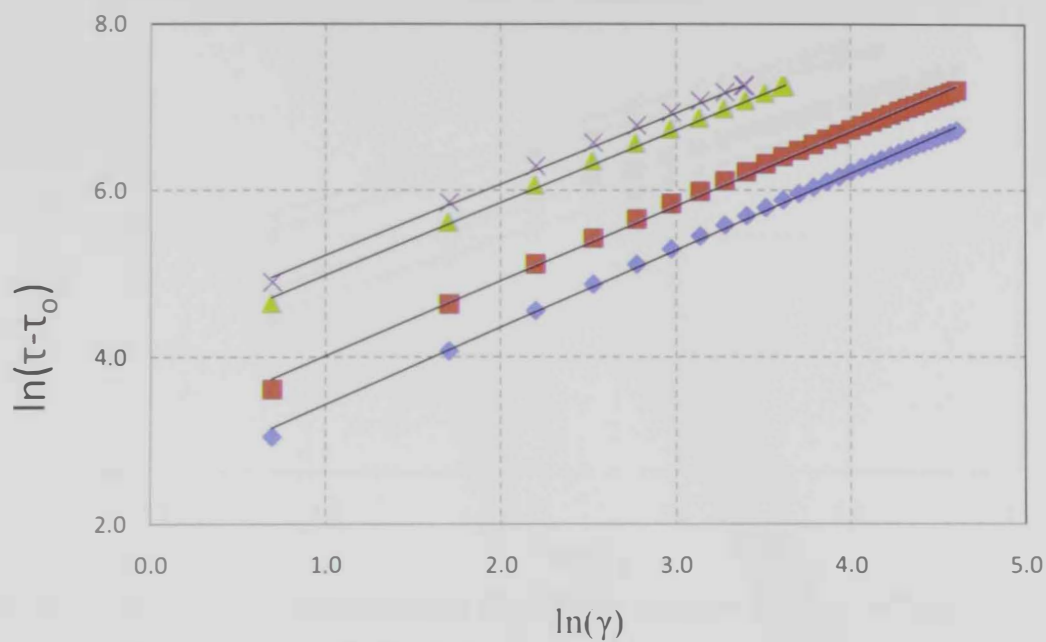


Figure 4. 8: Flow curves of CA solution fitted to the Herschel Bulkley model at $T = 25^{\circ}\text{C}$.

(♦ 0.15 CA, ■ 0.18 CA, ▲ 0.21 CA, × 0.24 CA, — H.B model)

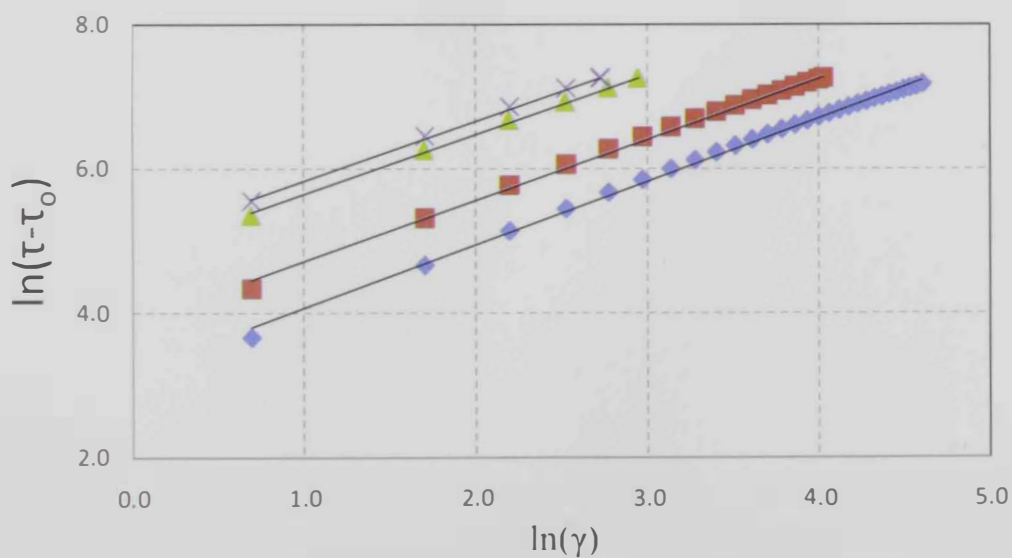


Figure 4. 9: Flow curves of CA solution fitted to the Herschel Bulkley model at $T = 35^{\circ}\text{C}$.

(♦ 0.15 CA, ■ 0.18 CA, ▲ 0.21 CA, × 0.24 CA, — H.B model)

4. Effect of Temperature, Composition and Shear Rate on CA /DMAc Solution Viscosity

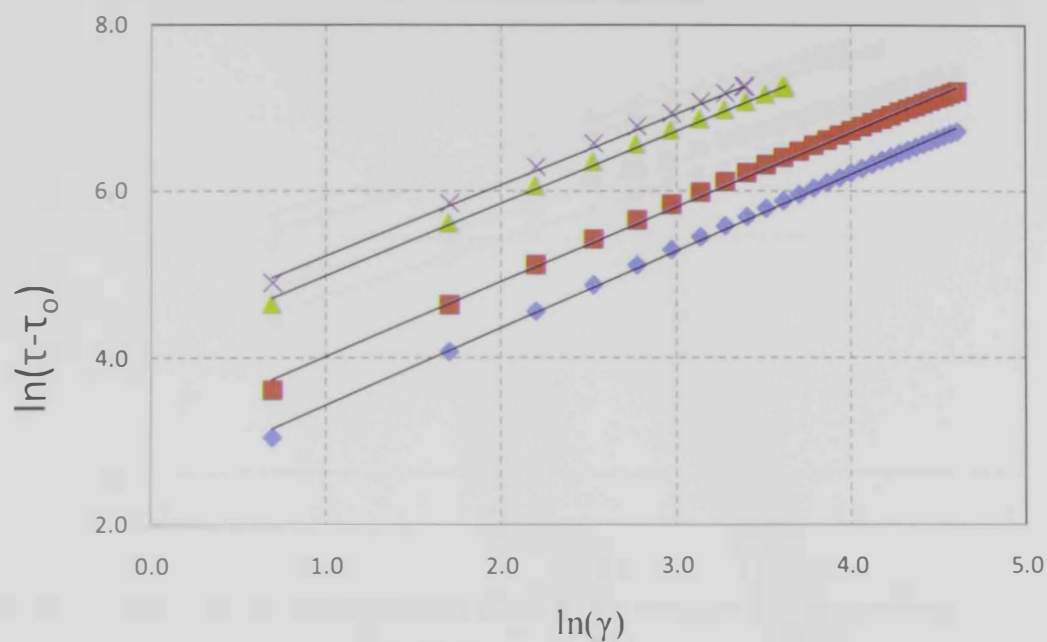


Figure 4. 8: Flow curves of CA solution fitted to the Herschel Bulkley model at $T = 25^{\circ}\text{C}$.

(♦ 0.15 CA, ■ 0.18 CA, ▲ 0.21 CA, ✕ 0.24 CA, — H.B model)

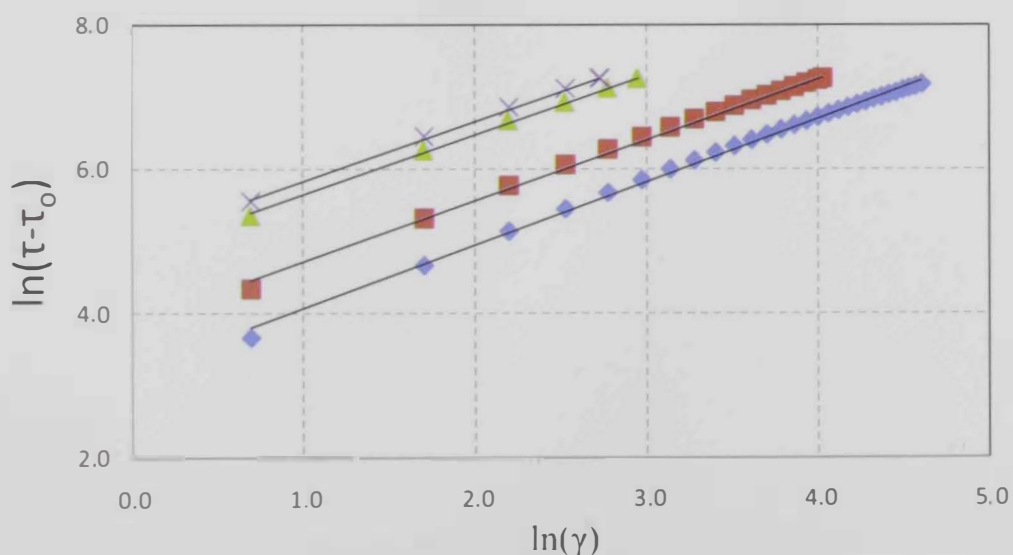


Figure 4. 9: Flow curves of CA solution fitted to the Herschel Bulkley model at $T = 35^{\circ}\text{C}$.

(♦ 0.15 CA, ■ 0.18 CA, ▲ 0.21 CA, ✕ 0.24 CA, — H.B model)

4. Effect of Temperature, Composition and Shear Rate on CA / DMAc Solution Viscosity

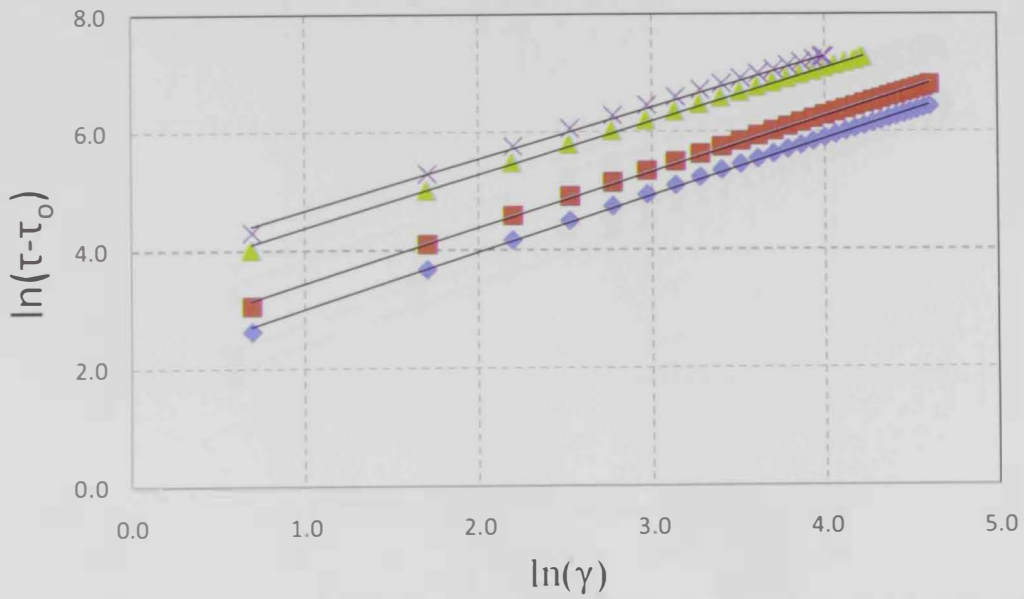


Figure 4. 10: Flow curves of CA solution fitted to the Herschel Bulkley model at $T = 45^\circ\text{C}$.

(• 0.15 CA, ■ 0.18 CA, ▲ 0.21 CA, ✕ 0.24 CA, — H.B model)

4. Effect of Temperature, Composition and Shear Rate on CA /DMAc Solution Viscosity

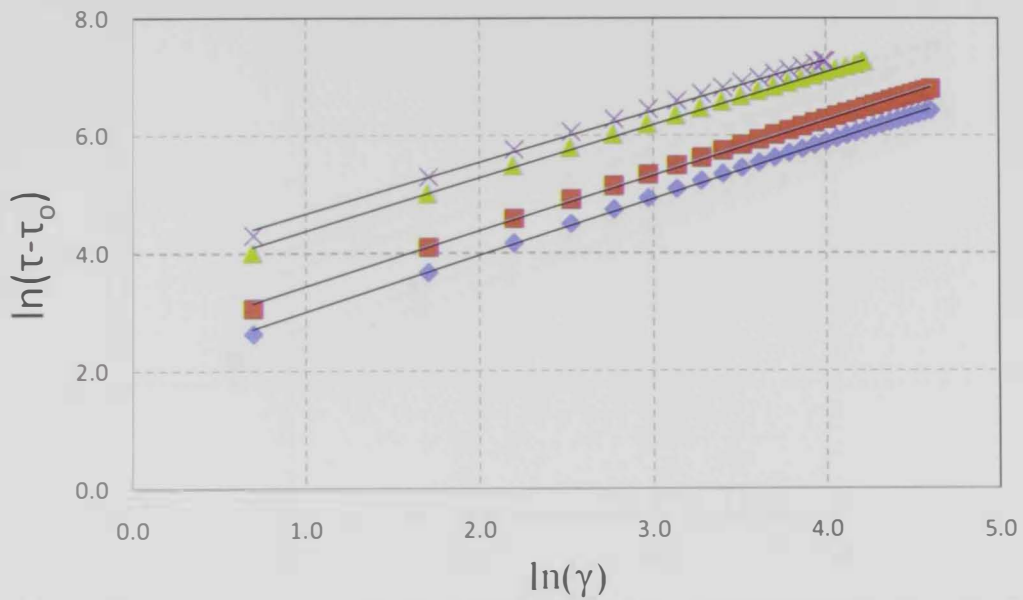


Figure 4. 10: Flow curves of CA solution fitted to the Herschel Bulkley model at $T = 45^\circ\text{C}$.

(♦ 0.15 CA, ■ 0.18 CA, ✕ 0.21 CA, ▲ 0.24 CA, — H.B model)

4. Effect of Temperature, Composition and Shear Rate on CA /DMAc Solution Viscosity

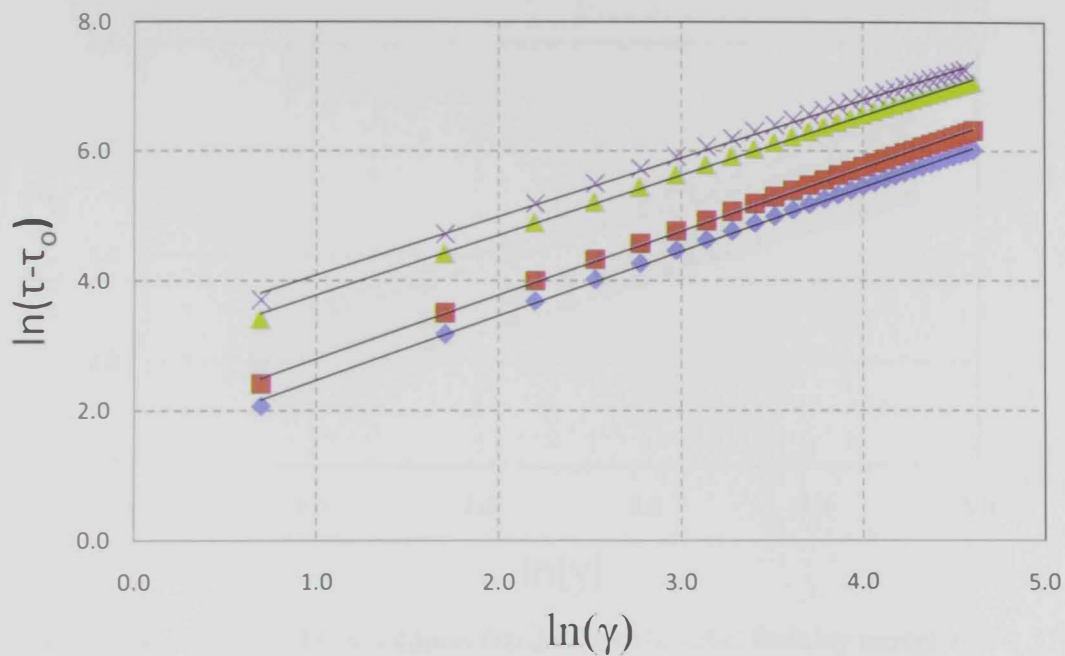


Figure 4. 11: Flow curves of CA solution fitted to the Herschel Bulkley model at T = 55°C.

(• 0.15 CA, ■ 0.18 CA, ▲ 0.21 CA, × 0.24 CA, — H.B model)

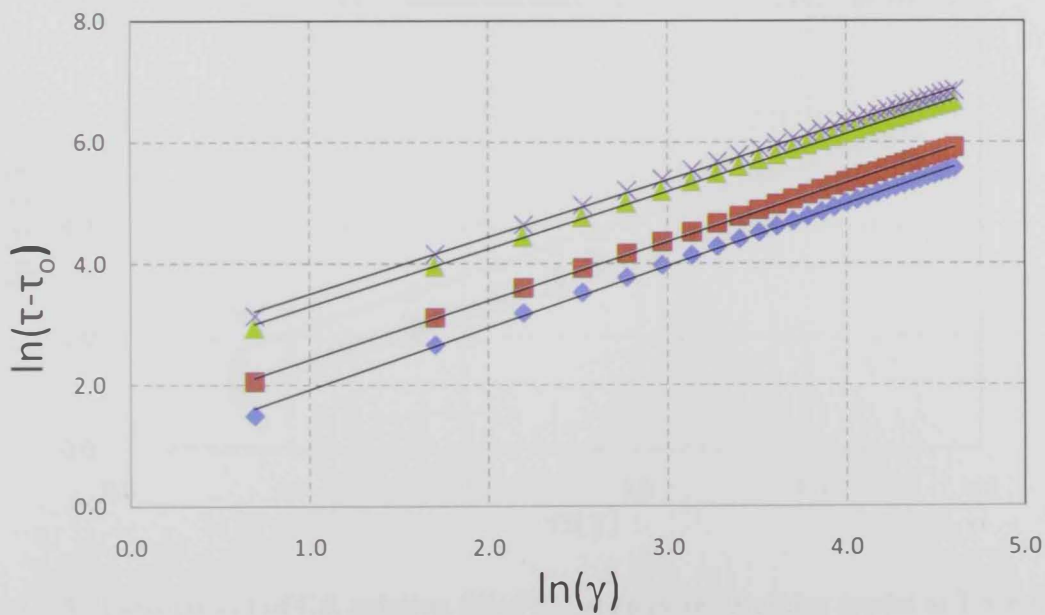


Figure 4. 12: Flow curves of CA solution fitted to the Herschel Bulkley model at T = 65°C.

(• 0.15 CA, ■ 0.18 CA, ▲ 0.21 CA, × 0.24 CA, — H.B model)

4. Effect of Temperature, Composition and Shear Rate on CA /DMAc Solution Viscosity

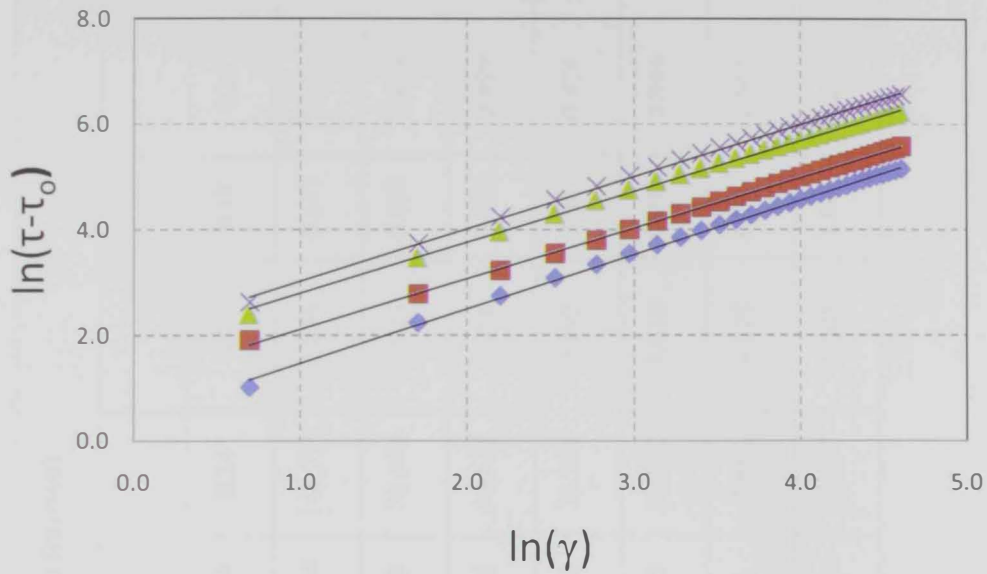


Figure 4. 13: Flow curves of CA solution fitted to the Herschel Bulkley model at T = 75°C.

(• 0.15 CA, ■ 0.18 CA, ▲ 0.21 CA, × 0.24 CA, — H.B model)

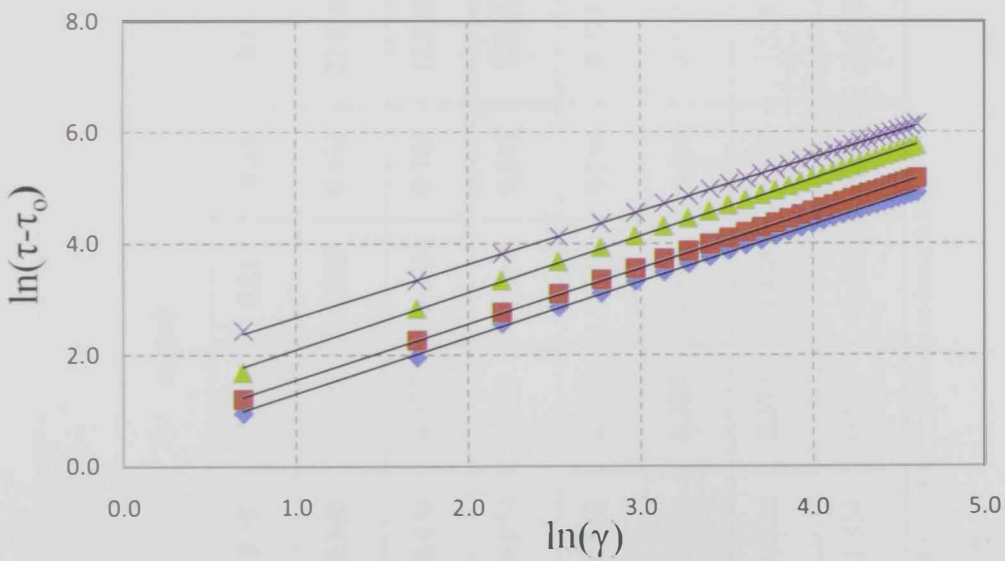


Figure 4. 14: .Flow curves of CA solution fitted to the Herschel Bulkley model at T = 85°C.

(• 0.15 CA, ■ 0.18 CA, ▲ 0.21 CA, × 0.24 CA, — H.B model)

Table4. 1: Parameters of Herschel Bulkley model for cellulose acetate prepared at different temperatures.

Temperature (°C)	*CA Concentration (mass fraction)											
	τ_0 (pa)				m (pa.s ⁿ)				n			
	0.15	0.18	0.21	0.24	0.15	0.18	0.21	0.24	0.15	0.18	0.21	0.24
25	0.100	0.230	0.356	0.432	22.966	48.038	123.594	148.710	0.876	0.843	0.826	0.826
35	0.170	0.912	0.230	0.786	12.244	22.533	61.008	78.649	0.924	0.898	0.869	0.853
45	0.670	0.463	0.214	0.947	7.714	12.110	32.266	44.434	0.958	0.939	0.899	0.871
55	0.872	0.734	0.785	0.254	4.371	6.104	17.305	24.216	0.992	0.983	0.924	0.901
65	0.756	0.375	0.638	0.384	2.472	4.212	10.465	12.962	1.019	0.973	0.946	0.938
75	0.845	0.375	1.436	1.657	1.550	3.171	6.278	7.652	1.028	0.957	0.961	0.988
85	1.534	0.575	1.465	0.684	1.344	1.719	2.915	5.557	1.008	1.006	1.023	0.956

*R², the coefficient of determination is at least 0.99.

4. Effect of Temperature, Composition and Shear Rate on CA /DMAc Solution Viscosity

The thermal properties of polymers include their behavior during heating (105). The effect of temperature on the rheological behavior of the polymers solutions was also studied. A decrease in viscosity was produced when the temperature increased. The influences of this are shown in Figures 15-17. Experiments showed a deviation from linear behavior. This effect decreased when the temperature and shear rate increased in value.

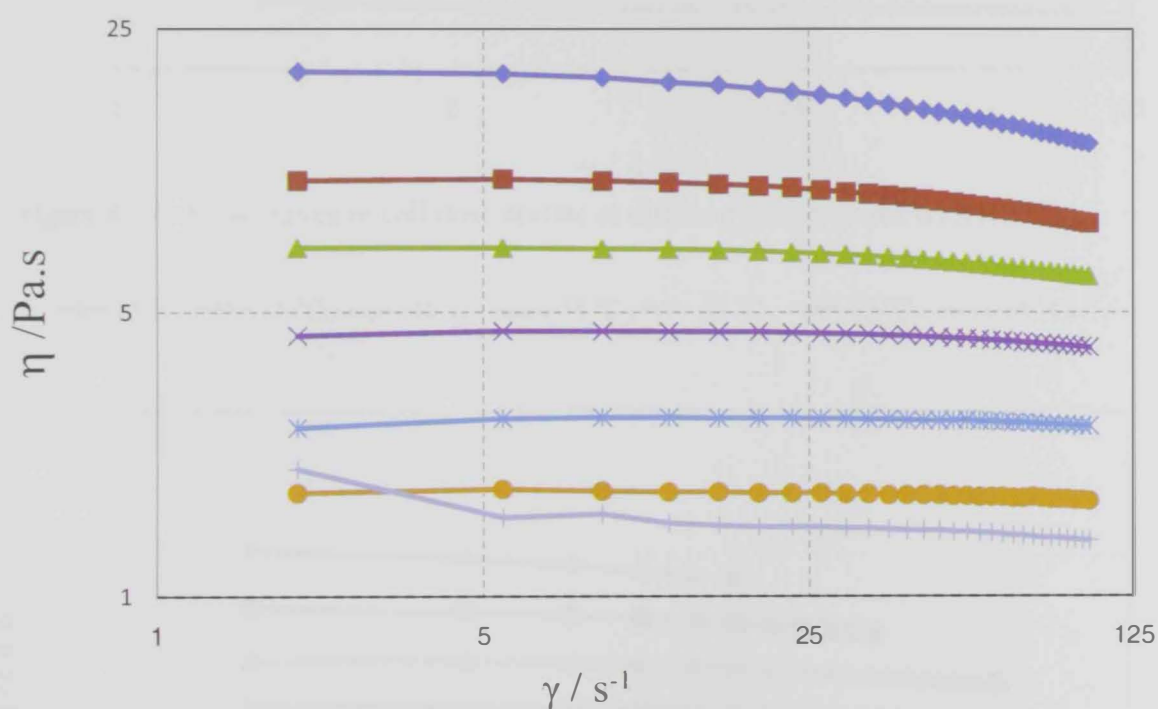


Figure 4. 15: Flow curves of cellulose acetate at different temperatures with 0.15 CA.

(\blacklozenge 25 °C, \blacksquare 35 °C, \blacktriangle 45 °C, \times 55 °C, \ast 65 °C, \bullet 75 °C, \oplus 85 °C)

4. Effect of Temperature, Composition and Shear Rate on CA /DMAc Solution Viscosity

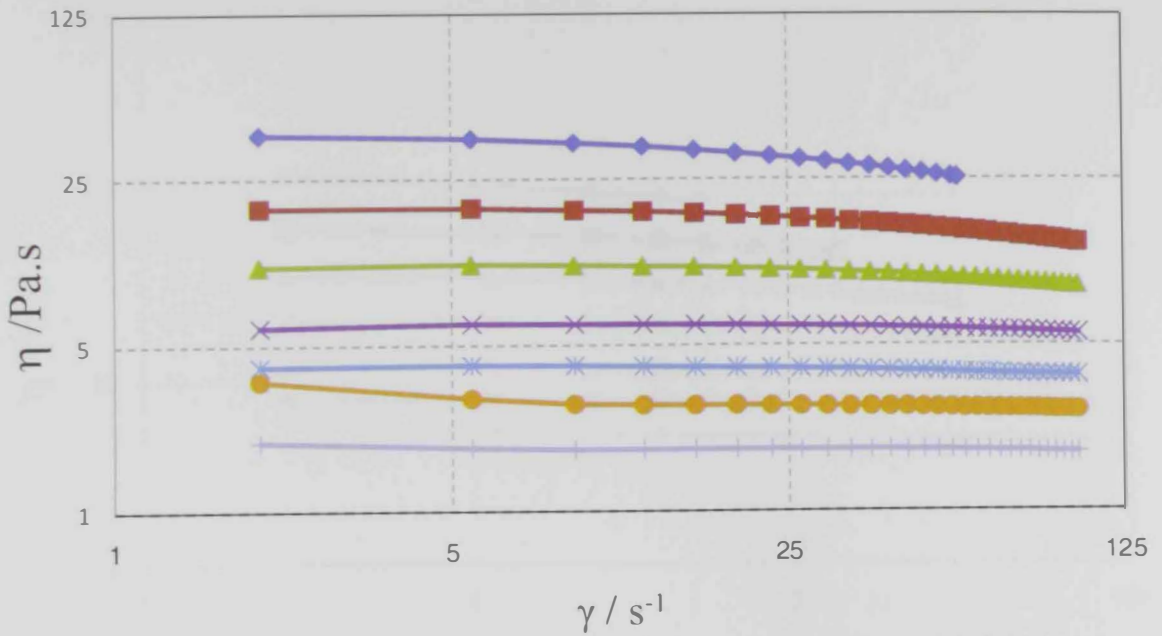


Figure 4. 16: Flow curves of cellulose acetate at different temperatures with 0.18 CA.

(—◆— 25 °C, —■— 35 °C, —▲— 45 °C, —×— 55 °C, —*— 65 °C, —●— 75 °C, —+— 85 °C)

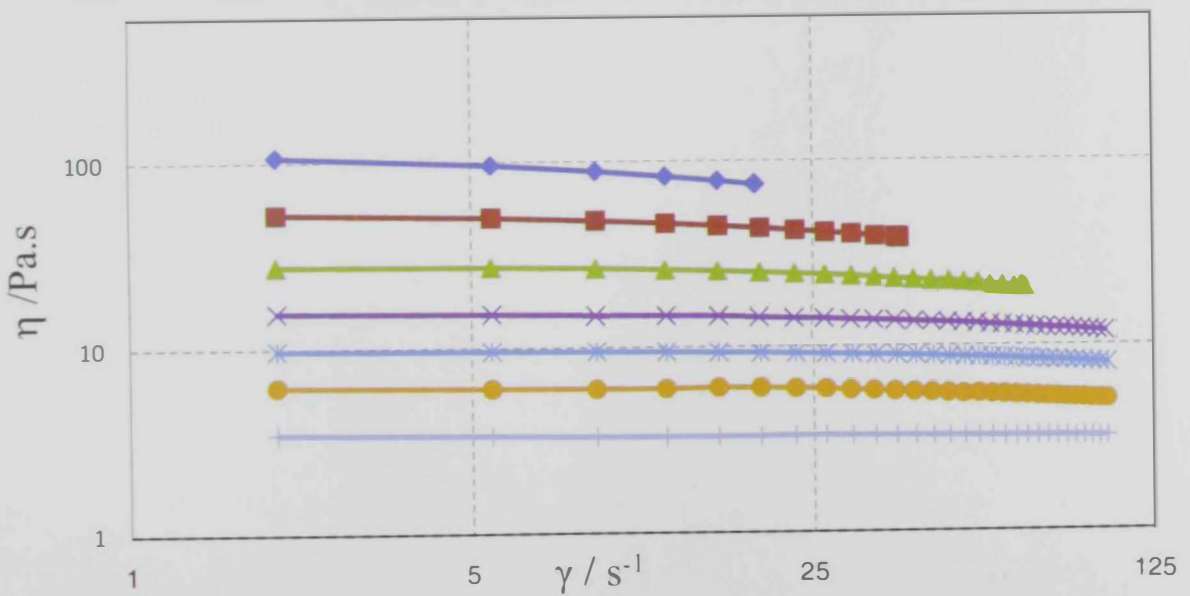


Figure 4. 17: Flow curves of cellulose acetate at different temperatures with 0.21 CA.

(—◆— 25 °C, —■— 35 °C, —▲— 45 °C, —×— 55 °C, —*— 65 °C, —●— 75 °C, —+— 85 °C)

4. Effect of Temperature, Composition and Shear Rate on CA /DMAc Solution Viscosity

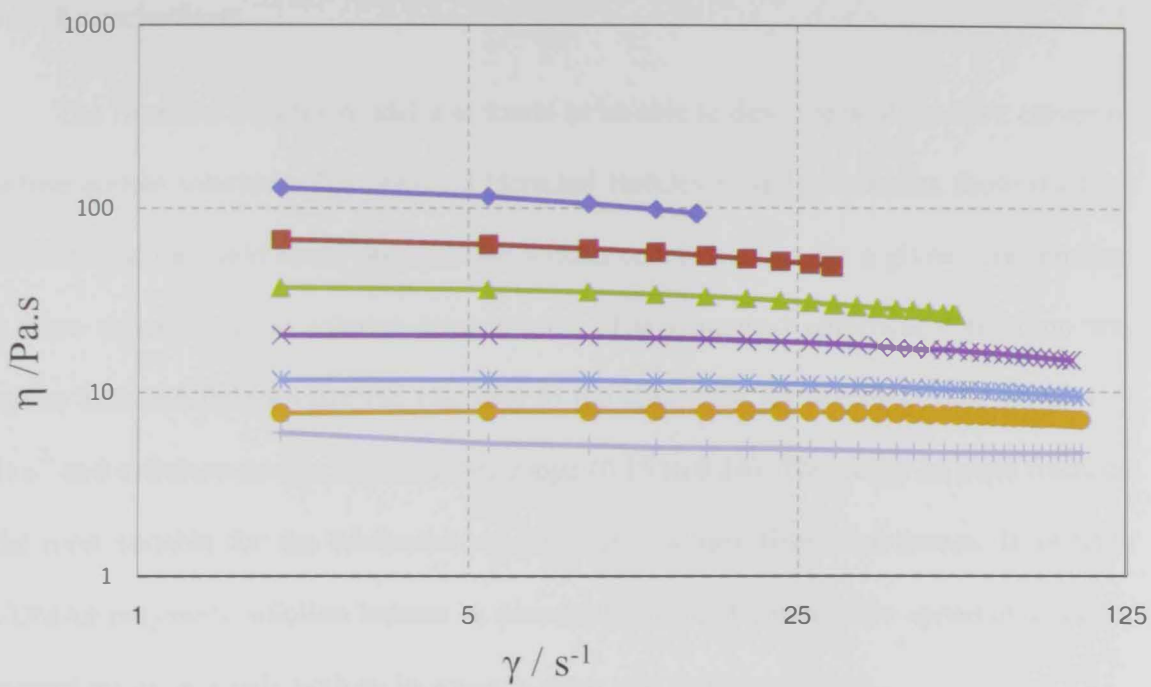


Figure 4. 18: Flow curves of cellulose acetate at different temperatures with 0.24 CA.

(\blacklozenge 25 °C, \blacksquare 35 °C, \blacktriangle 45 °C, \blackcross 55 °C, \ast 65 °C, \bullet 75 °C, \oplus 85 °C)

4.3. Conclusions

The Herschel Bulkley model was found to be able to describe well the flow curves of cellulose acetate solutions. The obtained Herschel Bulkley model parameters showed a high dependence of the yield stress on cellulose acetate concentrations for a given concentration and more dependence on solution temperatures. The generated empirical correlation was found to successfully correlate the viscosity to the shear rate for the shear rate range (1 to 125) s^{-1} and cellulose acetate mass fraction range (0.15 to 0.24). This range of mass fractions is the most suitable for the fabrication of polymeric hollow fiber membranes. In general, CA/DMAc polymeric solution behave as pseudoplastic fluids, where the apparent viscosity decreased instantaneously with an increase in shear rate and temperature.

Chapter Five: Effect of Cellulose Acetate Concentration and Dope Solution Flow Rate.

In this chapter the effect of cellulose acetate concentration and dope solution flow rate on fabricated fibers were discussed. Cellulose acetate/ DMAc mixtures were used for spinning hollow fibers using a non-solvent induced phase separation. Polymer dope solutions were prepared from different concentrations of cellulose acetate (15, 18, 21 and 24% CA) at different dope solution flows. The fabricated fibers were characterized by SEM, water permeability, water contact angle and stress/strain behavior.

5.1. Introduction

Improving membrane flux and rejection is not easy because there are many factors play a role in improving membrane performance such as the type of polymer, polymer composition, temperature of coagulant bath and dope solution concentration. Polymer concentration is important in study of the membrane characterized and also the same for the solvent used in spinning solution. In addition higher polymer concentration is needed in order to induce chain entanglement so that the formation of macrovoid in the skin layer is reduced (106). Study of the effect of cellulose acetate concentration and dope solution velocity was investigated in this chapter.

5.2. SEM Micrographs

SEM micrographs of membrane cross section were shown in Figures 5.1-5.16. These micrographs present SEM structure for different concentrations and dope solution flow rates.

SEM pictures for 15% CA/DMAc at different dope solution flow rate are shown in Figures 5.1-5.4 micrographs show the finger-like shape with sponge-like layer, the finger became shorter with increasing the flow rate of polymer solution. From Figures 5.5-5.8 show that the finger like structure became shorter and shorter with increased the polymer solution flow rate.

Figures 5.9-5.12 show the effect of dope solution flow rate at 21% CA on the structure of fabricated hollow fiber membranes. The micrographs show, as the dope solution flow rate was increased the finger-like shape shrunk at fixed time. Porosity increased with increasing concentration of dope polymer solution. Figures 5.13-5.16 indicate that sponge layer became more porous because more polymer coagulant.

Regarding the effect of polymer concentration (i.e. %CA in the cast solution) it was observed that the highly concentrated polymer solutions resulted in tight structure. This is attributed to the fact that increasing concentration of polymer in casting solution suppress the formation of macro-voids in membranes prepared by NIPS process. It was also observed that slow rate of membrane formation resulted in sponge-like structure; by contrast, finger-like structure was produced at high membrane formation rates.

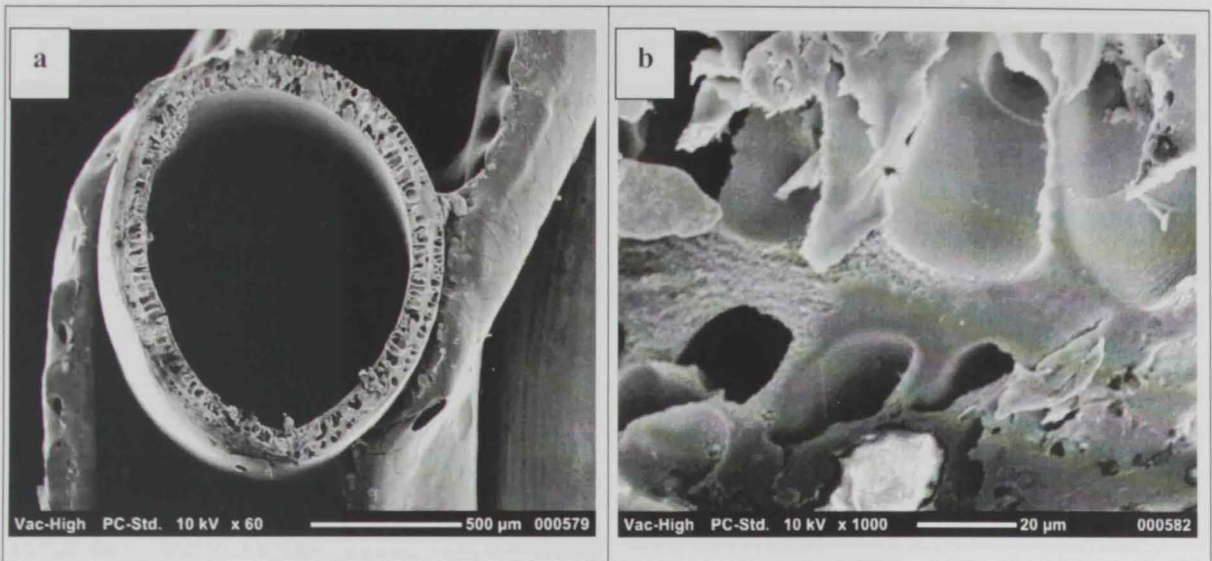


Figure 5. 1: SEM micrographs of 15% CA fiber at dope solution flow rate = 6 (g/min)
a) Whole cross section b) higher magnification of cross section

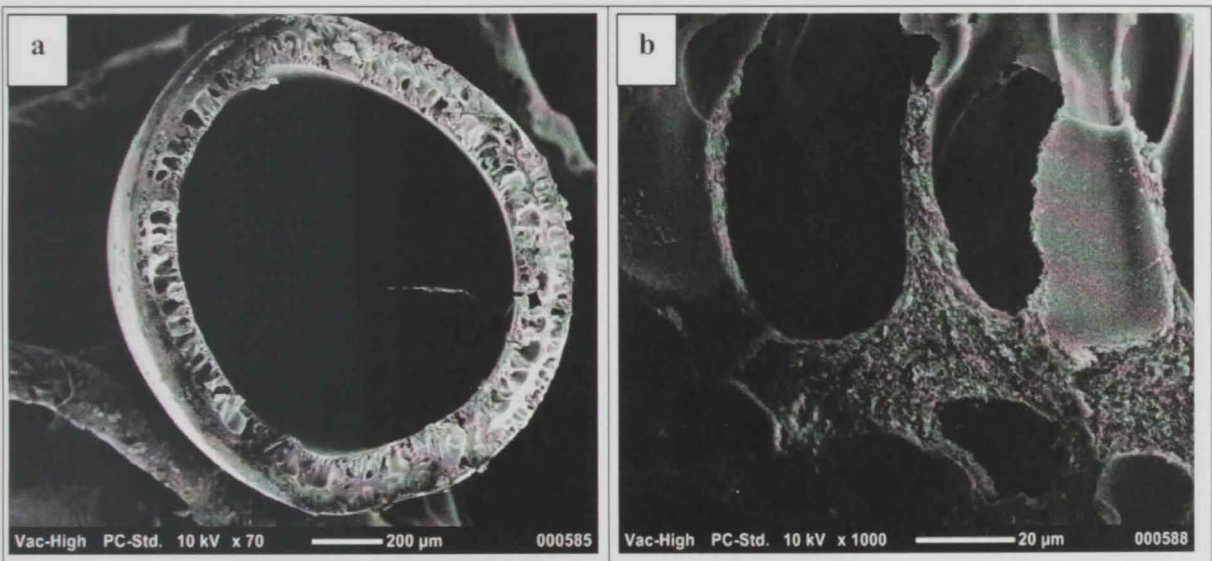


Figure 5.2: SEM micrographs of 15% CA fiber at dope solution flow rate = 7.5 (g/min)
a) Whole cross section b) higher magnification of cross section

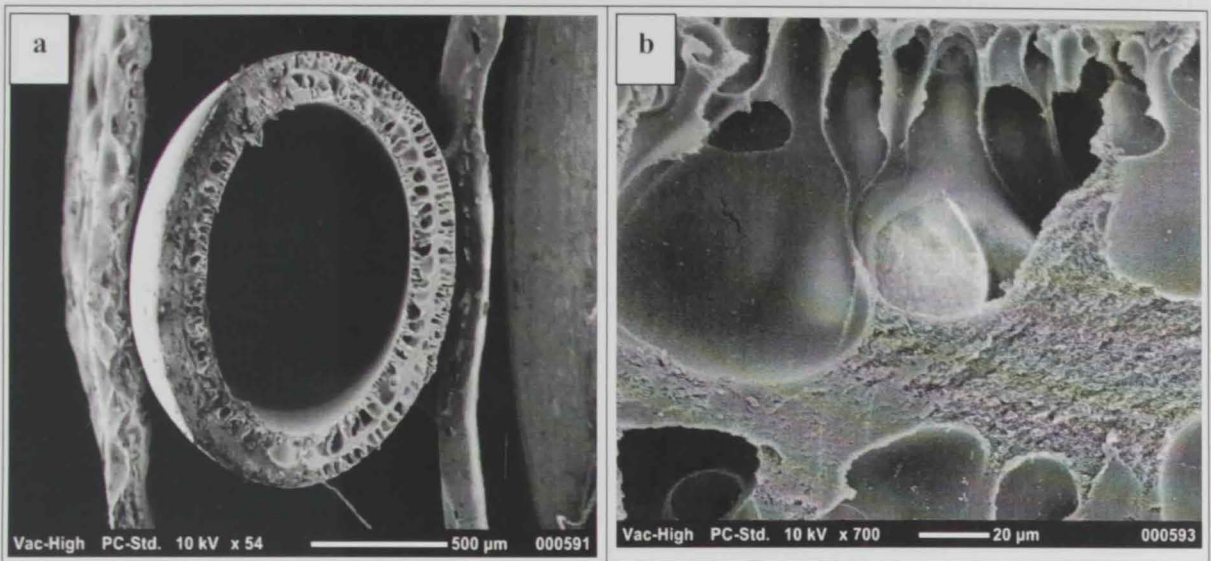


Figure 5.3: SEM micrographs of 15% CA fiber at dope solution flow rate = 9 (g/min)

a) Whole cross section b) higher magnification of cross section

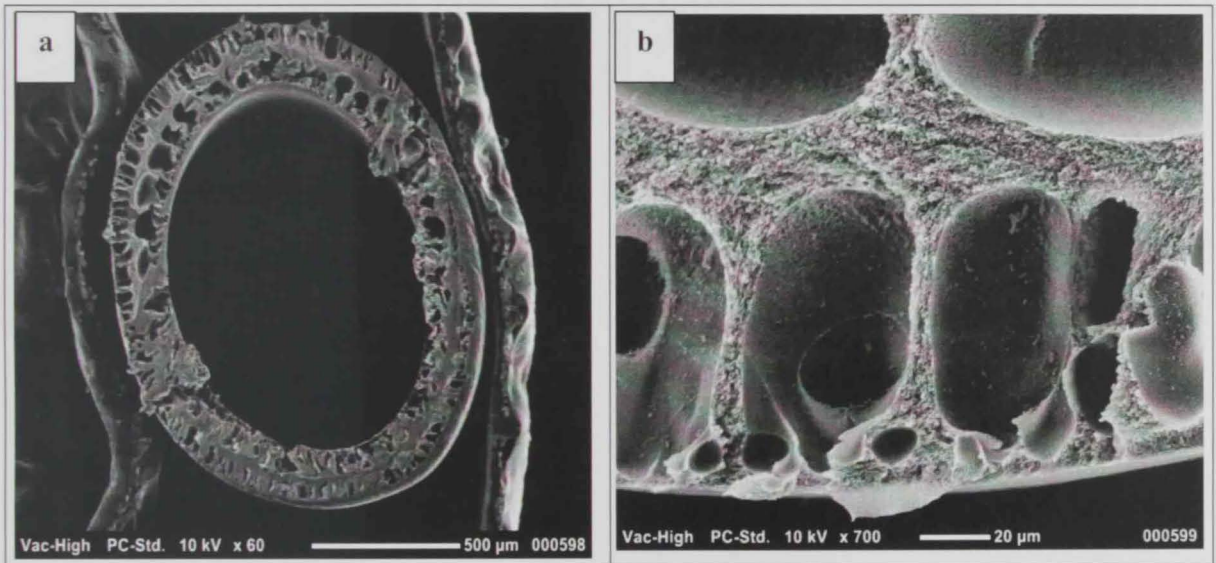


Figure 5.4: SEM micrographs of 15% CA fiber at dope solution flow rate = 10.5 (g/min)

a) Whole cross section b) higher magnification of cross section

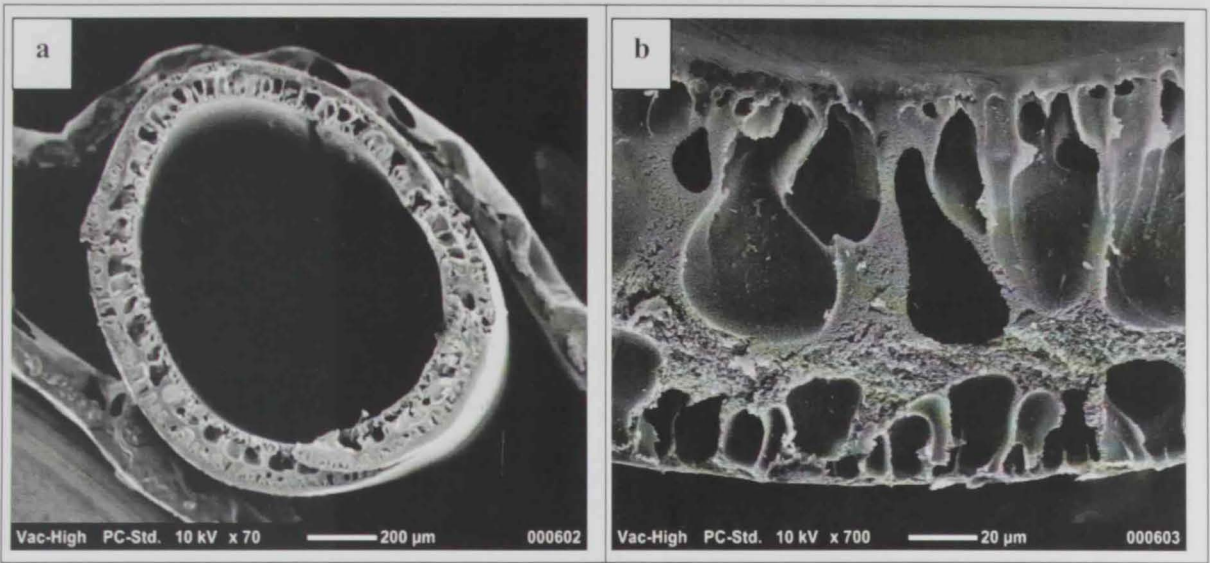


Figure 5.5: SEM micrographs of 18% CA fiber at dope solution flow rate = 6 (g/min)
a) Whole cross section b) higher magnification of cross section

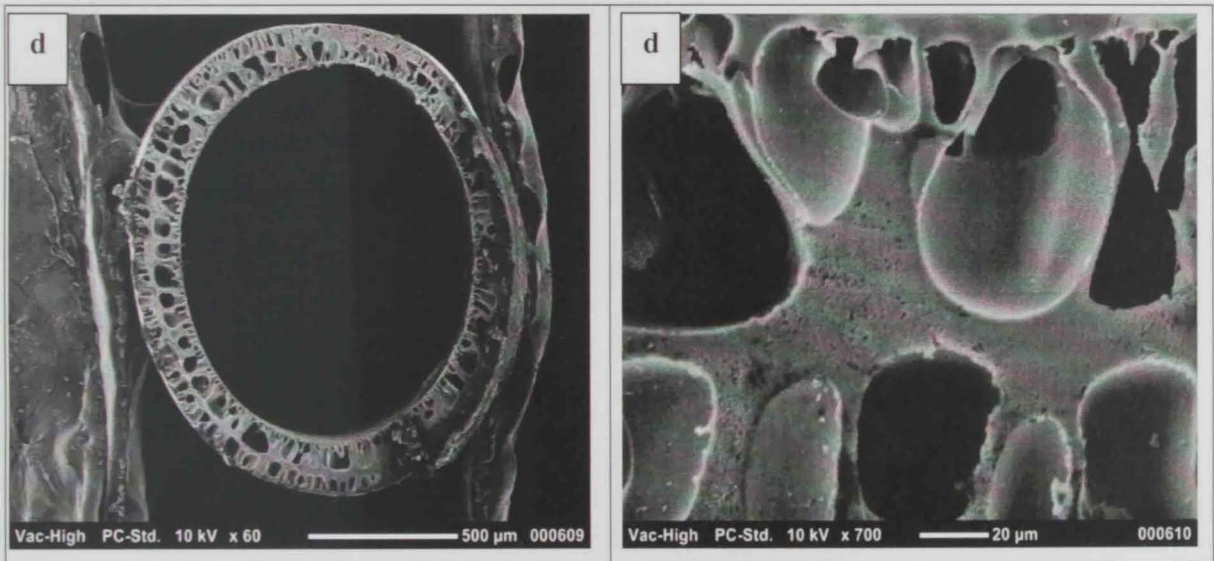


Figure 5.6: SEM micrographs of 18% CA fiber at dope solution flow rate = 7.5 (g/min)
a) Whole cross section b) higher magnification of cross section

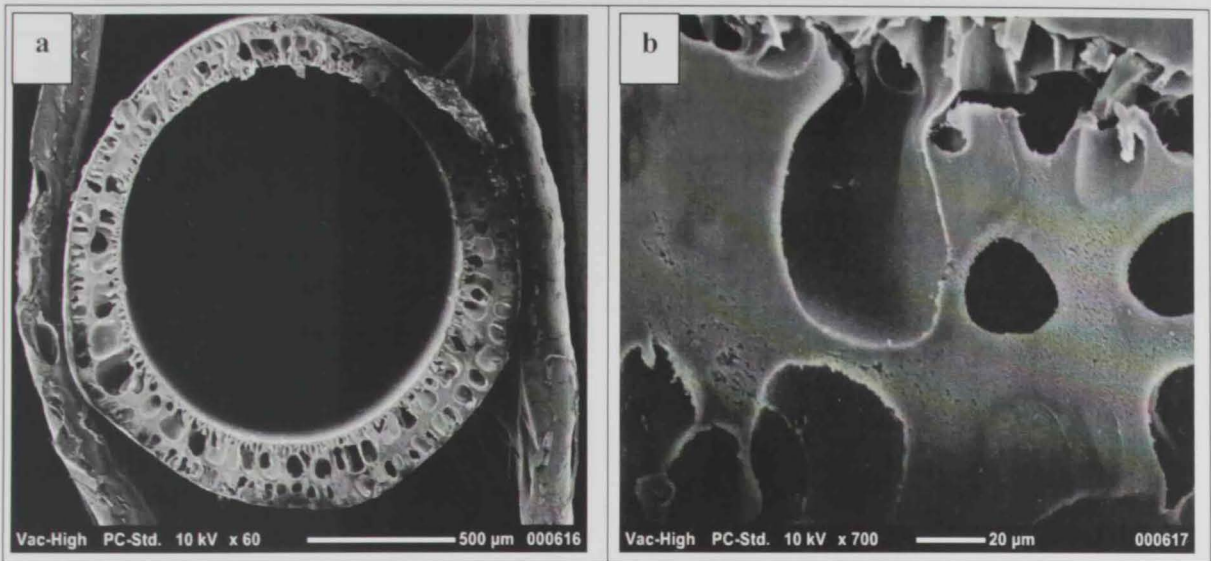


Figure 5.7: SEM micrographs of 18% CA fiber at dope solution flow rate = 9 (g/min)
a) Whole cross section b) higher magnification of cross section

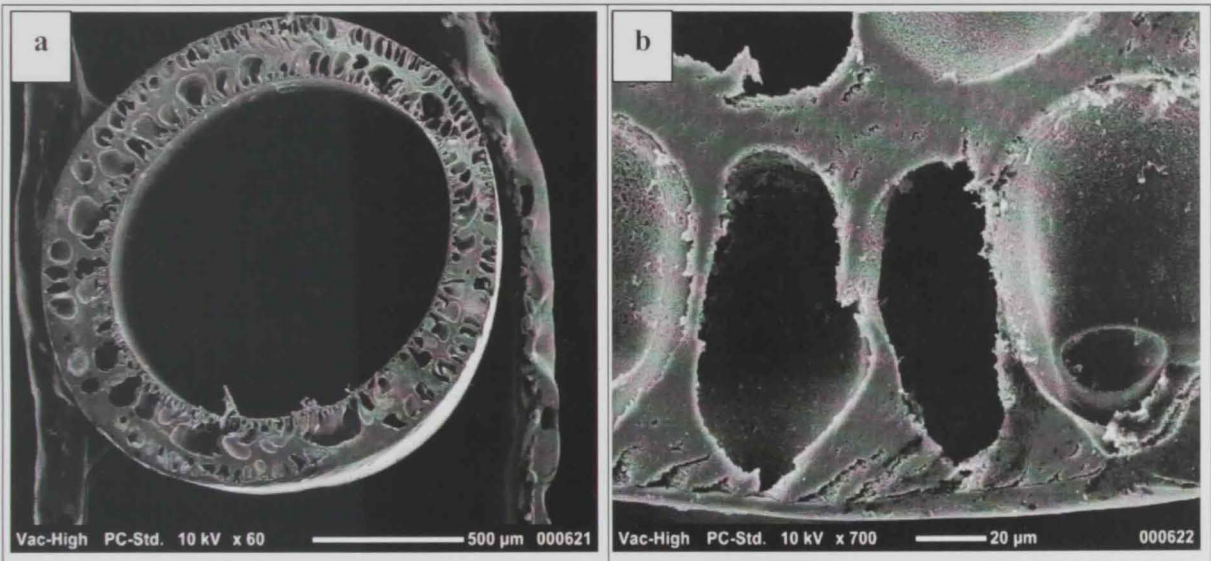


Figure 5.8: SEM micrographs of 18% CA fiber at dope solution flow rate = 10.5 (g/min)
a) Whole cross section b) higher magnification of cross section

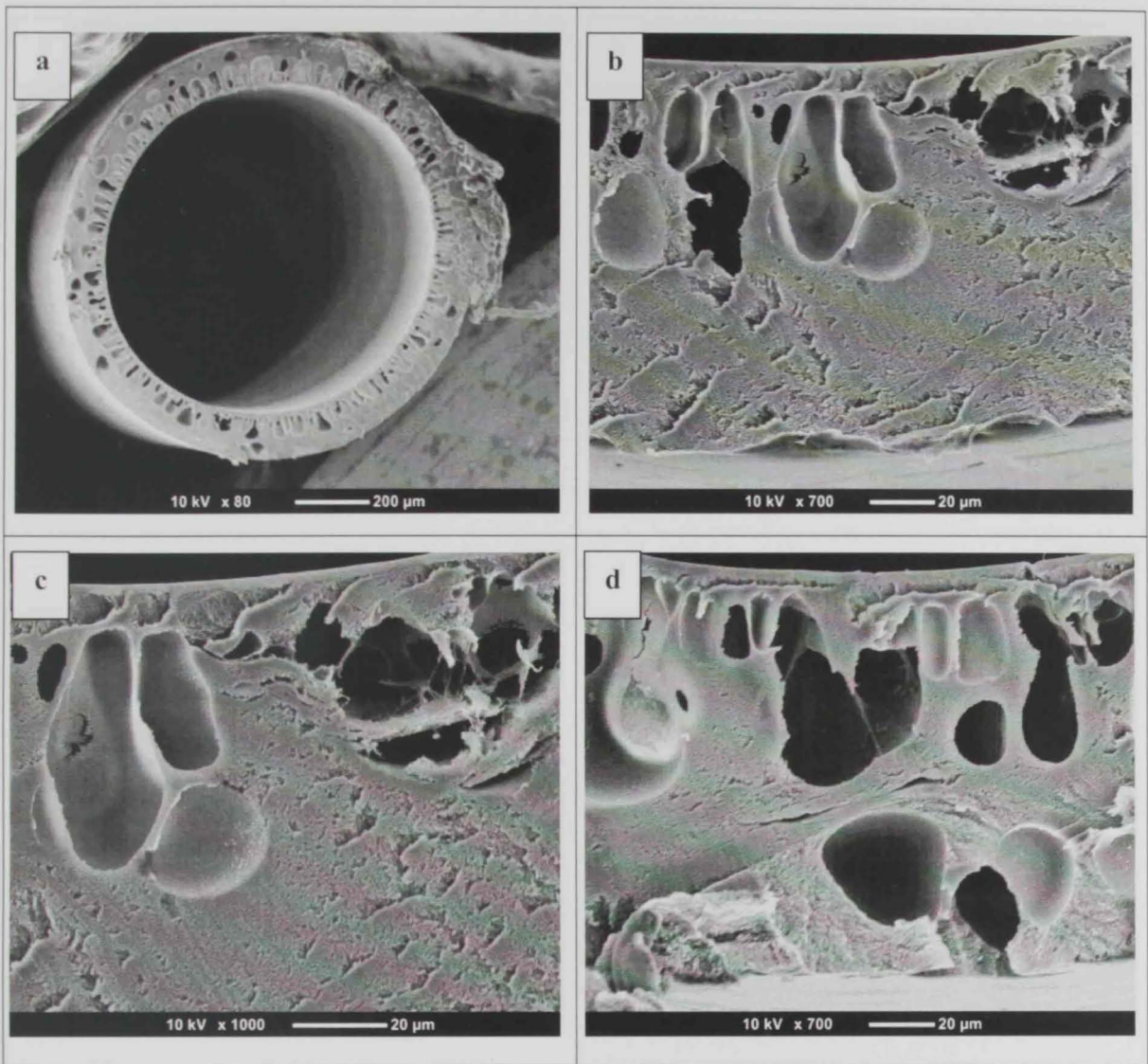


Figure 5.9: SEM micrographs of 21% CA fiber at dope solution flow rate = 6 (g/min)

- a) Whole cross section
- b) higher magnification of cross section
- c) higher magnification of out edge of the cross section
- d) higher magnification of the inner edge side.

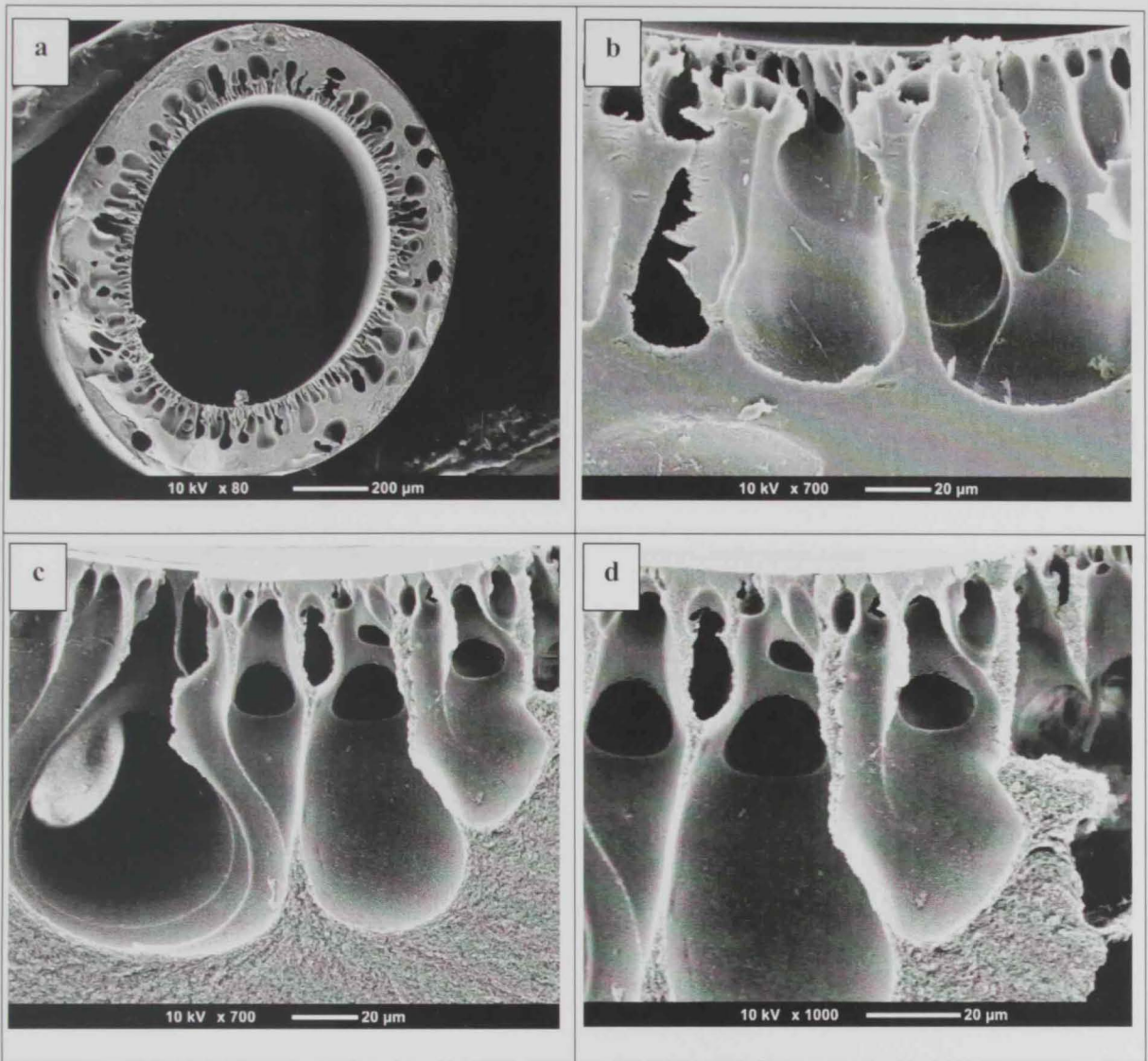


Figure 5.10: SEM micrographs of 21% CA fiber at dope solution flow rate = 7.5 (g/min)

- a) Whole cross section b) higher magnification of cross section c) higher magnification of out edge of the cross section d) higher magnification of the inner edge side.

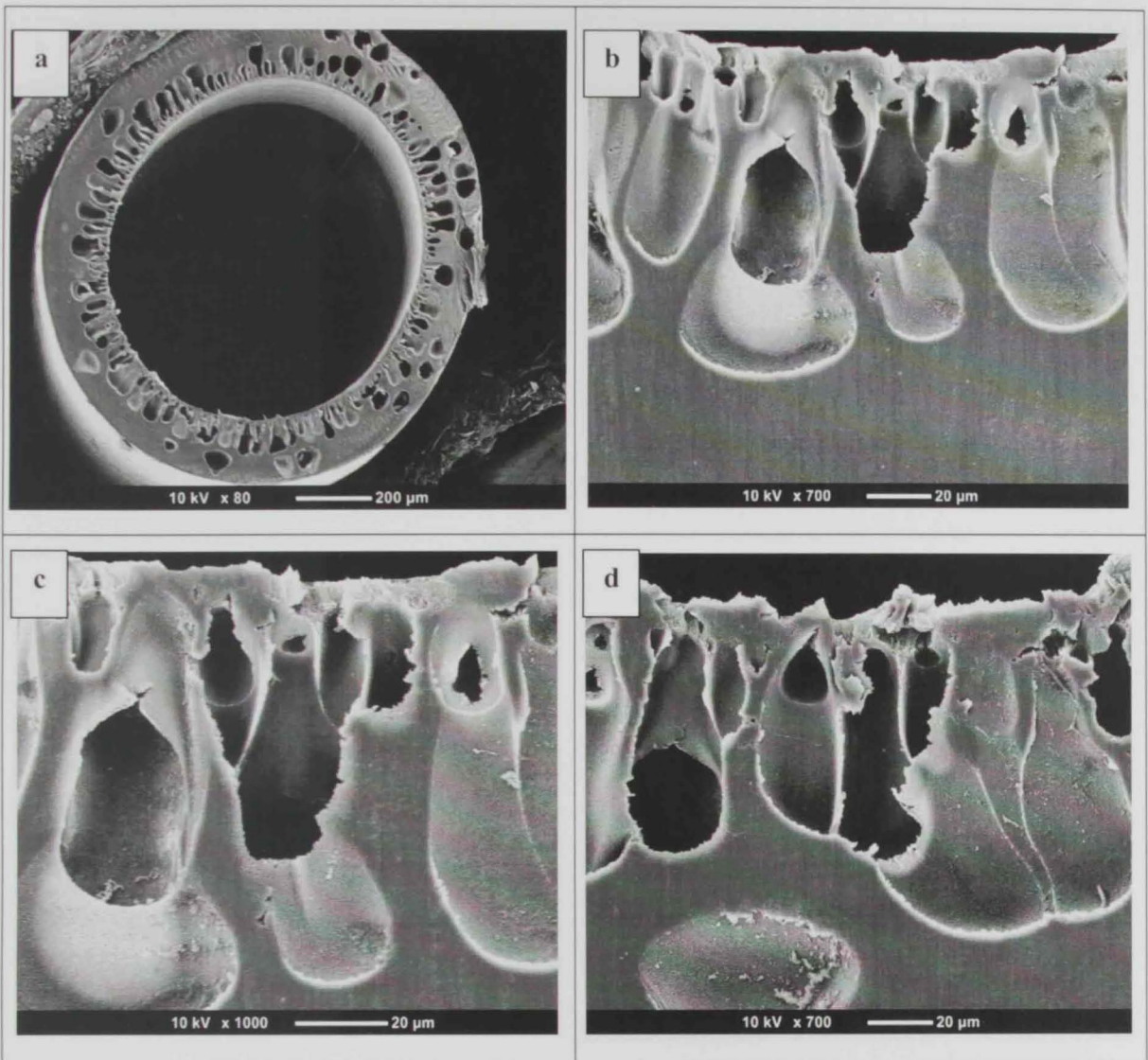


Figure 5.11: SEM micrographs of 21% CA fiber at dope solution flow rate = 9 (g/min)

- a) Whole cross section b) higher magnification of cross section c) higher magnification of out edge of the cross section d) higher magnification of the inner edge side.

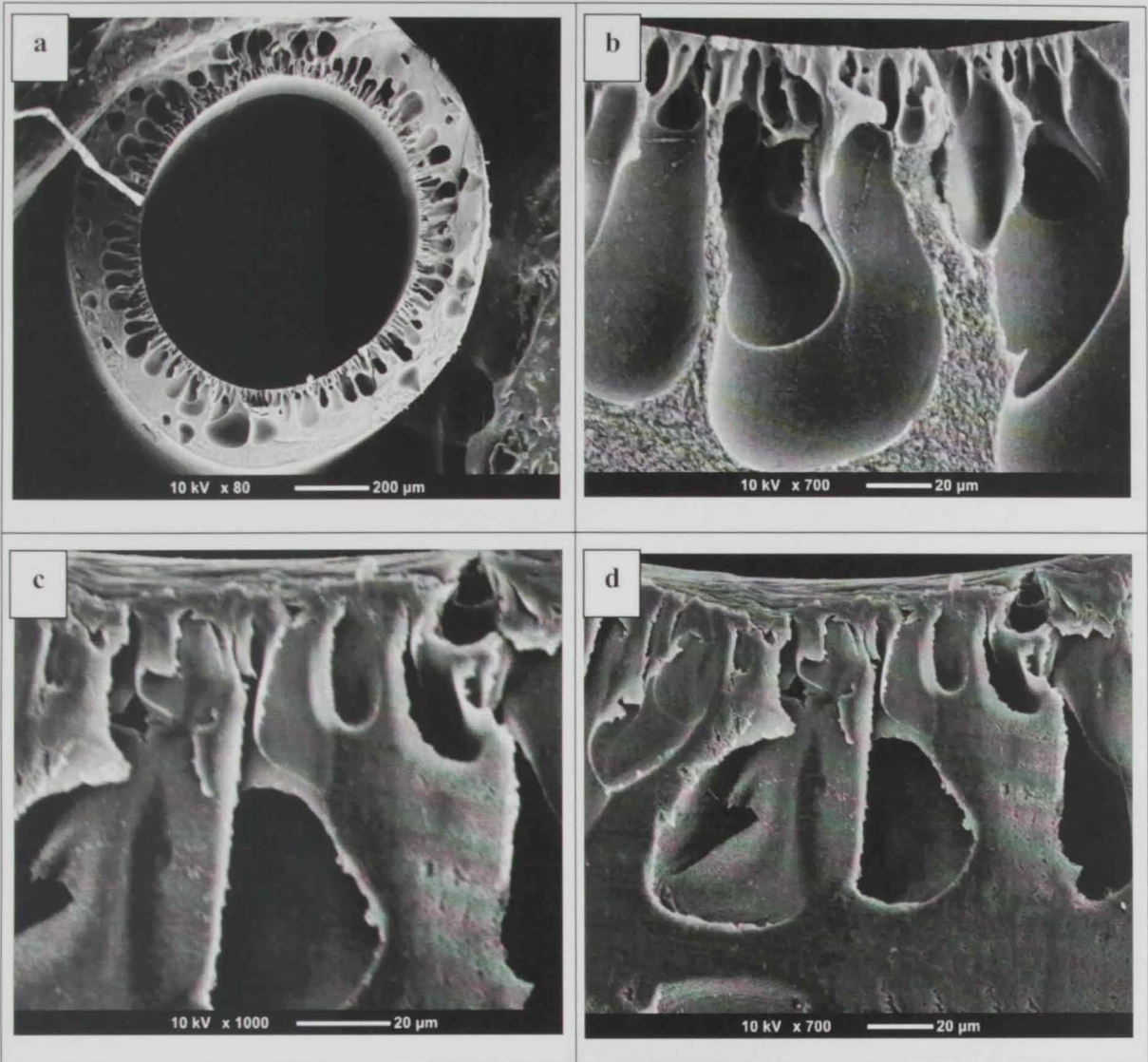


Figure 5.12: SEM micrographs of 21% CA fiber at dope solution flow rate = 10.5 (g/min)

- a) Whole cross section b) higher magnification of cross section c) higher magnification of out edge of the cross section d) higher magnification of the inner edge side.

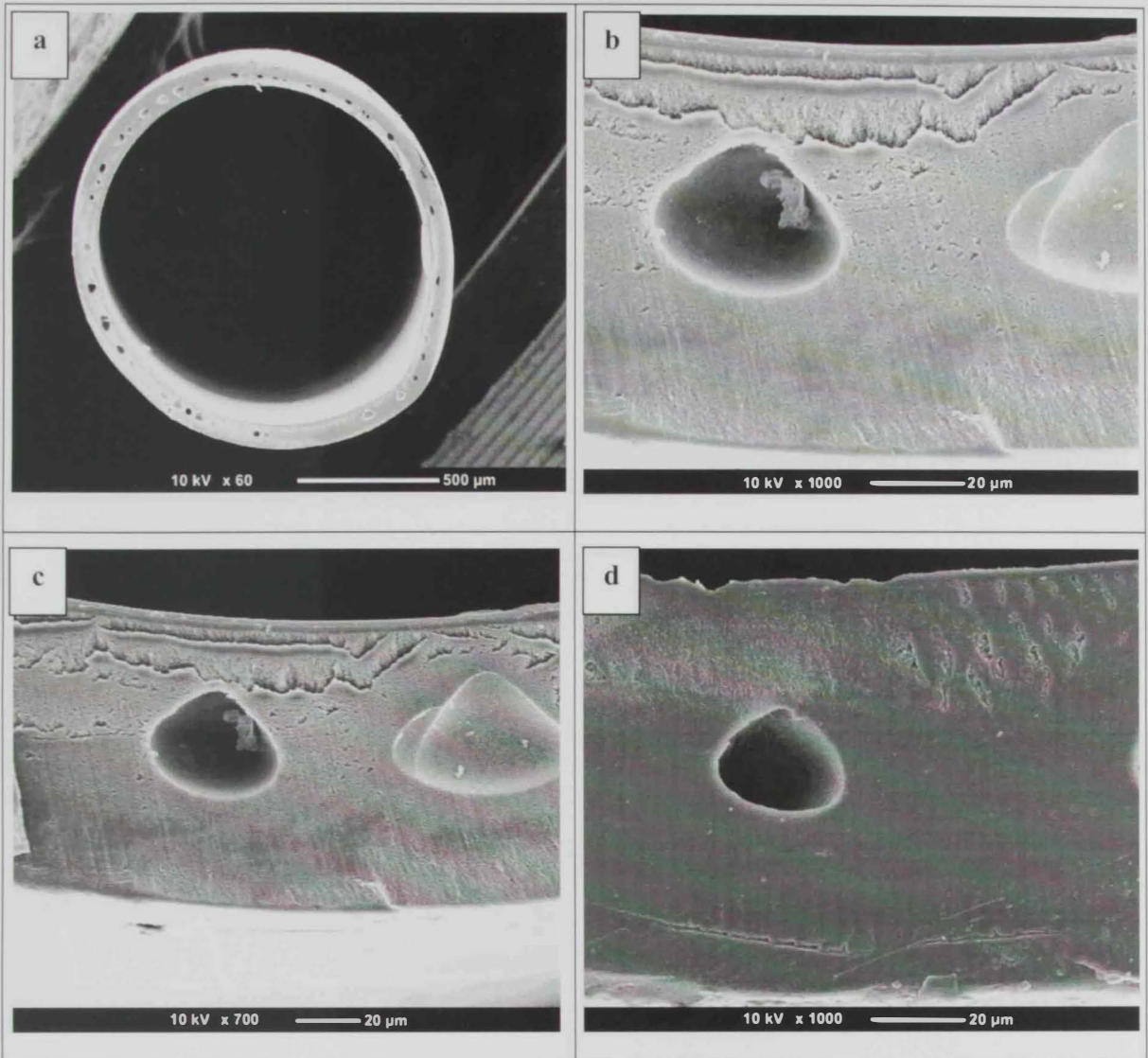


Figure 5.13: SEM micrographs of 24% CA fiber at dope solution flow rate = 6 (g/min)

- a) Whole cross section b) higher magnification of cross section c) higher magnification of out edge of the cross section d) higher magnification of the inner edge side.

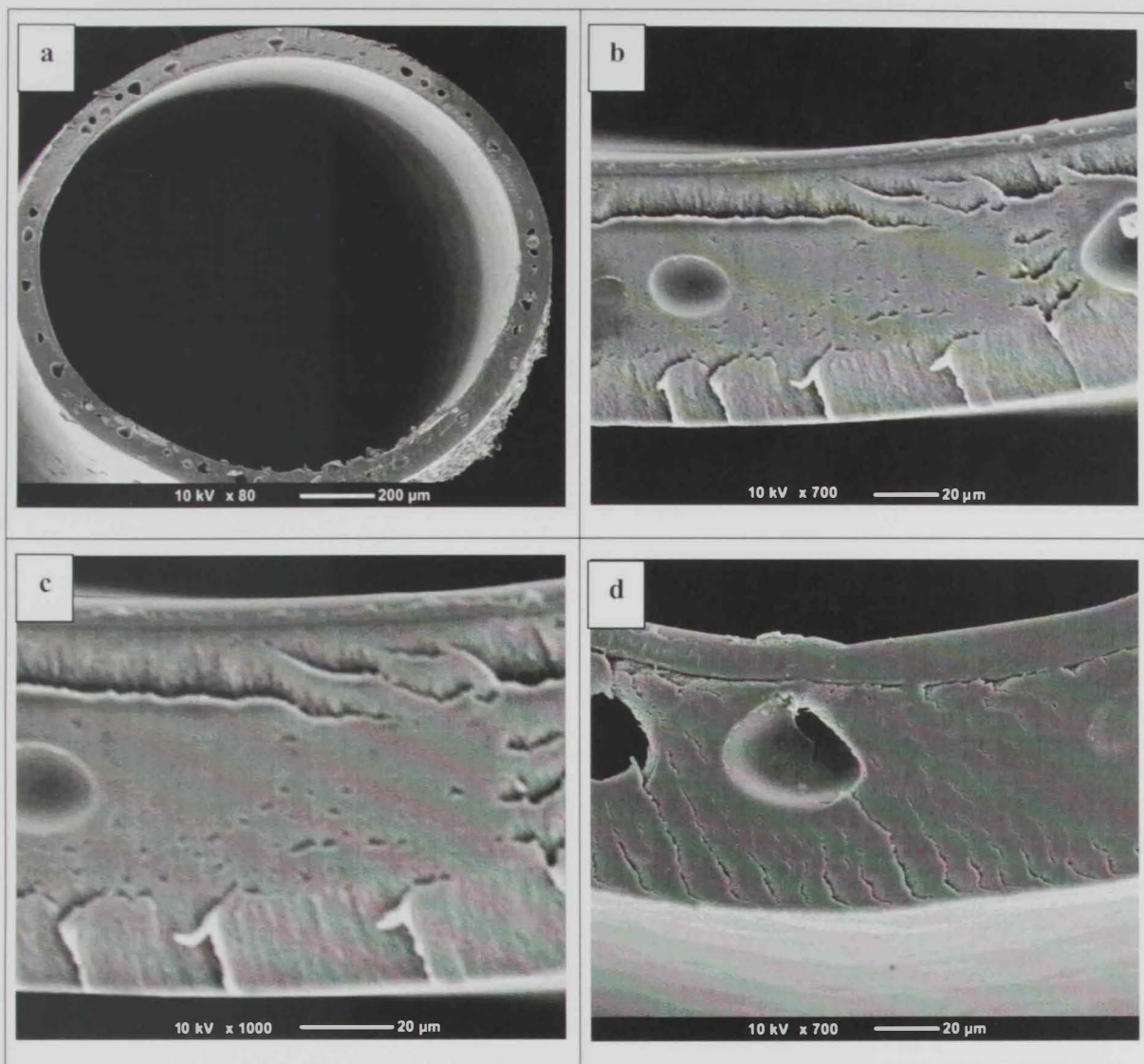


Figure 5.14: SEM micrographs of 24% CA fiber at dope solution flow rate = 7.5 (g/min)

- a) Whole cross section
- b) higher magnification of cross section
- c) higher magnification of out edge of the cross section
- d) higher magnification of the inner edge side.

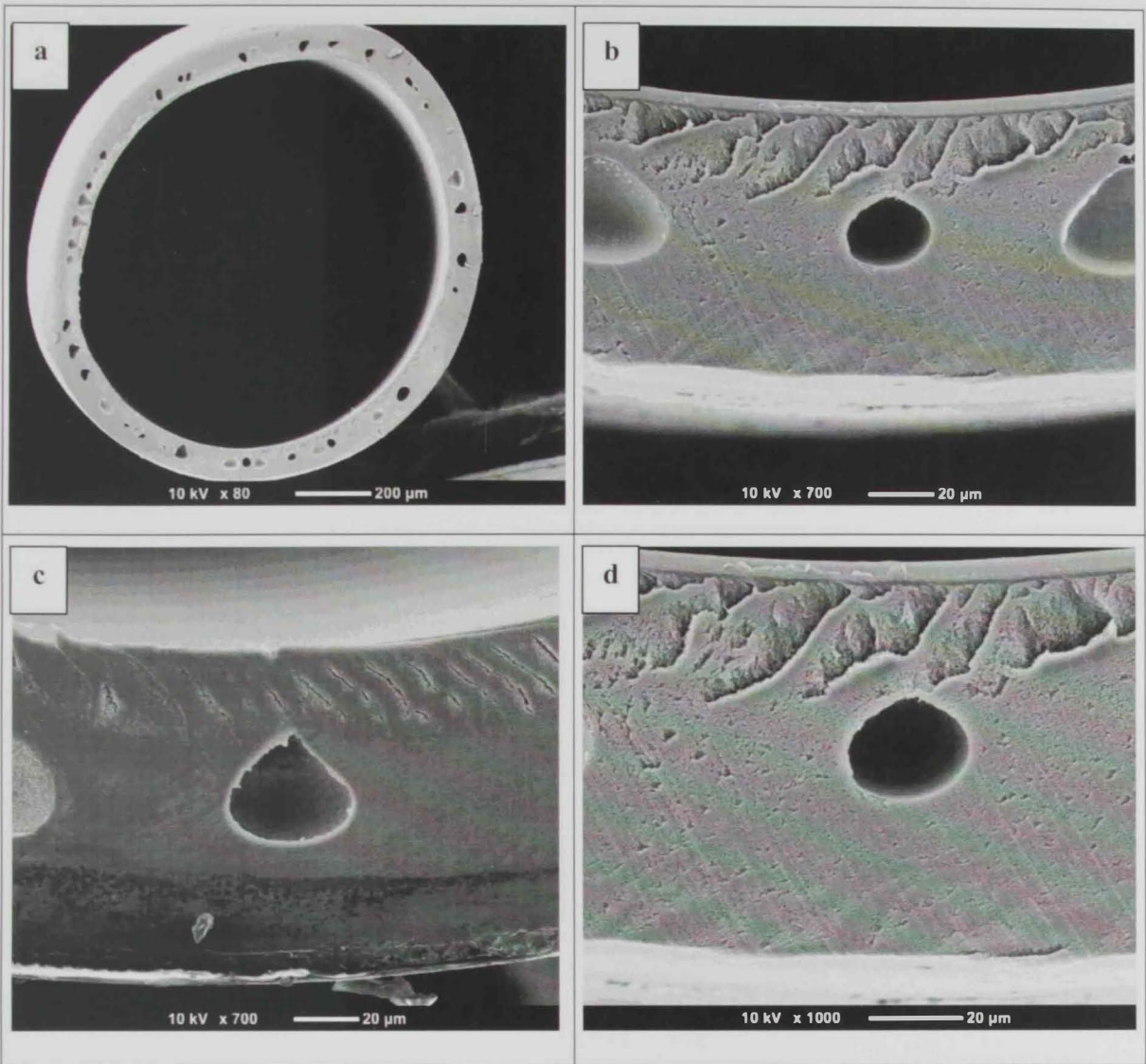


Figure 5.15: SEM micrographs of 24% CA fiber at dope solution flow rate = 9 (g/min)

- a) Whole cross section
- b) higher magnification of cross section
- c) higher magnification of out edge of the cross section
- d) higher magnification of the inner edge side.

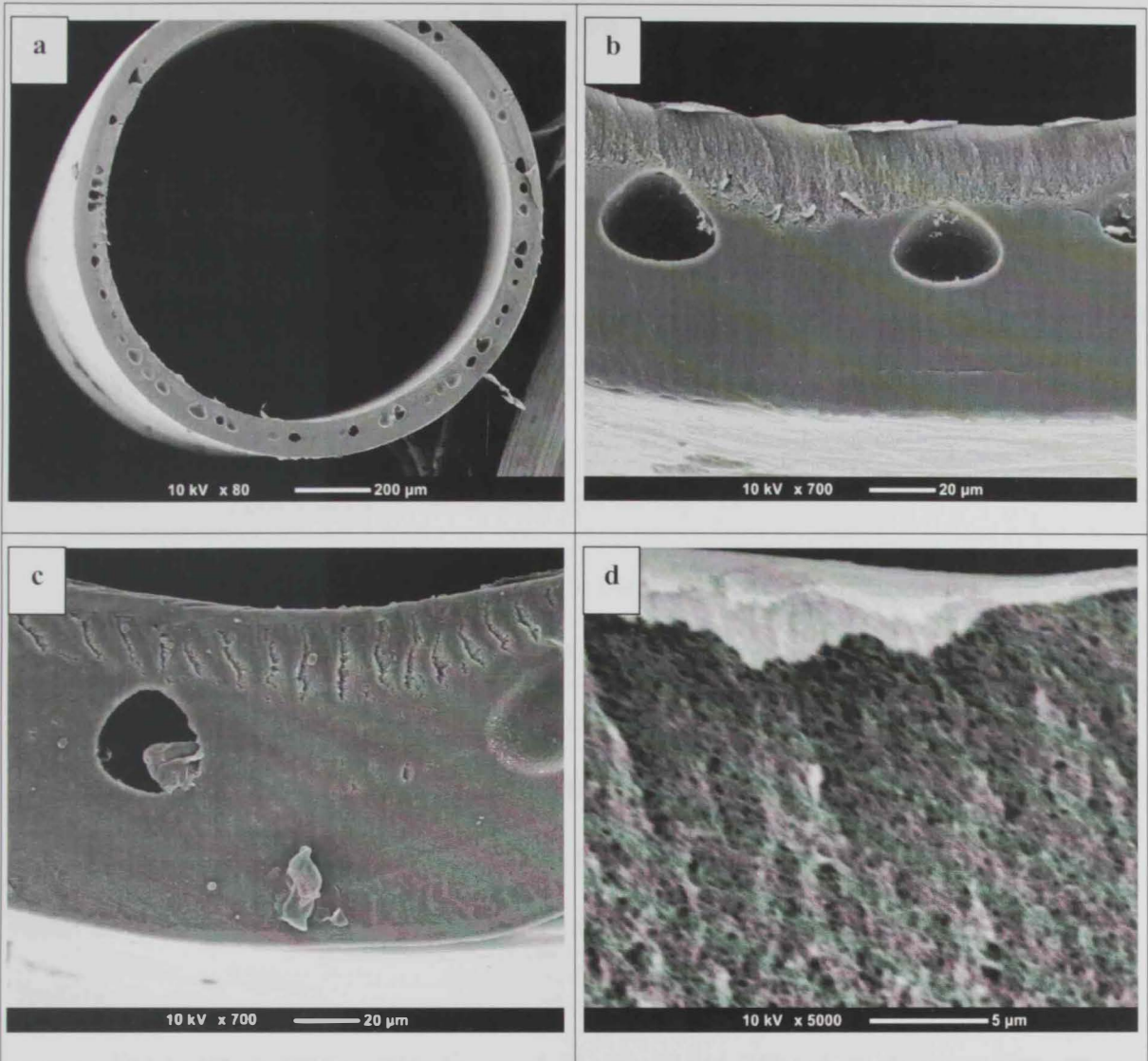


Figure 5.16: SEM micrographs of 24% CA fiber at dope solution flow rate = 10.5 (g/min)

- a) Whole cross section
- b) higher magnification of cross section
- c) higher magnification of out edge of the cross section
- d) higher magnification of the inner edge side.

5.3. Water Permeability and Rejection

To describe cellulose acetate fibers, the common way is to evaluate its performance in terms of pure water permeability and percent of solid rejection, the main aim of study water permeability and solid rejection of hollow fiber in order to reduce fouling in membrane. Five hours is the filtration time of water permeability test.

Permeate flux was calculated using the following equation (107);

$$\text{Permeate flux} = \frac{\text{Volume of Permeate}}{\text{Time} \times \text{Area of Membrane}} \quad (5)$$

The filtration experiments were done in the first two hours by using distilled water as a feed solution, and BSA solution (1g BSA /1000 ml water) used as feed solution for the next two hours. Finally after that in the last one hour, again distilled water was used as feed solution to clean the inner area of fiber from BSA, because BSA protein molecules could be absorbed on the pore surface and that lead to form BSA layer caused to decrease the flux of water in hollow fiber. The rejection percentage was calculated after two hours of BSA feeding.

The rejection ratio for the fibers of 15, 18, 21 and 24%CA at different flow rate is given in the Table 5.1. As the cellulose acetate concentration increased the rejection percentage decreased, because increasing polymer concentration was shown and form denser layers. 15% hollow fiber present the highest rejection compared with other CA concentration.

Table 5. 1: Rejection ratio of BSA at different CA concentrations.

Dope Solution concentration	Rejection %
15% CA/DMAc	16.62
18% CA/DMAc	15.42
21% CA/DMAc	12.90
24% CA/DMAc	9.311

Figure 5.17 shows that the filtration experiments for 15% CA concentration were performed in first two hours by using deionized water as a feed solution. The flux was almost the same at the beginning of filtration. BSA solution of 1g BSA /1000 ml water was used as a feed solution for the next three hours of filtration experiment. Flux of membrane was drastically decreased to about 50% based on initial flux of in the beginning of filtration for fibers produced at dope solution flow rate of 6 mg/min. The decreasing of flux at the initial filtration of BSA solution was attributed and absorption or convective deposition of BSA on the membrane surface. Parts of BSA molecules were adsorbed on the pore surface of membrane and in consequence the formed cake layer caused the decrease in flux. This result matches with previous studies, where cellulose acetate increased membrane hydrophilicity while permeability increased with cellulose acetate concentration because permeability depend on the degree of hydrophilic character of the polymer (108).

In the coming figures, the decreasing of flux at the initial filtration of BSA solution membrane decreased slightly and gradually mainly at high dope solution mass flow rate and at high dope solutions concentrations, such as for 21% CA (Figure 5.19) and 24 % CA (Figure 5.20), because high CA concentration in casting solution suppressed macro-void formation. In the figures 5.17-5.20, the drop in the permeability at beginning of the last hour

5. Results and Discussions: Effect of Cellulose Acetate Concentration and Dope Sol. Flow.

of permeability test because BSA particles bulk the pore at the beginning and then the water become step by step clean the inner area of hollow fiber.

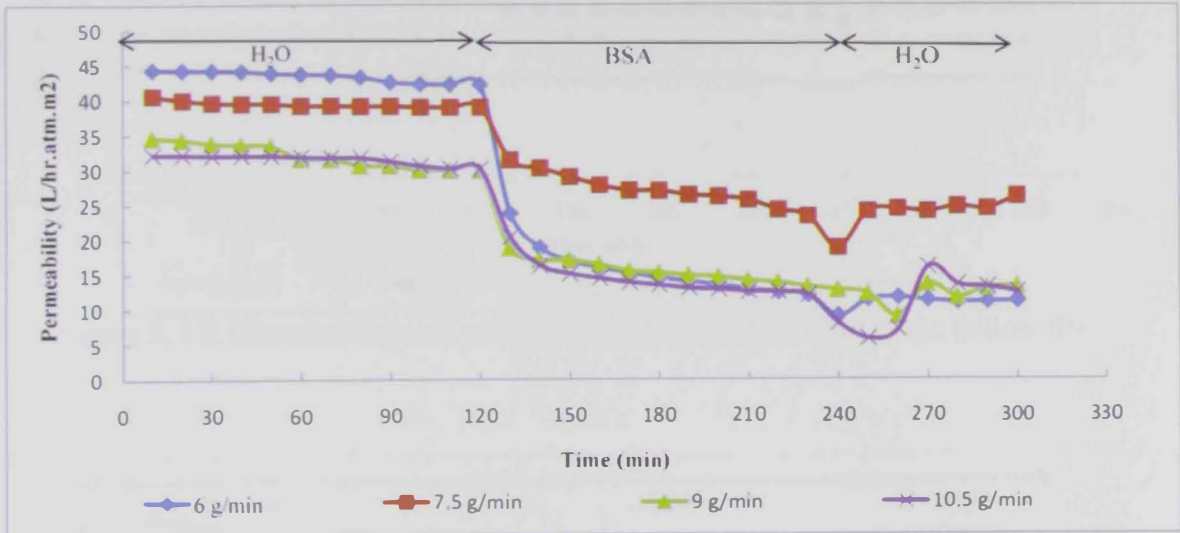


Figure 5.17: Filtration time of water permeability for 15% CA/DMAc hollow fiber.

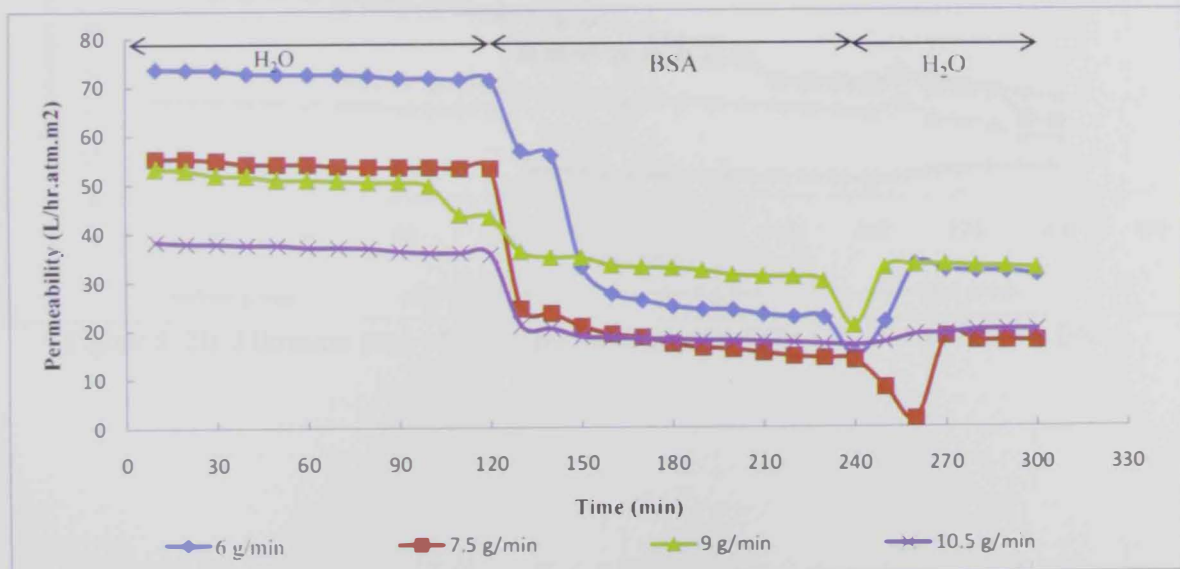


Figure 5.18: Filtration time of water permeability for 18% CA/DMAc hollow fiber.

5. Results and Discussions: Effect of Cellulose Acetate Concentration and Dope Sol. Flow.

of permeability test because BSA particles bulk the pore at the beginning and then the water become step by step clean the inner area of hollow fiber.

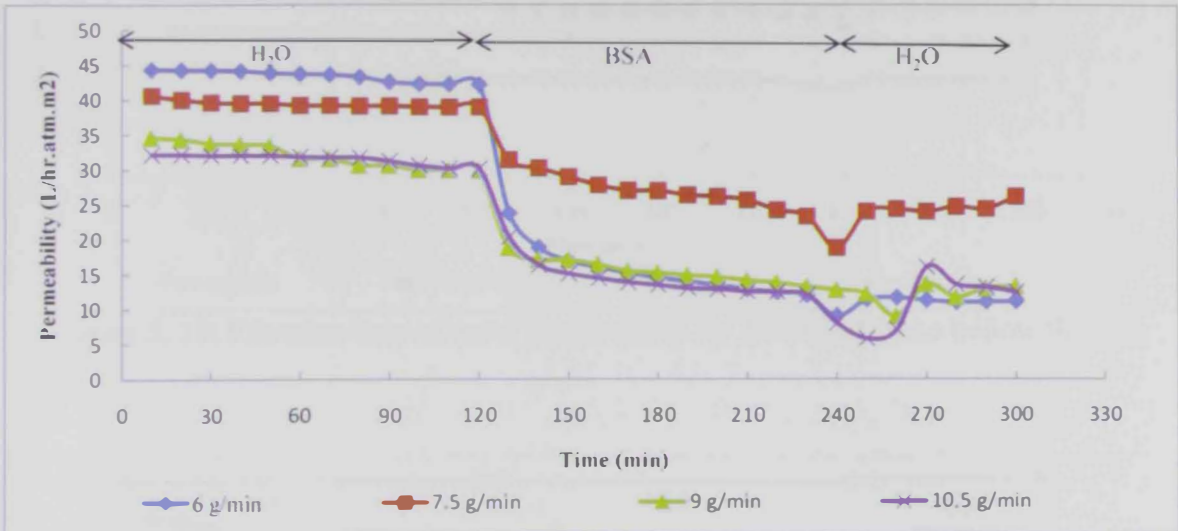


Figure 5.17: Filtration time of water permeability for 15% CA/DMAc hollow fiber.

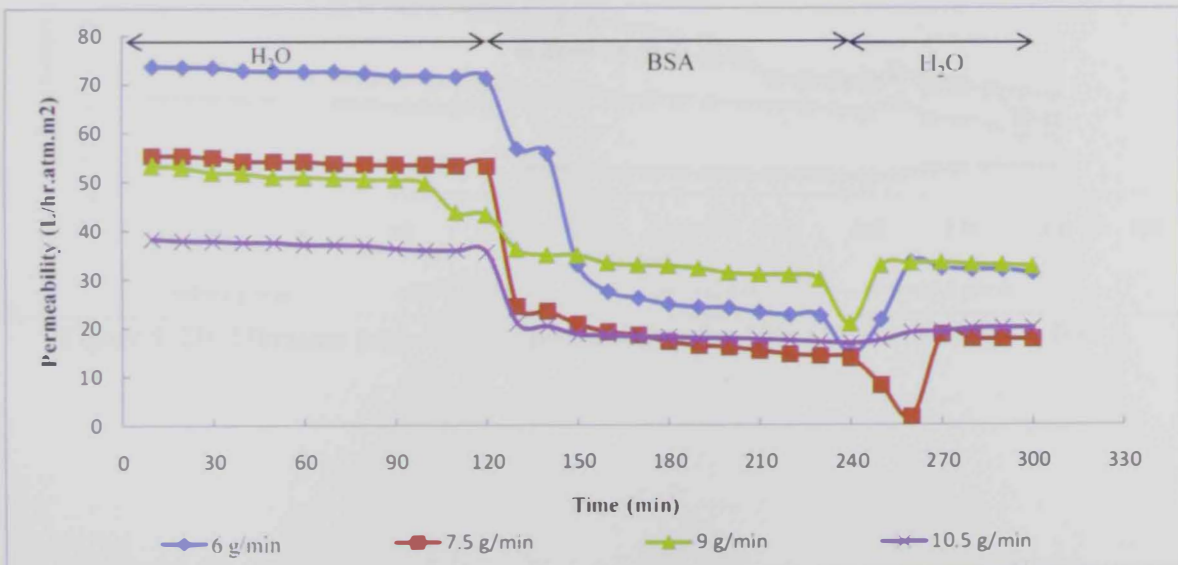


Figure 5.18: Filtration time of water permeability for 18% CA/DMAc hollow fiber.

5. Results and Discussions: Effect of Cellulose Acetate Concentration and Dope Sol. Flow.

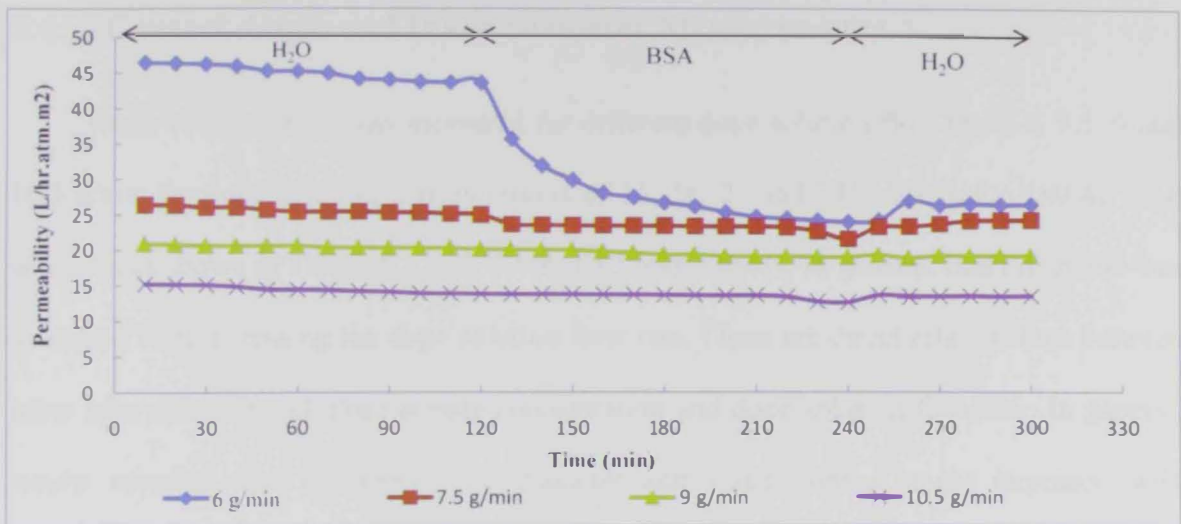


Figure 5. 19: Filtration time of water permeability for 21% CA/DMAc hollow fiber.

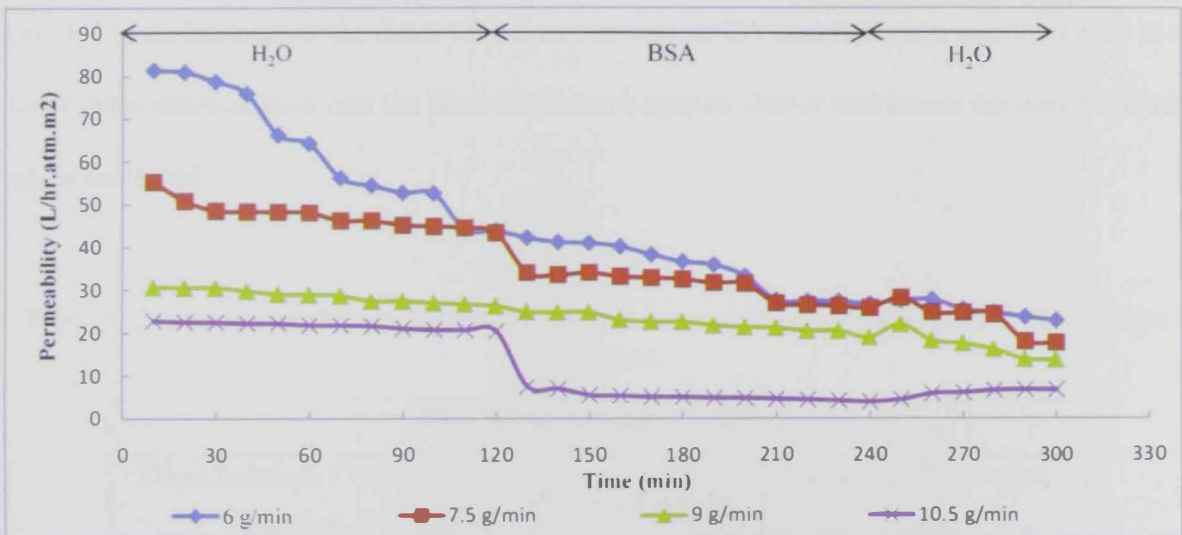


Figure 5. 20: Filtration time of water permeability for 24% CA/DMAc hollow fiber.

5.4. Contact Angle and Inner Diameter Measurements

Water contact angle was measured for different dope solution flow rates; 6, 7.5, 9 and 10.5 g/min for dope solution concentrations of 15, 18, 21 and 24% CA in CA/DMAc dope solutions as shown in Tables 5.2, 5.3, 5.4 and 5.5 respectively. In general, inner diameter was increased with increasing the dope solution flow rate. There are direct relationships between inner tube diameter, cellulose acetate concentration and dope solution flow rate. In general, results revealed that the inner tube diameter and water contact angle increased with increasing polymer concentration and dope solution flow rate. As the polymer dope solution mass flow rate increased, consequently the fibers take-up role speed should be increased and this led to an increase in the inner tube diameter and as CA concentration was increased at a fixed dope solution flow rate the fiber thickness becomes denser and hence the water contact angle increased.

Table 5. 2: Contact angle and inner diameter measurements of 15% CA with different dope flow rates.

Dope Solution Conc. 15% CA		
Dope Solution Flow Rate (g/min)	Measured Angle	Measured Diameter (mm)
6	54.0°	0.88
7.5	56.8°	1.01
9	64.0°	1.02
10.5	66.6°	1.05

5. Results and Discussions: Effect of Cellulose Acetate Concentration and Dope Sol. Flow.

Table 5. 3: Contact angle and inner diameter measurements of 18% CA with different dope flow rates.

Dope Solution Conc. 18% CA		
Dope Solution Flow Rate (g/min)	Measured Angle	Measured Diameter (mm)
6	63.52°	1.04
7.5	64.14°	1.08
9	65.46°	1.10
10.5	67.76°	1.11

Table 5. 4: Contact angle and inner diameter measurements of 21% CA with different dope flow rates.

Dope Solution Conc. 21% CA		
Dope Solution Flow Rate (g/min)	Measured Angle	Measured Diameter (mm)
6	65.80°	0.95
7.5	65.36°	1.01
9	69.06°	1.11
10.5	68.08°	1.18

5. Results and Discussions: Effect of Cellulose Acetate Concentration and Dope Sol. Flow.

Table 5. 5: Contact angle and inner diameter measurements of 24% CA with different dope flow rates.

Dope Solution Conc. 24% CA		
Dope Solution Flow Rate (g/min)	Measured Angle	Measured Diameter (mm)
6	66.01°	1.02
7.5	67.82°	1.07
9	70.08°	1.14
10.5	81.80°	1.18



5.5. Strength of Fabricated Fibers

The stress and strain were tested for hollow fiber membrane fabricated from dope solutions of 15, 18, 21 and 24% CA in CA/DMAc at variable dope solution mass flow rate of 6 to 9 g/min as shown in Figure 5.21 and Figure 5.22, respectively. At high CA concentration the stress and strain decreased as the dope solution flow rate increased. This is attributed to the decrease in dope solution residence time the water coagulation bath and hence not enough time for dope coagulation.

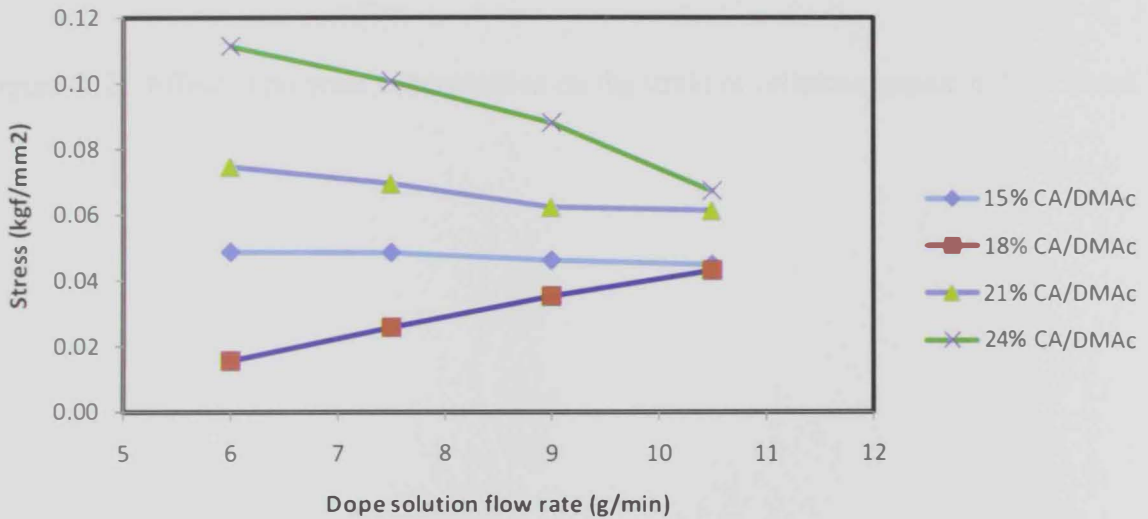


Figure 5. 21: Effect of polymer concentration on the stress of cellulose acetate hollow fibers.

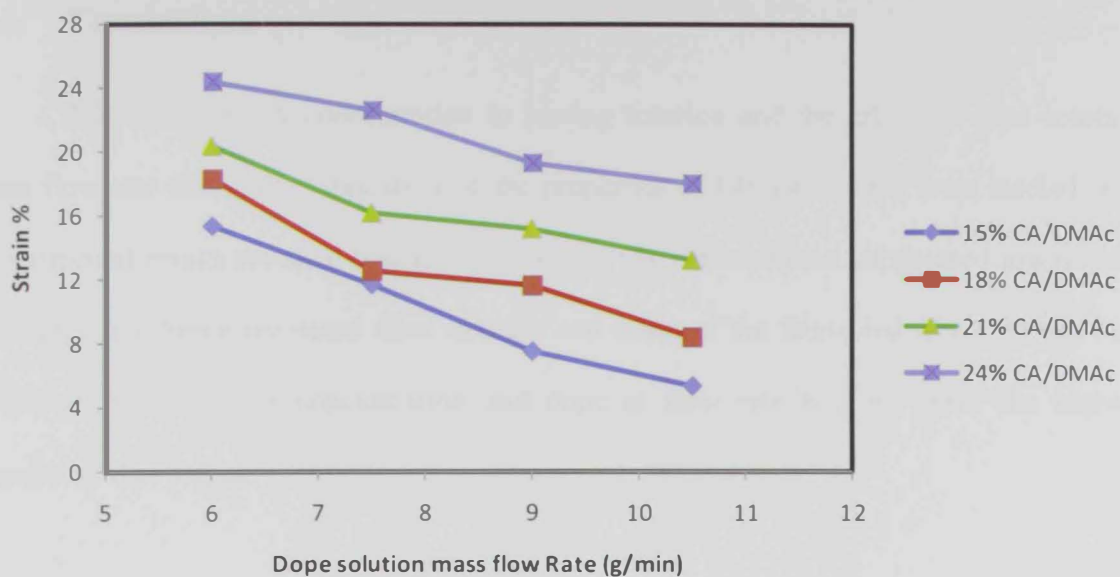


Figure 5. 22: Effect of polymer concentration on the strain of cellulose acetate hollow fibers.

5.6. Conclusions

The effect of CA concentration in casting solution and the effect of dope solution mass flow rate during the fabrication on the properties of fabricated fiber were studied. The experimental results revealed that an increase in CA concentration suppressed macro-void formation and hence increased fiber strength and strain of the fabricated fibers. It was also observed that 15% CA concentration and dope at flow rate 6 g/min gave the highest membrane flux values.

Chapter Six: Effect of Bore Fluid Flow Rate

In the present chapter the effect of bore fluid flow rate on the fabricated CA hollow fiber membrane morphology, water contact angle, water permeability, solute rejection, stress and strain were experimentally investigated. The bore fluid flow rate was studied at five different flow rates; 8, 10, 12, 13 and 16 g/min for a dope solution that was made of 21%CA and 79%DMC.

6.1. SEM Micrographs

SEM micrographs for 21% CA dope solution and bore fluid flow rate of 8, 10, 12, 13 and 16 g/min is shown in Figures 6.1, 6.2, 6.3, 6.4 and 6.5, respectively. The Figures show that with increasing the bore fluid flow rate the hollow fiber inner side diameter increased, wall thickness decreased and the tube bore side became more uniform. This is attributed to the reason that with increasing the bore fluid (non-solvent), the rate of separation of solvent/non-solvent increased, consequently coagulation rate increased. As bore fluid flow rate increased, the length of finger like structure decreased and the sponge like structure increased.

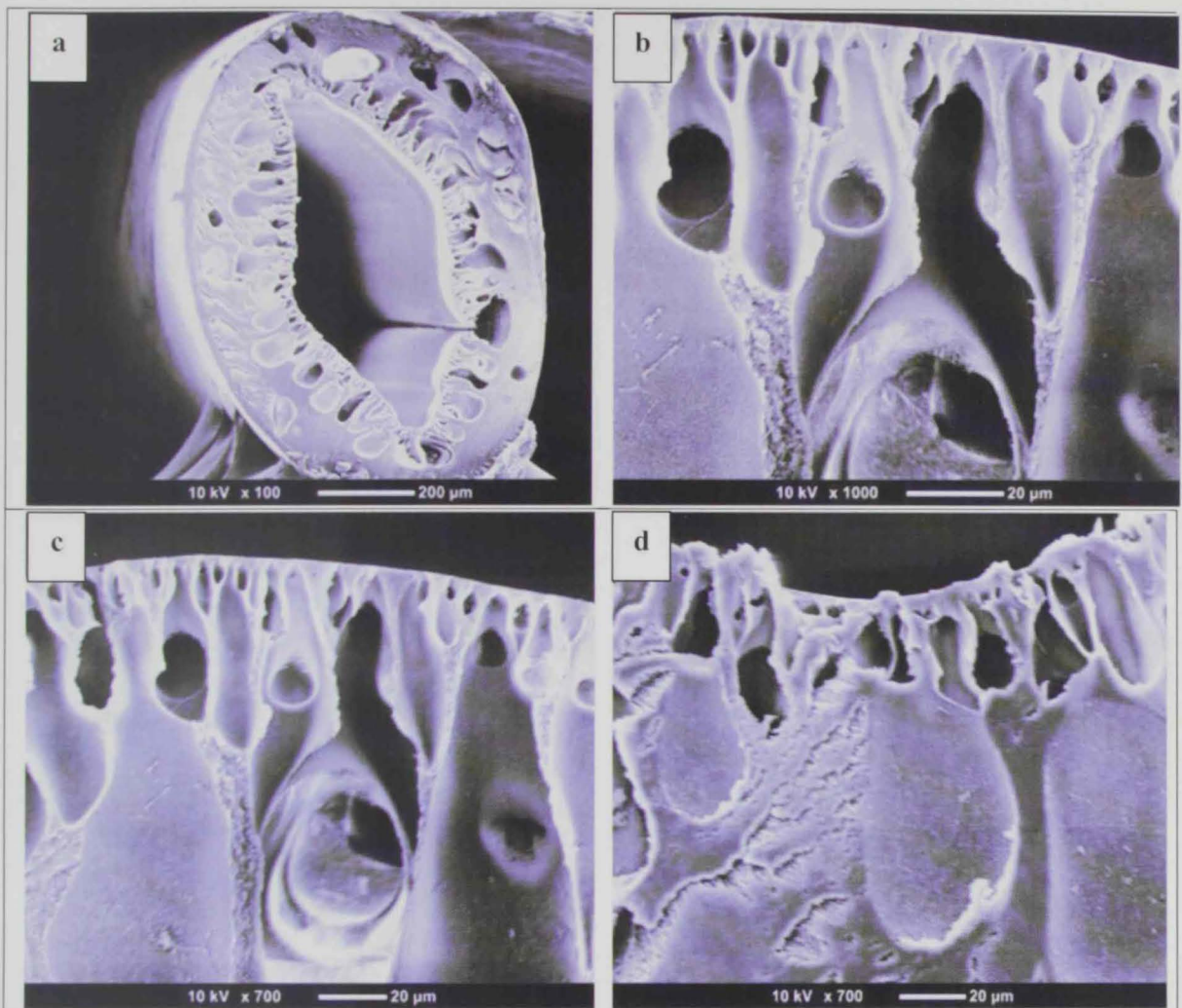


Figure 6. 1: SEM images of 21% cellulose acetate at bore flow rate = 8 (g/min)

- a) Whole cross section
- b) higher magnification of cross section
- c) higher magnification of out edge of the cross section
- d) higher magnification of the inner edge side.

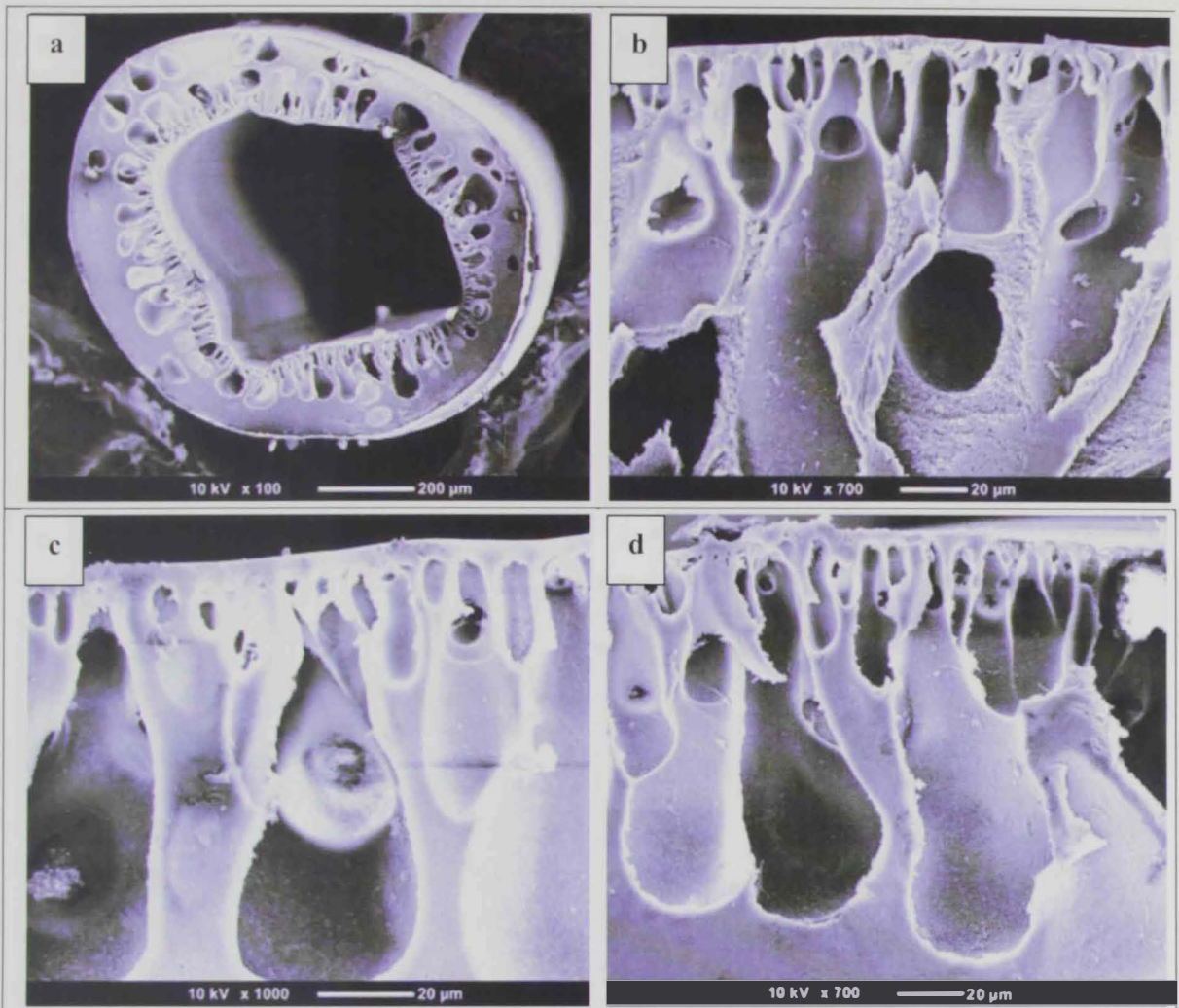


Figure 6. 2: SEM images of 21% cellulose acetate at bore flow rate = 10 (g/min)

b) Whole cross section b) higher magnification of cross section c) higher magnification of out edge of the cross section d) higher magnification of the inner edge side.

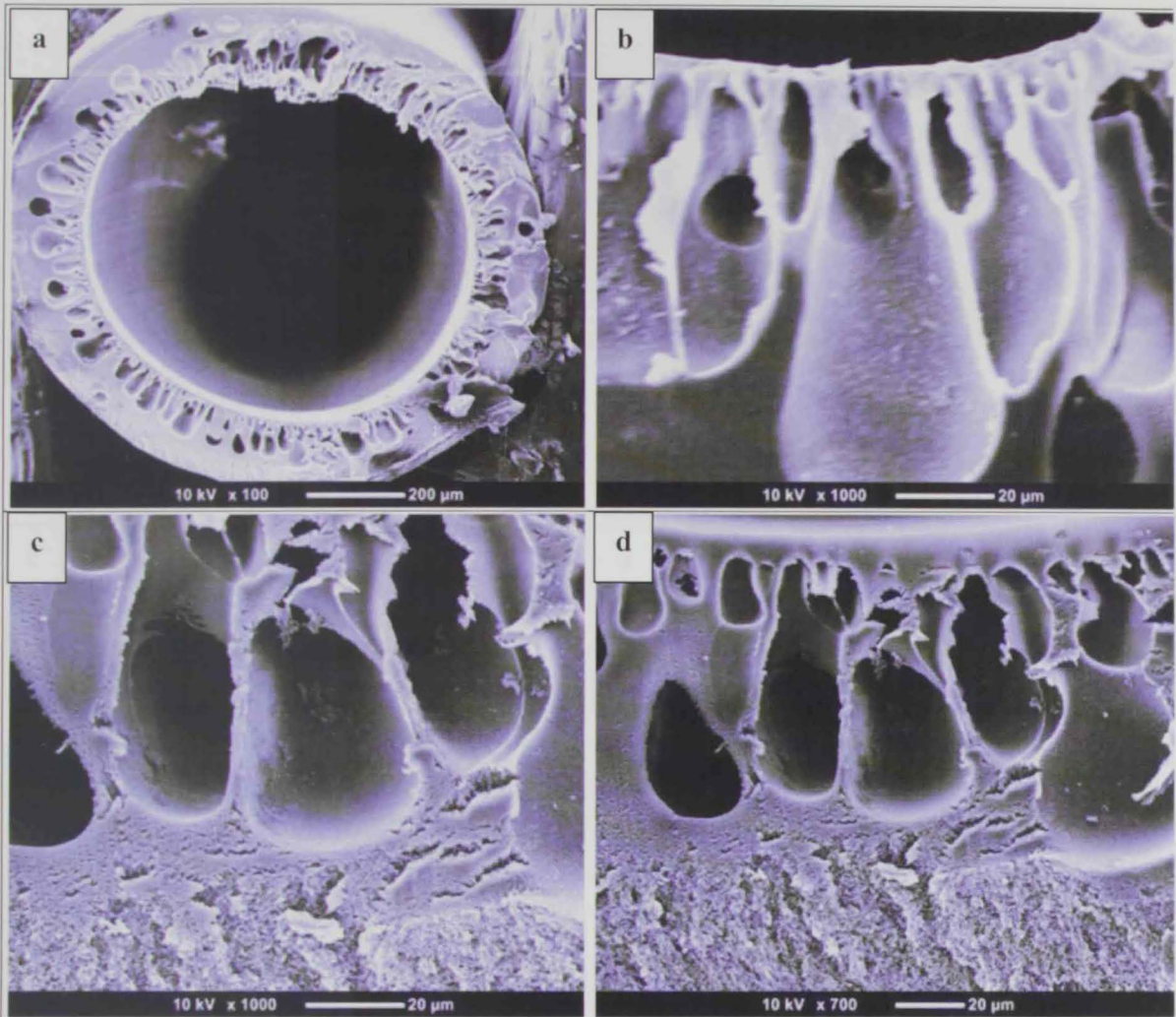


Figure 6. 3: SEM images of 21% cellulose acetate at bore flow rate = 12 (g/min)

- c) Whole cross section
- b) higher magnification of cross section
- c) higher magnification of out edge of the cross section
- d) higher magnification of the inner edge side.

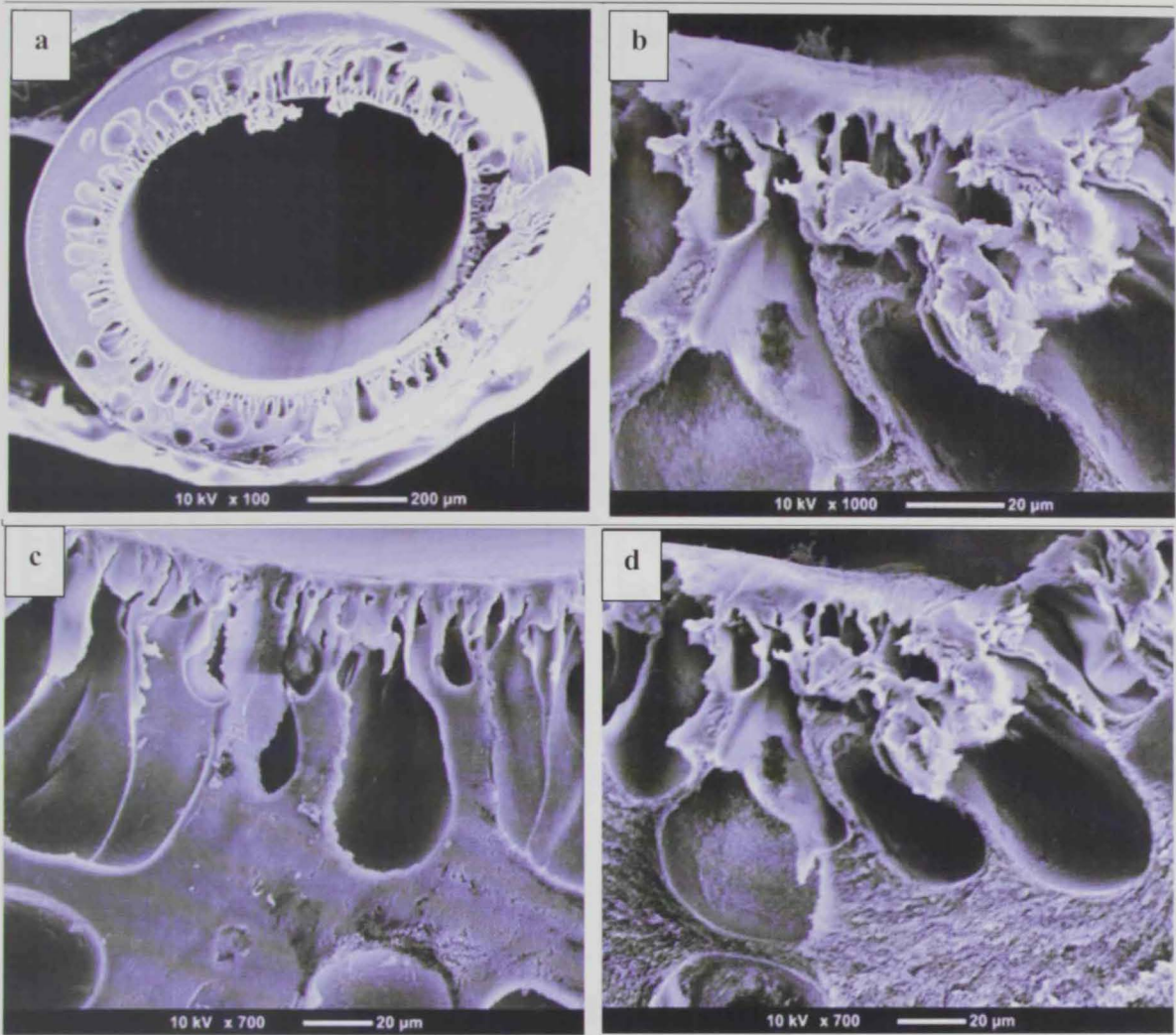


Figure 6. 4: SEM images of 21% cellulose acetate at bore flow rate = 13 (g/min)

- d) Whole cross section b) higher magnification of cross section c) higher magnification of out edge of the cross section d) higher magnification of the inner edge side.

6. Results and Discussions: Effect of Bore Fluid Flow Rate.

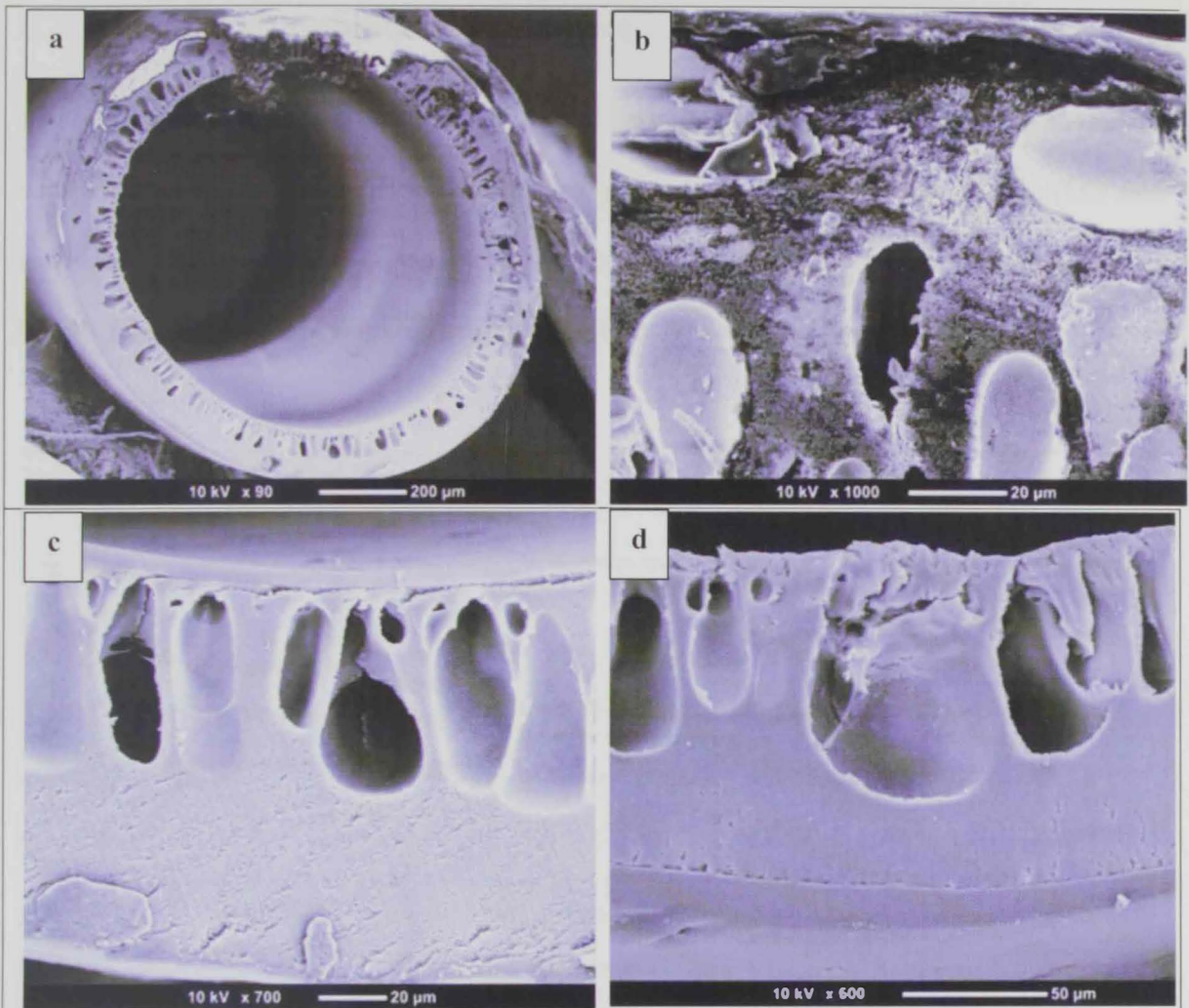


Figure 6. 5: SEM images of 21% cellulose acetate at bore flow rate = 16 (g/min)

- e) Whole cross section b) higher magnification of cross section c) higher magnification of out edge of the cross section d) higher magnification of the inner edge side.

6.2. Water Permeability and Rejection

Water permeability is obtained by measuring the volume of water flow due to constant pressure. In this section the volume of permeate water is a function of bore flow rate and inner diameter. From Figure 6.6 it can be observed that, the water flux through the hollow fiber was decreased with increasing the flow rate of bore fluid (water).

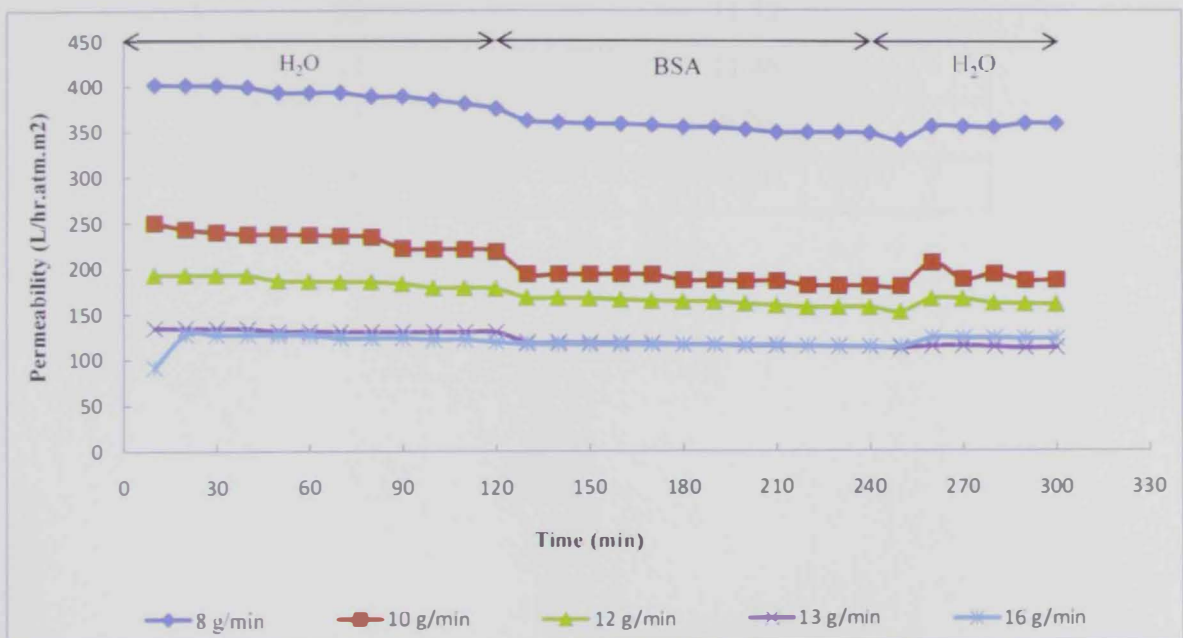


Figure 6. 6: Filtration time of water permeability at different bore flow rate.

6. Results and Discussions: Effect of Bore Fluid Flow Rate.

The percentage rejection increased with the decreasing in the bore fluid flow rate, Table 6.1 illustrates the BSA rejection by changing the bore fluid flow rate in the fibers.

Table 6. 1:Rejection ratio of BSA at different bore flow rates.

Bore Flow Rate (g/min)	Rejection %
8	12.01
10	11.72
12	11.46
13	9.96
16	8.11

6.3. Contact Angle and Diameter Measurements

Table 2 shows the effect of bore fluid flow rate on the water contact angle for dope solution consists 21% CA in DMAc. The results shows that water contact angle and inner diameter increased with increasing bore fluid flow rate. This is related to the bore fluid flow rate increased the wall thickness of the hollow fiber membrane decreased due the fast rate of exchange of solvent (DMAc) and the nonsolvent (water). The water contact angle increased from 62° to 75.8° with the increase in the bore fluid flow rate from 8 to 16 g/min.

Table 6. 2: Contact Angle and diameter measurements cellulose acetate at different bore flow rates.

Dope Solution Conc. 21% CA		
Bore fluid flow rate (g/min)	Water contact angle	Inner side diameter (mm)
8	62.0	0.50
10	68.0	0.56
12	69.8	0.62
13	74.8	0.71
16	75.8	0.84

6.4. Strength of Fabricated Fibers

Figure 6.6 shows the effect of the stress of the hollow fiber as a function of bore fluid flow rate for 21% CA dope solution. The results show that the stress decreased as the bore fluid flow rate decreased. This result is expected since with the increase in bore fluid flow rate, the rate of exchange of solvent (DMAc) in the dope solution to non solvent (water) increased and resulted in thin wall thickness. Strain was also observed to decrease due to the think walls and the increase in the hollow fiber diameter (Figure 6.8)

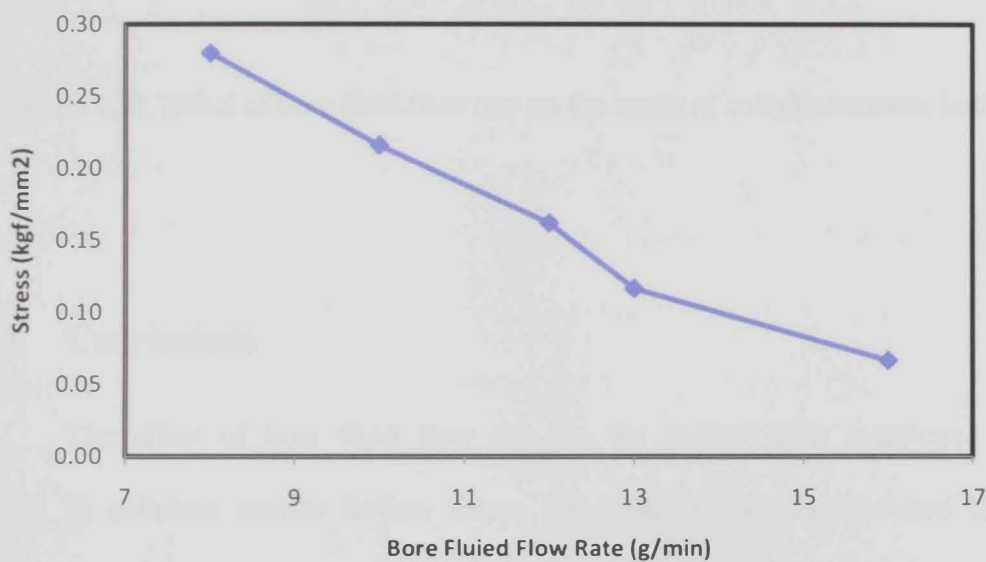


Figure 6. 7: Effect of bore fluid flow rate on the stress of cellulose acetate hollow fibers.

6. Results and Discussions: Effect of Bore Fluid Flow Rate.

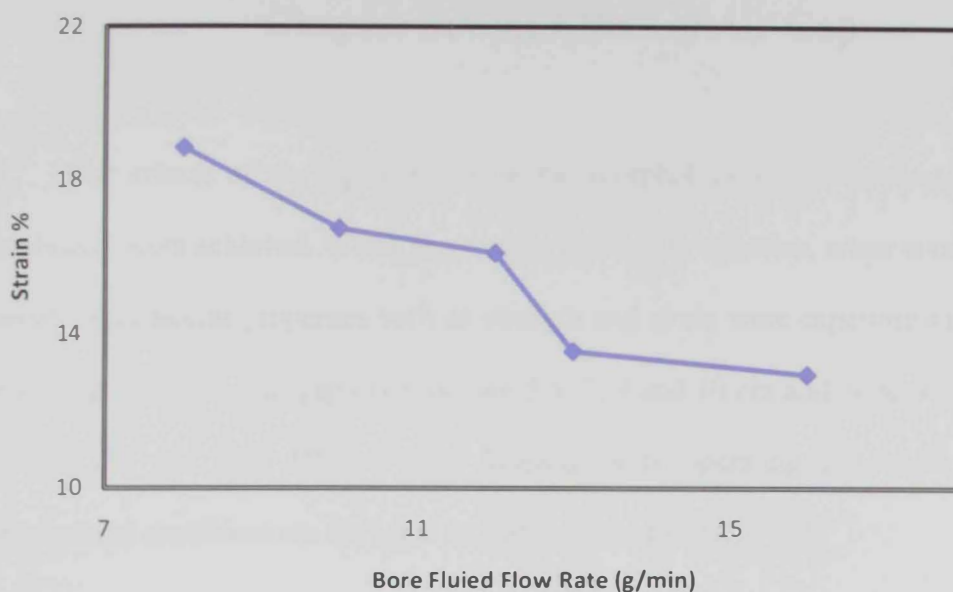


Figure 6. 8: Effect of bore fluid flow rate on the strain of cellulose acetate hollow fibers.

6.5. Conclusions

The effect of bore fluid flow rate on the hollow fiber membrane morphology of 21 % cellulose acetate hollow fibers was studied. Results disclosed that with the increase in bore fluid flow rates both strength and stain decreased. As the bore fluid flow rate increased the rate of solvent/non solvent transfer between inner side fiber and bore fluid (non solvent) increased, consequently, finger like structure at the inner structure increased. The inner side of fiber became more porous and the fiber strength decreased. Retention or solute rejection decreased as the bore fluid flow rate increased due to the increase in the macro-voids.

Chapter Seven: Effect of Air Gap

The effects of air gap distance on the morphology of the fabricated hollow fiber membranes were achieved. Water permeation and solute rejection, water contact angle, fiber diameter mechanical properties such as strength and strain were experimentally investigated for air gap distances. Air gap distances are 5.5, 7, 9 and 10 cm and dope solution consisting of 21% CA and 79% DMAc while keeping other operating conditions constant. The experimental conditions are the same as that presented in Table 3.3.

7.1. Introduction

Many parameters affect the structure of hollow fiber membranes such as rheological properties of spinning solution, type of bore fluid, type of external coagulant, dope solution flow rate and length of the air gap. Chung and others showed that air gap distance and elongation stress played important roles on the mass transfer in hollow fibers (110). M. Khayet et al (2009) pointed out that many fiber characteristics could be affected with the change in the air gap distance such as water permeability which is expected to decrease as the air gap distance increases. This is attributed to the increase in the skin layer thickness with increasing the air gap spinning distance (111). The main objective in this chapter was to define the effect of air gap distance on the hollow fiber configuration, water permeability and mechanical properties of manufactured hollow fibers.

7.2. SEM Micrographs

Scanning Electron Microscopy (SEM) was used to study the morphology of the hollow fibers at different distances of air gap (5.5, 7, 9 and 10 cm) at fixed dope solution concentration (21% CA). The SEM micrographs are shown in Figures 7.1, 7.2, 7.3 and 7.4, respectively. The inner side of the fibers shows finger like structure in all cases, the finger like structure became shorter and sponge layer increased with increasing air gap distance. The external layer of the fibers became denser with the increase in air gap up to 9 cm. The formation of the dense layer is expected due the slow exchange rate of solvent/non-solvent and the consequent slow coagulation rate.

7. Results and Discussions: Effect of Air Gap.

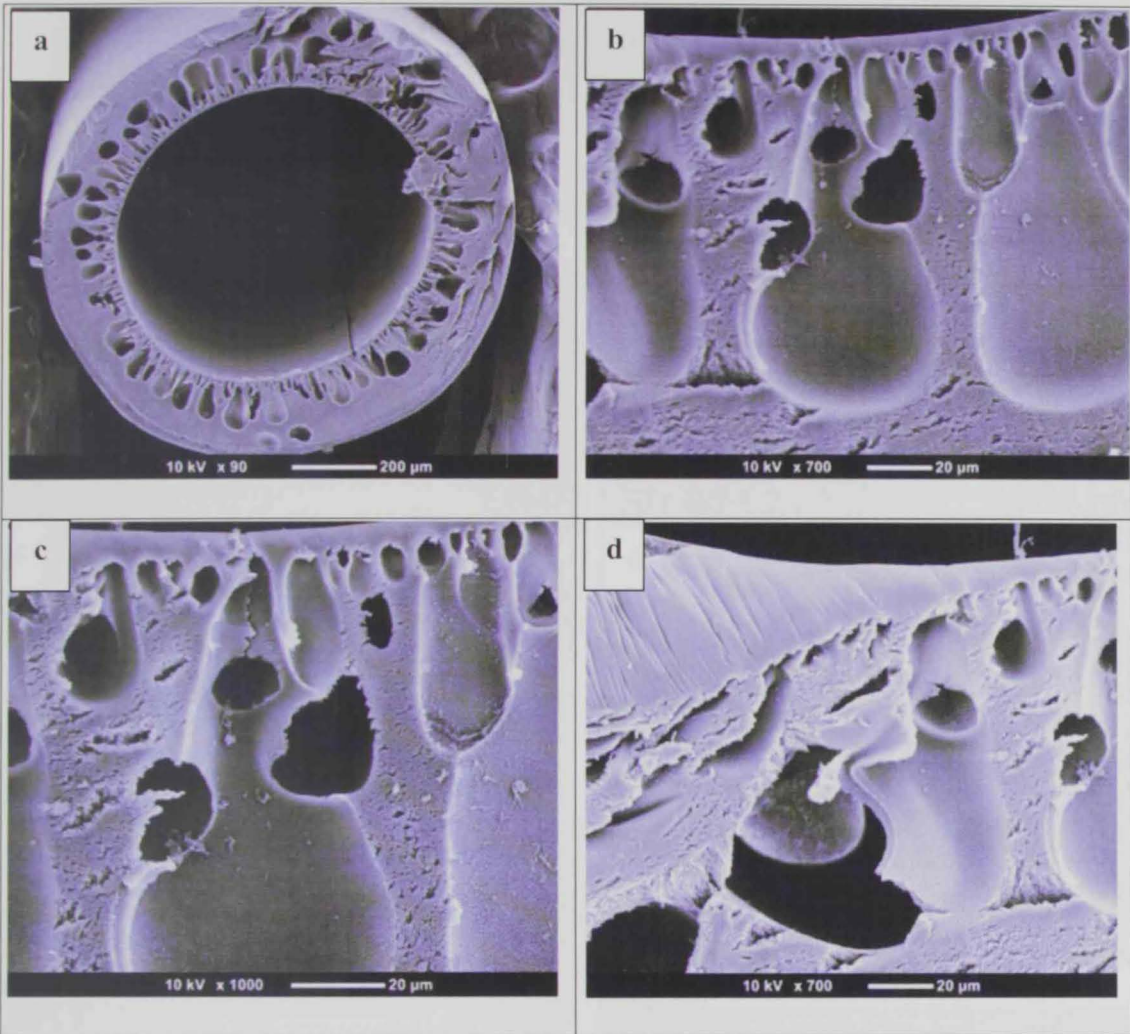


Figure 7. 1: SEM images of 21%CA at air gap = 5.5cm.

- a) Whole cross section b) higher magnification of cross section c) higher magnification of out edge of the cross section d) higher magnification of the inner edge side.

7. Results and Discussions: Effect of Air Gap.

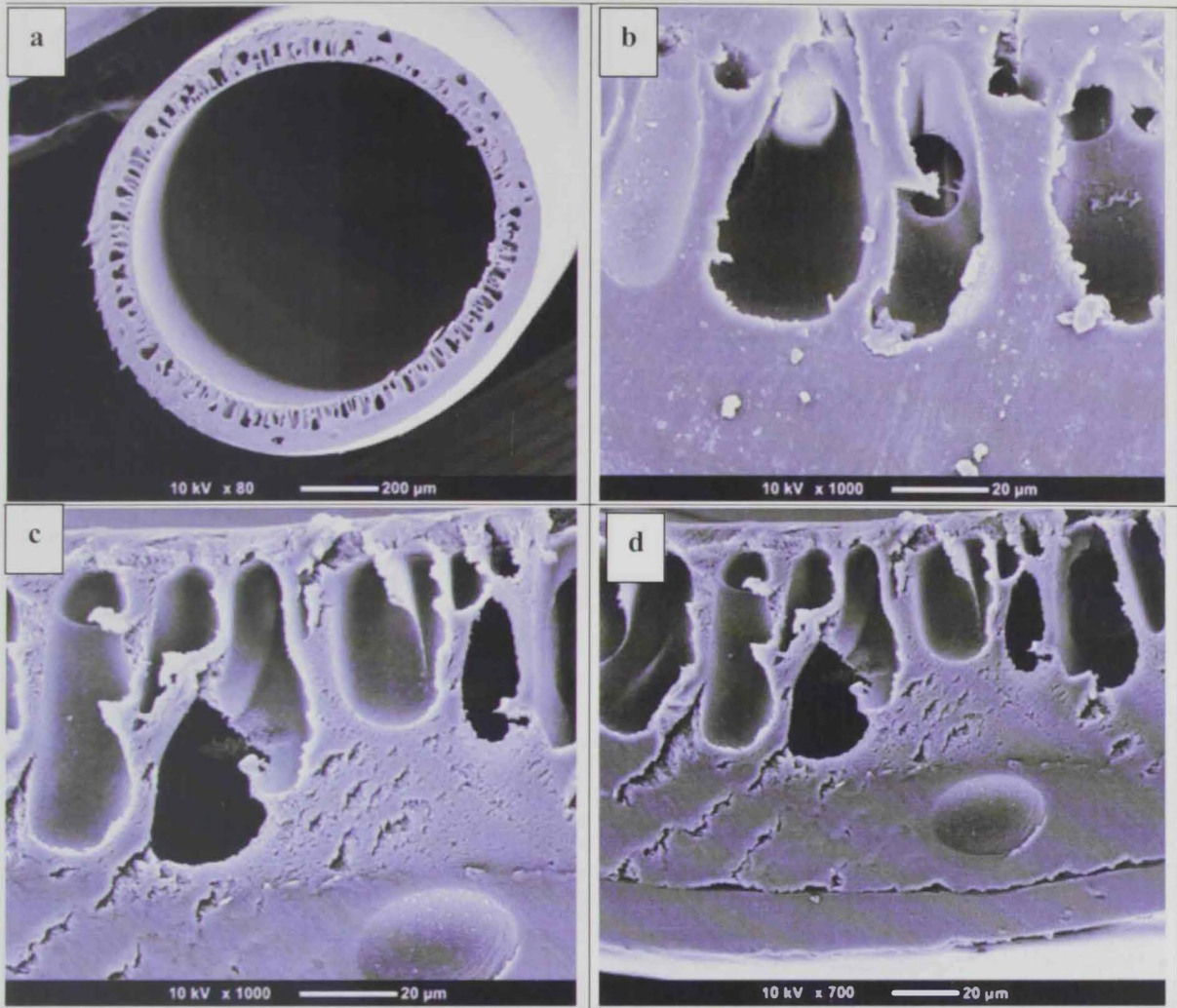


Figure 7. 2: SEM images of 21%CA at air gap = 7cm.

- a) Whole cross section b) higher magnification of cross section c) higher magnification of out edge of the cross section d) higher magnification of the inner edge side.

7. Results and Discussions: Effect of Air Gap.

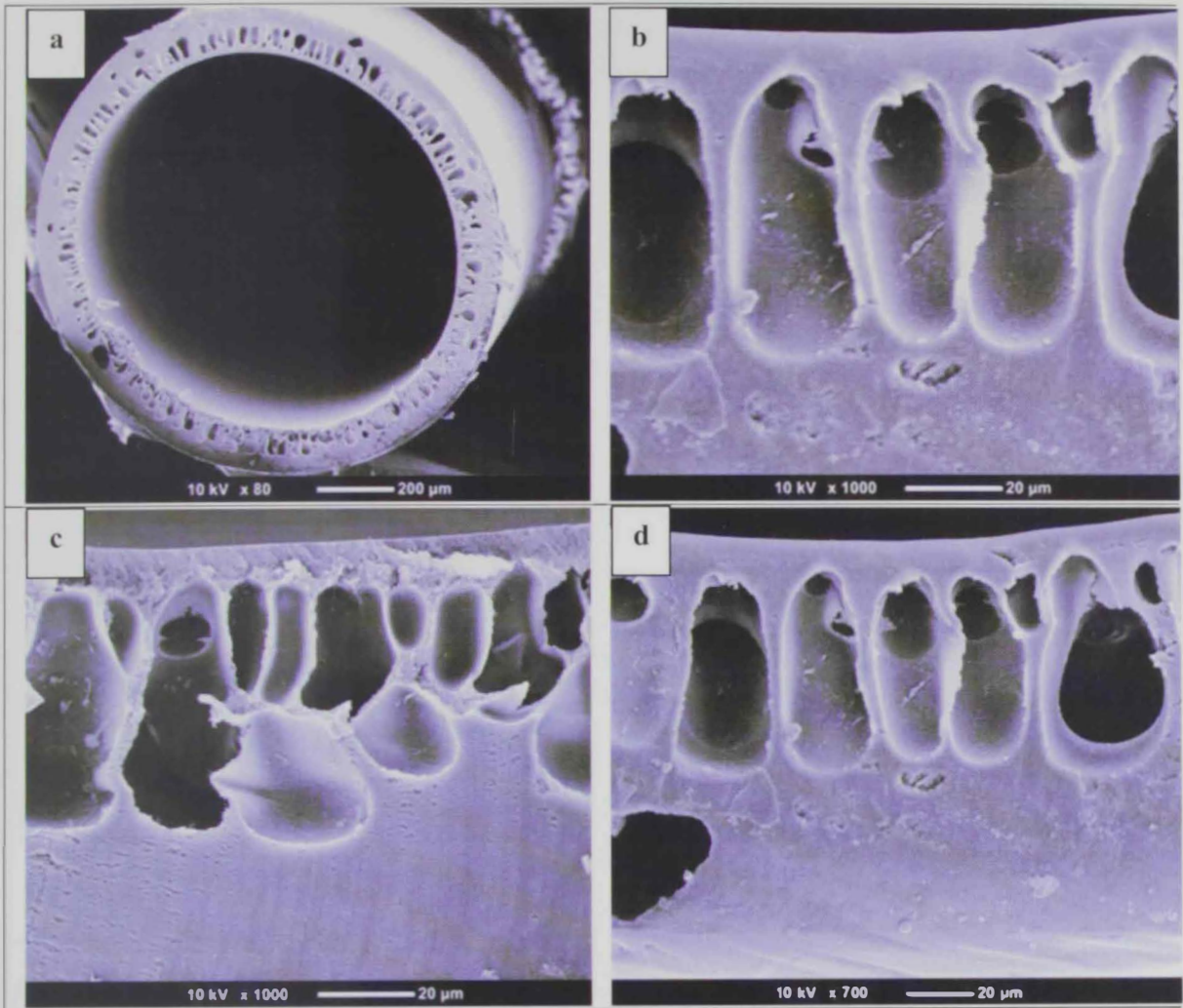


Figure 7. 3: SEM images of 21% CA at air gap = 9cm.

- a) Whole cross section
- b) higher magnification of cross section
- c) higher magnification of out edge of the cross section
- d) higher magnification of the inner edge side.

7. Results and Discussions: Effect of Air Gap.

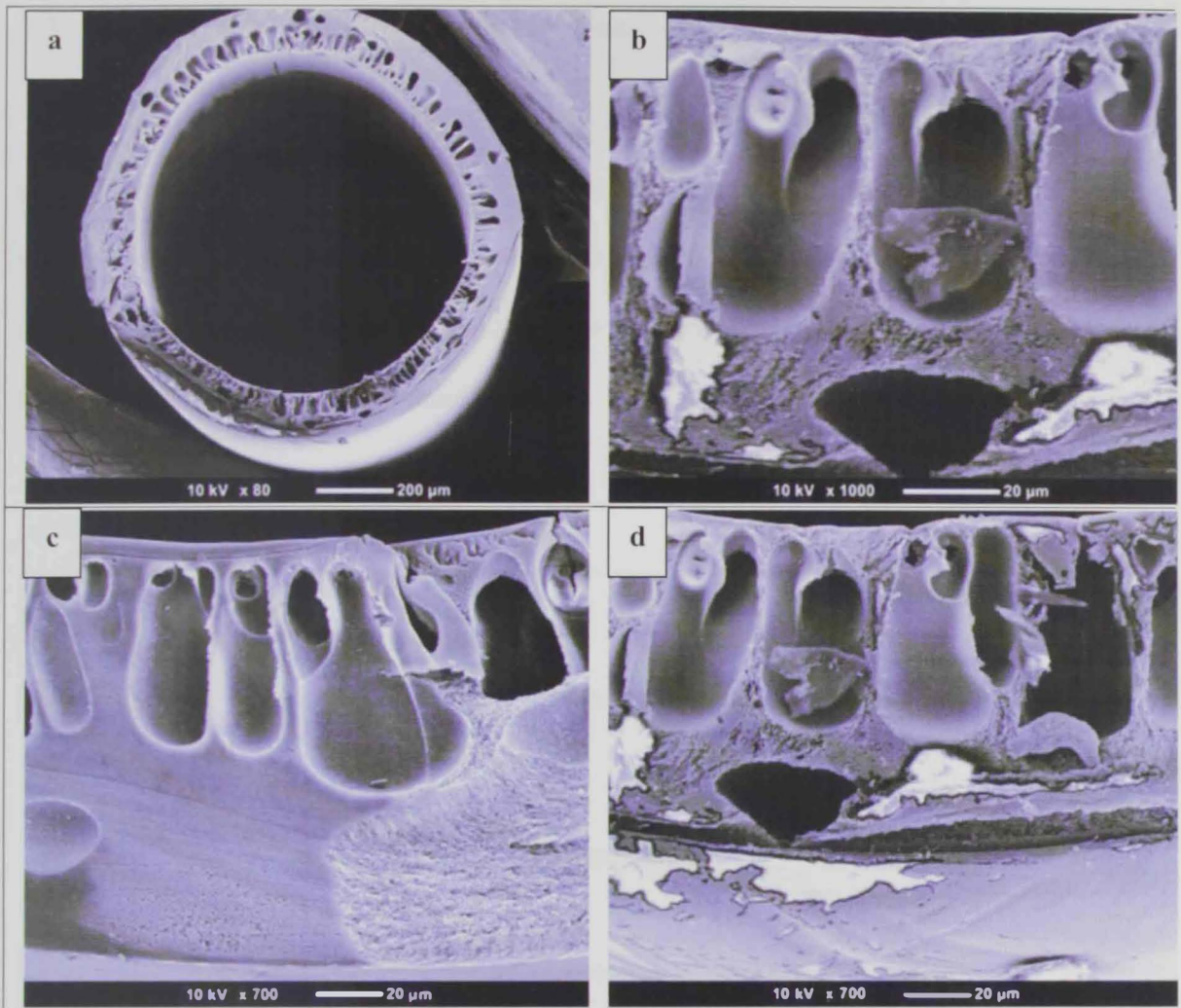


Figure 7. 4: SEM images of 21% CA at air gap = 10 cm.

- a) Whole cross section
- b) higher magnification of cross section
- c) higher magnification of out edge of the cross section
- d) higher magnification of the inner edge side.

7.3. Water Permeability and Rejection

The water flux through the hollow fiber was increased with the increase in the air gap distance as shown in Figure 7.5. At air gap length 9 cm and 10 cm the water permeability values coincide. According to water permeability results, the hollow fiber membrane showed more hydrophilic behavior with the increase in the air gap length. Air gap distances facilitated phase separation and induced orientation.

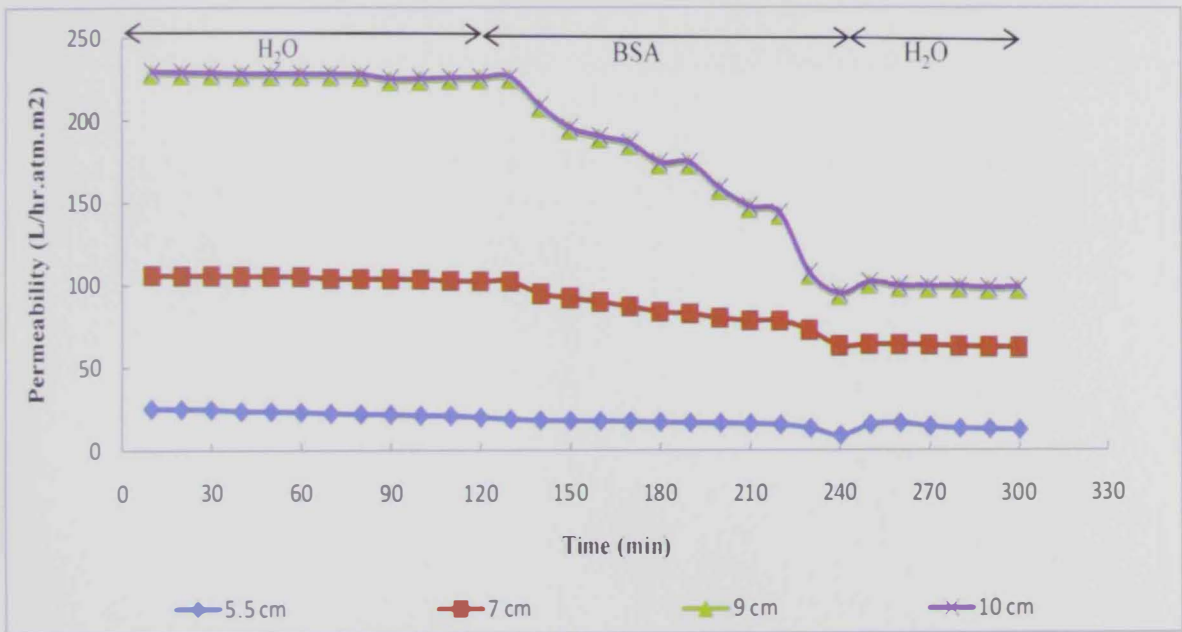


Figure 7. 5: Filtration time of water permeability at different air gap distance.

Table 7.1 shows the rejection percentage at each length for air gap. The highest percentage of rejection of BSA was 81.49 % at 5.5 cm. As the air gap length increased, the rejection decreased. These results suggest that increasing the air gap length will form a denser layer.

7. Results and Discussions: Effect of Air Gap.

Table 7. 1: Rejection ratio of BSA at different air gap lengths.

Air Gap Distance (cm)	Rejection %
5.5	81.49
7	18.61
9	15.29
10	15.01

7.4. Contact Angle and Diameter Measurements

Table 7.2 shows the effect of air gap distance on the fabricated fiber contact angle hollow fibers inner diameter. The table shows that both water contact angle and hollow fiber inner side increased with increasing air gap distance. The results were in agreement with M. Khayet (2003) findings. The slow rate of coagulation resulted in dense external surface of the fibers. The higher the polymer concentration in the surface the higher the water contact angle.

Table 7. 2: Contact Angle and diameter measurements cellulose acetate at different air gap distance.

Dope Solution Conc. 21% CA		
Air Gap Distance (cm)	Measured Angle	Measured Diameter (mm)
5.5	64.24°	0.87
7	65.80°	0.95
9	66.70°	0.97
10	71.66°	1.06

7.5. Strength of Fabricated Fibers

The effect of the air gap flow rate on the fibers strength is shown in Figure 7.6. The figure discloses that, as the air gap distance increased, stress decreased. This could be a result of phase separation that causes molecular chains to pull.

The inner surface of cellulose acetate hollow fibers membranes decreased when the air-gap length increased due to the nascent fiber being stretched and elongated by the gravity force.

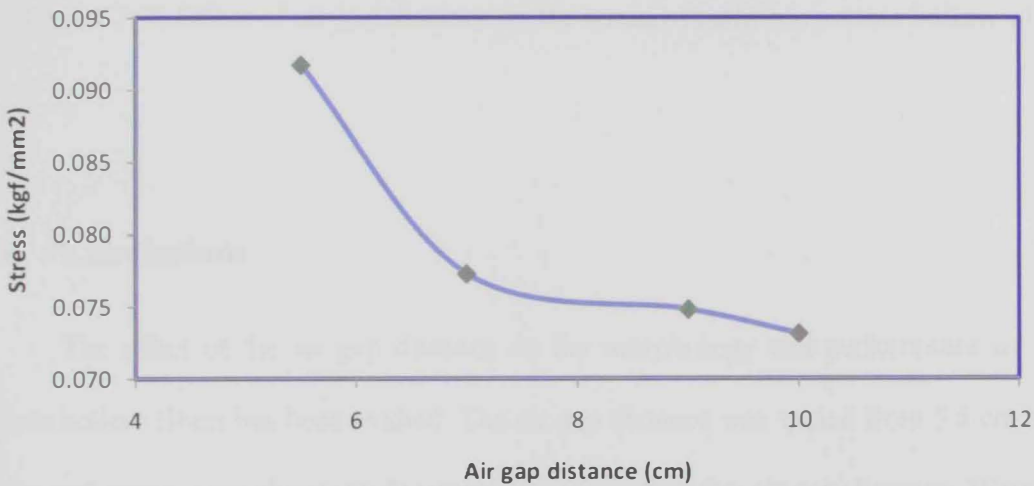


Figure 7. 6: Effect of air gap distance on the stress of fibers fabricated from 21% CA.

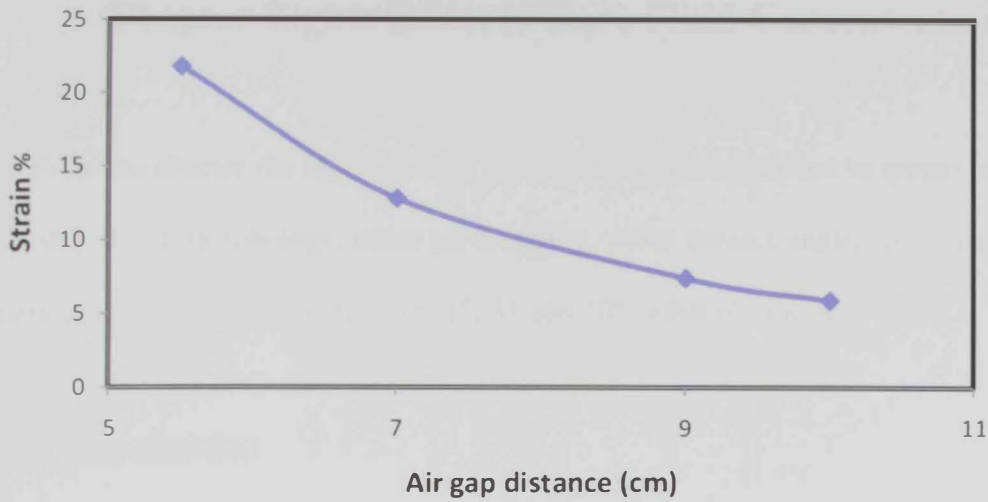


Figure 7. 7: Effect of air gap distance on the strain of cellulose acetate hollow fibers.

7.6. Conclusions

The effect of the air gap distance on the morphology and performance of cellulose acetate hollow fibers has been studied. The air gap distance was varied from 5.5 cm to 10 cm. Stress and strain were shown to decrease with increasing the air gap distance. Water contact angle and inside diameter of the hollow fibers were found to increase with increasing the air gap distance. The longer the nascent hollow fiber membrane is exposed to a humid air gap, the higher the water content in the top layer before demixing occurs, resulting in more porous structure and higher permeation rate.

Chapter Eight: Effect of Bore Fluid Concentration.

In this chapter the effect of bore fluid concentration (ethanol in water) on the hollow fiber membrane morphology, water permeability, water contact angle, stress and strain were investigated for concentrations 0, 18, 25, 35 and 50% ethanol in water.

8.1. Introduction

In order to manufacture hollow fibers in good properties there are many factors that control the prepared fibers during their manufacturing such as structure and dimension of the spinneret, bore fluid composition, polymer solution viscosity, flow rate of the bore fluid, the dope extrusion rate, the length of the air gap and take up roll speed (112). Effect of ethanol composition in water coagulation both was studied in the present chapter.

8.2. SEM Micrographs

The cross section of hollow fibers were examined by using SEM. Figures 8.1, 8.2, 8.3 8.4 and 8.5 show SEM micrographs of fibers fabricated with bore fluid concentrations of 0, 18, 25, 35 and 50%, respectively.

8. Results and Discussions: Effect of Pore Fluid Concentration.

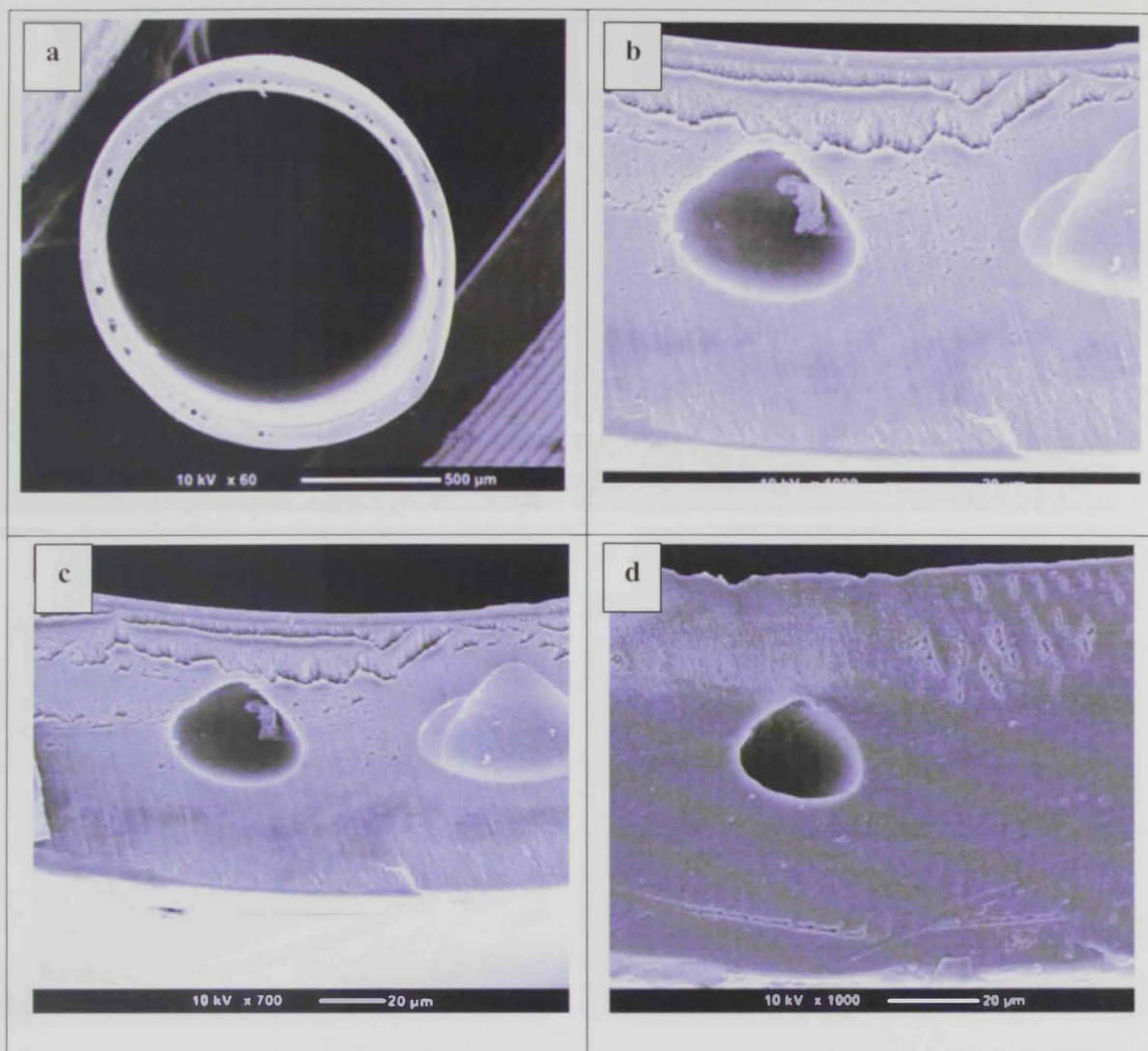


Figure 8. 1: SEM micrographs of 24% CA at bore fluid concentration 0% Ethanol/H₂O.

- a) Whole cross section b) higher magnification of cross section c) higher magnification of out edge of the cross section d) higher magnification of the inner edge side.

8. Results and Discussions: Effect of Pore Fluid Concentration.

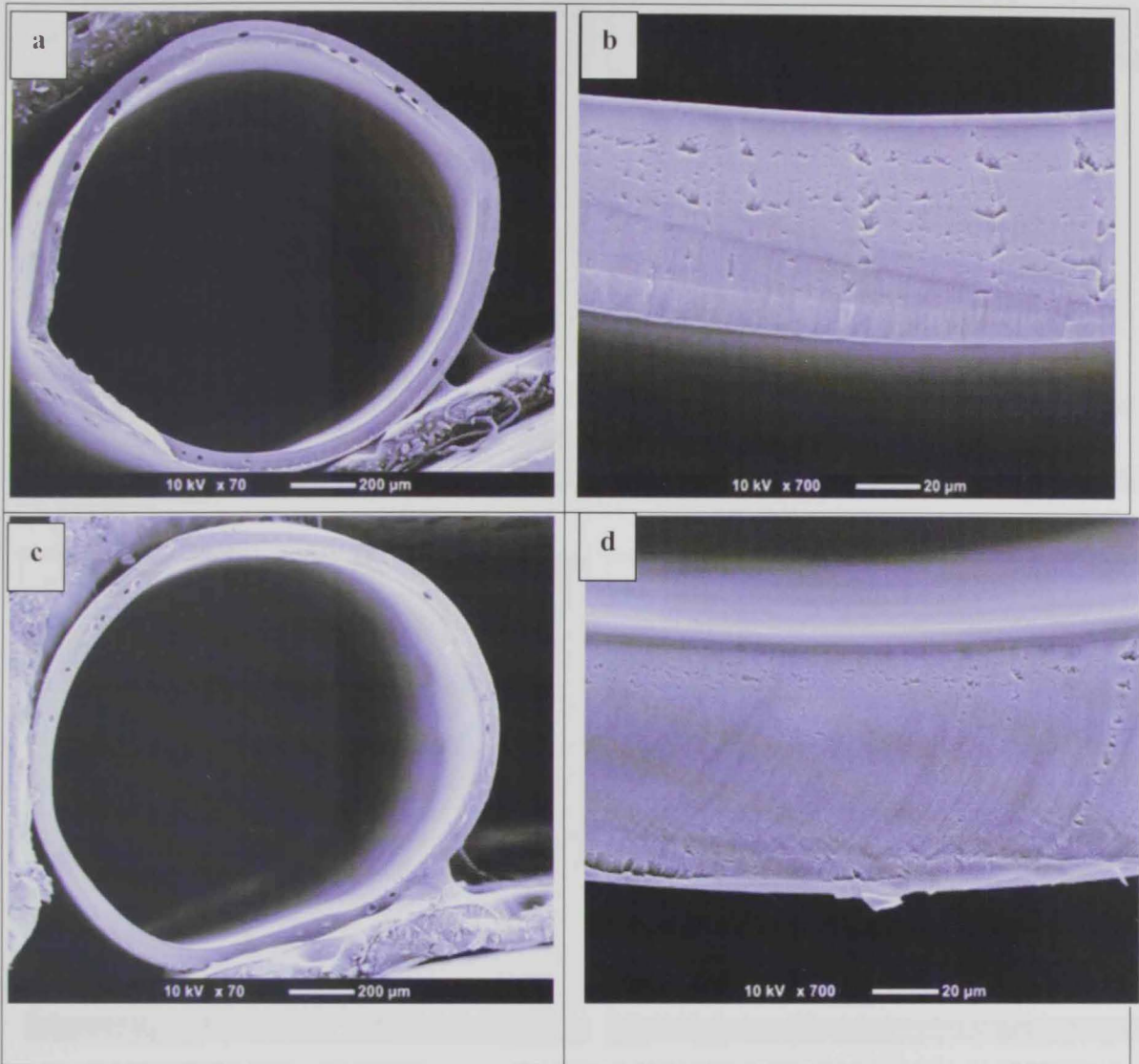


Figure 8. 2: SEM micrographs of 24% CA at bore fluid concentration 18% Ethanol/H₂O.

- a) Whole cross section b) higher magnification of cross section c) higher magnification of out edge of the cross section d) higher magnification of the inner edge side.

8. Results and Discussions: Effect of Pore Fluid Concentration.

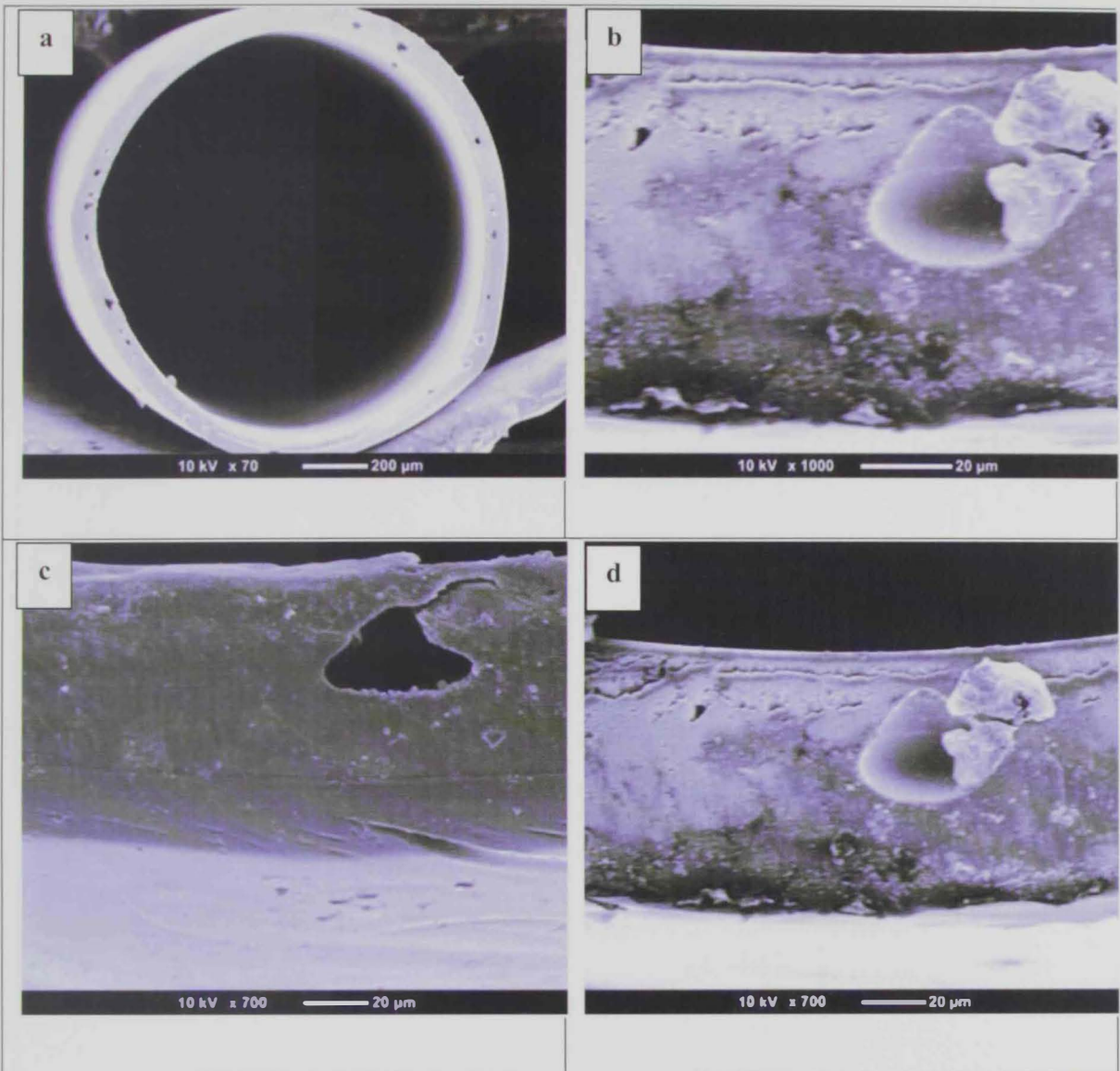


Figure 8. 3: SEM micrographs of 24% CA at bore fluid concentration 25% Ethanol/H₂O.

- b) Whole cross section b) higher magnification of cross section c) higher magnification of out edge of the cross section d) higher magnification of the inner edge side.

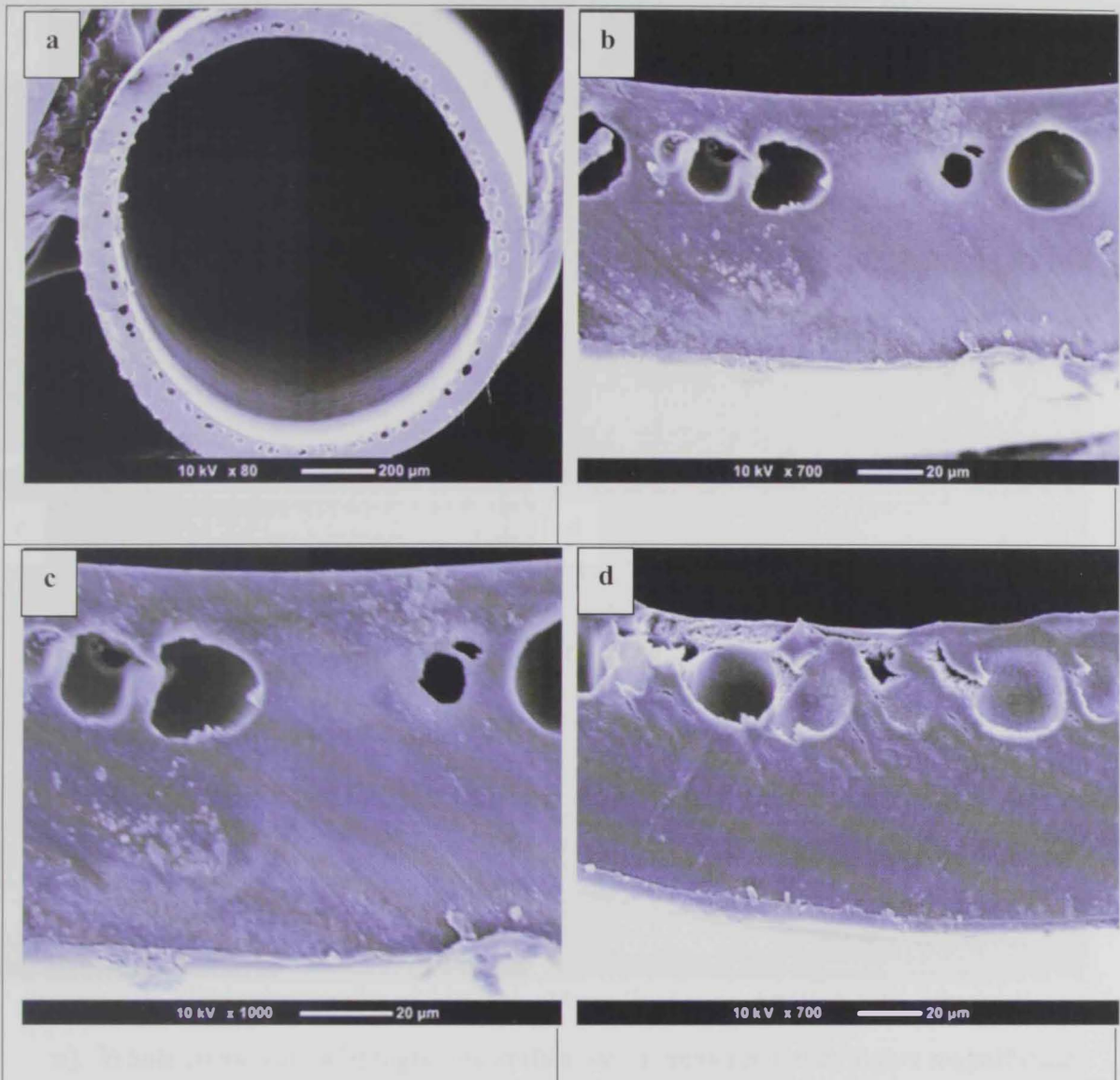


Figure 8. 4: SEM micrographs of 24% CA at bore fluid concentration 35% Ethanol/H₂O.

- a) Whole cross section b) higher magnification of cross section c) higher magnification of out edge of the cross section d) higher magnification of the inner edge side.

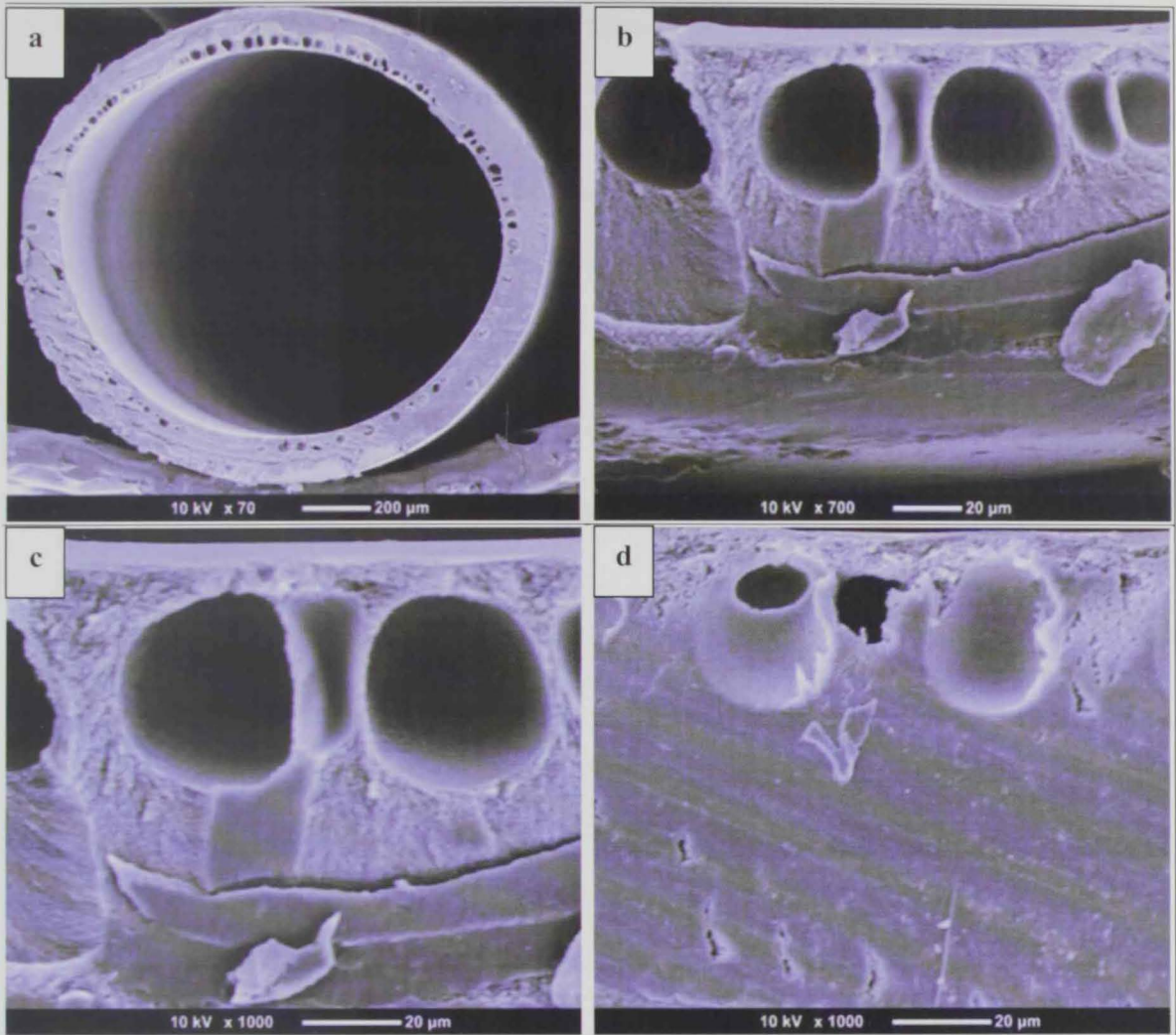


Figure 8. 5: SEM micrographs of 24% CA at bore fluid concentration 50% Ethanol/H₂O.

- a) Whole cross section
- b) higher magnification of cross section
- c) higher magnification of out edge of the cross section
- d) higher magnification of the inner edge side.

8.3. Water Permeability and Rejection

Figure 8.6 shows that water permeability decreased as the ethanol concentration in the bore fluid increased. The presence of 0% ethanol in bore fluid showed the highest pure water permeation flux and the highest BSA rejection. Table 8.1 shows the rejection percentage at each concentration.

Table 8. 1: Rejection % of BSA at different concentrations of bore fluid.

Ethanol Concentration in Bore Fluid	Rejection %
0% Ethanol/H ₂ O	12.10
18% Ethanol/H ₂ O	10.90
25% Ethanol/H ₂ O	8.31
35% Ethanol/H ₂ O	5.45
50% Ethanol/H ₂ O	4

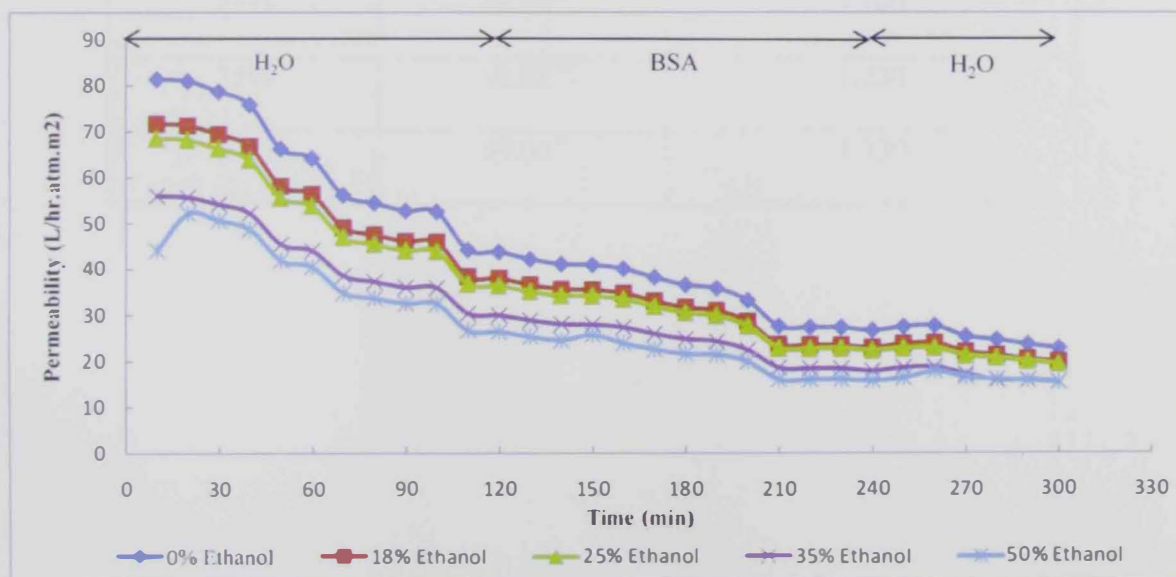


Figure 8. 6: Filtration time of water permeability for different concentration of bore fluid.

8.4. Contact Angle and Diameter Measurements

The contact angle and inner diameter for manufactured fibers at different concentrations of ethanol in bore fluid was examined. From the table below the contact angle and inner diameter were increased with increasing the ethanol concentration.

Table 8. 2: Contact Angle and inner diameter measurements for different concentrations of bore fluid.

Dope Solution Conc. 24% CA/DMAc		
Ethanol Concentration	Measured Angle	Measured Diameter (mm)
0%	66.01°	1.02
18%	66.48°	1.073
25%	68.84°	1.100
35%	68.92°	1.220
50%	69.00°	1.330

8.5. Strength of Fabricated Fibers

The mechanical properties are very important for the hollow fiber performance. Therefore, stress and strain of hollow fibers were determined. Figure 8.7 shows that the stress decreased with increasing the ethanol concentration in bore fluid. Figure 8.8 also shows a decrease in the strain percentage when the ethanol concentration was increased.

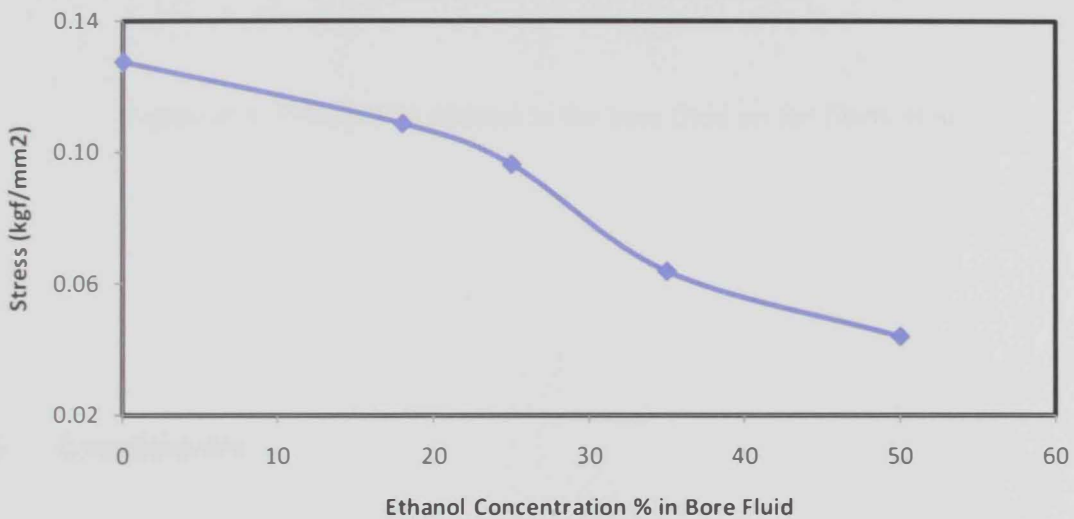


Figure 8.7: Effect of % ethanol in the bore fluid on the fibers stress.

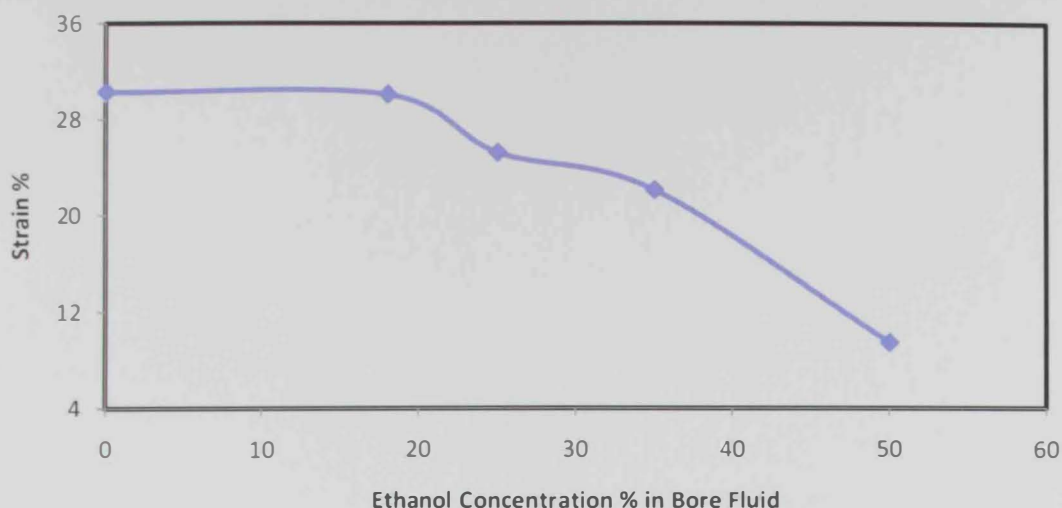


Figure 8. 8: Effect of % ethanol in the bore fluid on the fibers strain.

8.6. Conclusions

In this study, effects of bore fluid composition on the morphology and performance of cellulose acetate hollow fibers were investigated by using ethanol in water with different concentrations. The ethanol concentrations used in bore fluid were; 0, 18, 25, 35 and 50%. The morphology of hollow fiber was found to depend on the concentration of bore fluid. The best spinning process was achieved when using pure water as bore fluid. In addition the BSA rejection was 12.10% and that was acceptable. The addition of ethanol (non solvent) to the bore fluid suppressed the formation of macro-voids and resulted in low porous membranes.

Conclusions and Recommendations

Chapter Nine: Conclusions and Recommendations

9.1. Conclusions

Many preparation factors are known to control the hollow fiber performance. Such as dope solution flow rate, air gap distance, the type of bore fluid, bore fluid flow rate and the concentration of polymer in the blending solution.

From the present study, the results indicated that there are direct relationships between contact angle measured and permeability. Water flux was decreased with increasing contact angle at fixed others conditions. When hollow fiber became more porous, a drop in strength resulted, and more porous mean hollow fibers became more hydrophilic.

Herschel Bulkley model parameters illustrated a high dependence of the yield stress on cellulose acetate concentration and temperature.

The strength of hollow fiber and hydrophilicity was improved when the cellulose acetate concentration increased in the starting polymer solutions. On the other hand, at a constant cellulose acetate concentration and variable bore flow rate, strength and stain decreased. But when the strength was evaluated, the highest value of strength was achieved at bore flow 8 g/min (air gap= 7cm, 21% CA, dope solution flow= 6 g/min and using water as bore fluid). The best BSA rejection was obtained at air gap 5.5 cm with 81.49% of BSA rejection. This value of rejection was achieved at bore flow =15 g/min, dope solution flow= 6 g/min, 21%CA and using water as bore fluid.

The effects of inner coagulation composition on the morphology and performance of cellulose acetate hollow fibers by using different concentrations of ethanol in water indicated that the best results were achieved when using pure water flux as an alternative of using ethanol in water.

9.2. Recommendations

Due to the time limitations, author of this work was not able to conduct some experimental works that help to study polymer properties. Thus, future interested researchers are recommended to test the following:

1. Measure the bending stress that was induced at fabricated hollow fibers. And consider it as a part of mechanical studies.
2. Study the effect of roll up speed on the properties of cellulose acetate hollow fibers.
3. Study the hollow fibers inner surface and outer surface before and after BSA filtration by scanning electronic microscope.

References

References

1. **Jinzhu Ma, Zhenyn Ding, Guoxiao Wei, Hua Zhao, Tianming Huang.** *Sources of Water Pollution and Evolution of Water Quality in the Wuwei Basin of Shiyang River, Northwest China.* 2009, Environmental Management, Vol. 90, pp. 1168-1177.
2. **Solda'n, Pr'emyšl.** *Toxic risk of surface water pollution six years of experience.* 2003, Environment International, Vol. 28, pp. 677– 682.
3. **C.A. Brebbia, J.S.Antunes do Carmo.** *Water Pollution VIII.* s.l.: Science and Technology, 2006. p. 18. Vol. 7.
4. **D.Bellos, T.Sawidis.** *Chemical Pollution Monitoring of the River Pinios (Thessalia-Greece).* Environmental Management : s.n., 2005, Vol. 76, pp. 282-292.
5. **R. H. Foy, S. D. Lennox and R. V. Smith.** *Assessing the Effectiveness of Regulatory Controls on Farm Pollution using Chemical and Biological Indices of Water Quality and Pollution Statistics.* 2001, Water Research , Vol. 35, pp. 3004-3012.
6. **P.J. Oberholster, A.-M. Botha, T.E. Cloete.** *Biological and chemical Evaluation of Sewage Water Pollution in the Rietvlei Nature Reserve Wetland Area, South Africa.* 2008, Environmental Pollution, Vol. 156, pp. 184-192.
7. **S. Mondal, S. Ranil Wickramasinghe.** *Produced Water Treatment by Nanofiltration and Reverse Osmosis Membranes.* 2008, Membrane Science, Vol. 322, pp. 162–170.

References

8. **Mehmet Çakmakce, Necati Kayaalp, Ismail Koyuncu.** *Desalination of Produced Water from Oil Production Fields by Membrane Processes.* 2008, *Desalination*, Vol. 222, pp. 176–186.
9. **Helmer, Richard.** *Water Pollution Control.* 2nd Ed. London : behalf of WHO by F & FN Spon, 1997. p. 24.
10. *Guidelines for Drinking Water Quality.* 3rd Ed. Switzerland : World Health Organization, 2004. p. 6. Vol. 1.
11. **Lidia Po Catalao Dionisio, G. Rheinheimerà and Juan J. Borrego.** *Microbiological Pollution of Ria Formosa (South of Portugal).* 2000, *Marine Pollution Bulletin* , Vol. 40, pp. 186-193.
12. *Guidelines for Drinking Water Quality.* 3rd Ed. Switzerland : World Health Organization, 2004. p. 3. Vol. 1.
13. **April Clark, Torrey Turner, K. Padma Dorothy, J. Goutham, C. Kalavati, Bettaiya Rajanna.** *Health Hazards due to Pollution of Waters along the Coast of Visakhapatnam, East Coast of India.* 2003, *Ecotoxicology and Environmental Safety*, Vol. 56, pp. 390-397.
14. *Guidelines for Drinking Water Quality.* 3rd Ed. Switzerland : World Health Organization, 2004. p. 4. Vol. 1.
15. Cyanobacteria. *Wikipedia.* [Online] [Cited: May 30, 2009.] [http://en.wikipedia.org/wiki/Cyanobacteria.](http://en.wikipedia.org/wiki/Cyanobacteria)

References

16. **Hyo-Joon Jeong, Won-Tae Hwang, Eun-Han Kim, Moon-Hee Han.** *Radiological Risk Assessment for an Urban Area: Focusing on a Drinking Water Contamination.* 2009, *Annals of Nuclear Energy* , Vol. 36, pp. 1313–1318.
17. **P. P. Povinec, I. Osvath, M. S. Baxter, S. Ballestra, J. Carroll, J. Gastaud, I. Harms, L. Huynh-Ngoc, L. Liong Wee Kwong, H. Pettersson.** *Summary of IAEA-MEL's Investigation of Kara Sea Radioactivity and Radiological Assessment.* 2009, *Annals of Nuclear*, Vol. 36, pp. 1313-1318.
18. Water Purification. *Wikipedia.* [Online] [Cited: April 25, 2010.] [http://en.wikipedia.org/wiki/Water_purification.](http://en.wikipedia.org/wiki/Water_purification)
19. **Ronald N. Kostoff, Jeffrey L. Solka, Robert L. Rushenberge and Jeffrey A. Wyatt.** *Literature related discovery (LRD): Water purification.* 2008, *Technological Forecasting & Social Change*, Vol. 75, pp. 256-275.
20. **Ritu D. Ambashtaa, Mika Sillanpääa.** *Water purification using magnetic assistance: A review.* 2010, *Journal of Hazardous Materials*, Vol. 180, pp. 38–49.
21. **Raffaele Molinari, Leonardo Palmisano, Enrico Drioli, Mario Schiavello.** *Studies on various reactor configurations for coupling photocatalysis and membrane processes in water purification.* 2002, *Journal of Membrane Science* , Vol. 206, pp. 399–415.
22. **Xia Huang, Yaobin Meng, Peng Liang, Yi Qian.** *Operational conditions of a membrane filtration reactor coupled with photocatalytic oxidation.* 2007, *Separation and Purification Technology*, Vol. 55 , pp. 165–172.

References

23. **Sylwia Mozia, Antoni W. Morawski, Masahiro Toyoda, Michio Inagaki.** *Effectiveness of photodecomposition of an azo dye on a novel anatase phase TiO₂ and two commercial photocatalysts in a photocatalytic membrane reactor (PMR).* 2008, Vol. 63, pp. 386-391.
24. **Mozia, Sylwia.** *Photocatalytic membrane reactors (PMRs) in water and wastewater treatment. A review.* 2010, Separation and Purification Technology, Vol. 73, pp. 71-91.
25. **Yiran Li, Jun Wang, Ying Zhao, Zhaokun Luan.** *Research on magnetic seeding flocculation for arsenic removal by superconducting magnetic separation.* 2010, Separation and Purification Technology, Vol. 73, pp. 264-270.
26. **A.S. Bahaj, P.A.B. James, F.D. Moeschler.** *Wastewater treatment by bio-magnetic separation: A comparison of iron oxide and iron sulphide biomass recovery.* 1998, Water Science and Technology, Vol. 38, pp. 311-317.
27. **CHARLES P. GERBA, JAIME E. NARANJO, BS.** *Microbiological water purification without the use of chemical disinfection.* 2000, Wilderness and Environmental Medicine, Vol. 11, pp. 12-16.
28. **SU Fengyi, LUO Mingfang, ZHANG Fei, LI Peng, LOU Kai, XING Xinhui,.** *Performance of microbiological control by a point of use filter system for drinking water purification.* 2009, Journal of Environmental Sciences, Vol. 21, pp. 1237-1246.
29. **Catherine N. Mulligan, Neginmalak Davarpanah, Masaharu Fukue, Tomohiro Inoue.** *Filtration of contaminated suspended solids for the treatment of surface water.* 2009, Chemosphere, Vol. 74, pp. 779-786.

References

30. **Lain-Chuen Juang, Dyi-Hwa Tseng and He-Yin Lin.** *Membrane processes for water reuse from the effluent of industrial park wastewater treatment plant: a study on flux and fouling of membrane.* 2007, *Desalination*, Vol. 202, pp. 302–309.
31. **Rijn, C.J.M. van.** *Membrane Science and Technology. Series 10.* Netherlands : Elsevier, 2004, pp. 1-3. Vol. 10.
32. **Porter, Mark C.** *Handbook of Industrial Membrane Technology.* New Jersey : NOYES, 1990. p. VI.
33. **Katsuki Kimura, Tomohiro Maeda, Hiroshi Yamamura, Yoshimasa Watanabe.** *Irreversible membrane fouling in microfiltration membranes filtering coagulated surface water.* 2008, Irreversible membrane fouling in micrJournal of Membrane Science , Vol. 320, pp. 356–362.
34. **T. Wintgens a, T. Melin a, A. Schiller b, S. Khan b, M. Muston b, D. Bixio c and C. Thoeys.** *The role of membrane processes in municipal wastewater reclamation and reuse..* 2005, *Desalination*, Vol. 178, pp. 1-11.
35. **Aldo Bottino, Gustavo Capannelli, Antonio Comite, Fiorenza Ferrari, Raffaella Firpo, Silvia Venzano.** *Membrane technologies for water treatment and agroindustrial sectors.* 2009, *Comptes Rendus Chimie*, Vol. 12, pp. 882-888.
36. **Wickramasinghe, S. Mondal and S. Ranil.** *Produced water treatment by nanofiltration and reverse osmosis membranes.* 2008, *Journal of Membrane Science*, Vol. 322, pp. 162–170.

References

37. **Wirth, Corinne Cabassud and David.** *Membrane distillation for water desalination: how to chose an appropriate membrane.* 2003, *Desalination* , Vol. 157, pp. 307-314.
38. **Roger C. Viadero Jr, James A. Noblet.** *Membrane filtration for removal of fine solids from aquaculture process water.* 2002, *Aquacultural Engineering*, Vol. 26, pp. 151-169.
39. **Argimiro R. Secchi, Keiko Wada, Isabel C. Tessaro.** *Simulation of an ultrafiltration process of bovine serum albumin in hollow-fiber membranes.* 1999, *Journal of Membrane Science*, Vol. 160, pp. 255-265.
40. **K. Boussu, Y. Zhang, J. Cocquyt, P. Van der Meeren, A. Volodin, C. Van Haesendonck, J.A. Martens and B. Van der Bruggen.** *Characterization of polymeric nanofiltration membranes for systematic analysis of membrane performance.* 2006, *Journal of Membrane Science*, Vol. 278, pp. 418-427.
41. **A.M. Hassan, M. A.K. Al-Sofi, A.S. Al-Amoudi, A.T.M. Jamaluddin, A.M. Farooque, A. Rowaili, A.G.I. Dalvi, N.M. Kither, G.M. Mustafa, I.A.R. Al-Tisan.** *A new approach to membrane and thermal seawater desalination processes using nano-filtration membranes (Part I).* 1998, *Desalination*, Vol. 118, pp. 35-51.
42. **Baker, Richard W.** *Membrane Technology and Applications.* 2nd Edition. England : John Wiley & Sons Ltd, 2004. p. 17.
43. **Ismail, Woei-Jye Lau and A.F.** *Polymeric nanofiltration membranes for textile dye wastewater treatment: Preparation, performance evaluation, transports modelling, and fouling control-a review.* 2009, *Desalination*, Vol. 245, pp. 321-348.

References

44. Paul, D.R. *Reformulation of the solution diffusion theory of reverse osmosis*. 2004, *Journal of Membrane Science*, Vol. 241, pp. 371–386.
45. S. Senthilmurugan, Sharad K. Gupta. *Separation of inorganic and organic compounds by using a radial flow hollow-fiber reverse osmosis module*. 2006, *Desalination*, Vol. 196, pp. 221–236.
46. A. Bédalo-Santoyo, J.L. Gómez-Carrasco, E. Gómez-Gómez, F. Muximo-Martin, A.M. Hidalgo-Montesinos. *Application of reverse osmosis to reduce pollutants present in industrial wastewater*. 2003, *Desalination*, Vol. 155, pp. 101–108.
47. Shudong Sun, Yilun Yue, Xiaohua Huang, Deying Meng. *Protein adsorption on blood contact membranes*. 2003, *Journal of Membrane Science*, Vol. 222, pp. 3–18.
48. Diana J. Hellman, Alan R. Greenberg, William B. Krantz. *A novel process for membrane fabrication: thermally assisted evaporative phase separation (TAEPS)*. 2004, *Journal of Membrane Science*, Vol. 230, pp. 99–109.
49. Liao-Ping Chenga, Tai-Horng Youngb, Lin Fanga, Jy-Jie Gaa. *Formation of particulate microporous poly(vinylidene fluoride) membranes by isothermal immersion precipitation from the 1-octanol/dimethylformamide/poly(vinylidene fluoride) system*. 1999, *Polymer*, Vol. 40, pp. 2395–2403.
50. Jian-Jun Qin, Juan Gaa, Tai-Shung Chunga. *Effect of wet and dry-jet wet spinning on the shear induced orientation during the formation of ultrafiltration hollow fiber membranes*. 2001, *Journal of Membrane Science*, Vol. 182, pp. 57–75.

References

51. **Sina Bonyadi, Tai Shung Chung, William B. Krantz.** *Investigation of corrugation phenomenon in the inner contour of hollow fibers during the non solvent induced phase separation process.* 2007, *Journal of Membrane Science*, Vol. 299, pp. 200–210.
52. **Dimitrios F. Stamatialis, Bernke J. Papenburg, Miriam Giron'es, Saiful Saiful, Srivatsa N.M. Bettahalli, Stephanie Schmitmeier, Matthias Wessling.** *Medical applications of membranes: Drug delivery, artificial organs and tissue engineering.* 2008, *Journal of Membrane Science*, Vol. 308, pp. 1–34.
53. **B. D. Bhide, S. A. Stern.** *Membrane processes for the removal of acid gases from natural gas. II. Effects of operating conditions, economic parameters, and membrane properties.* 1993, *Journal of Membrane Science*, Vol. 81, pp. 239-252.
54. **Kevin W. Lawson, Douglas R. Lloyd.** *Membrane distillation.* 1997, *Journal of Membrane Science*, Vol. 124, pp. 1-25.
55. **A. Mansourizadeh, A.F. Ismail.** *Effect of additives on the structure and performance of polysulfone hollow fiber membranes for CO₂ absorption.* 2010, *Journal of Membrane Science*, Vol. 348, pp. 260-267.
56. **Ehsan Saljoughia, Mohtada Sadrzadeha, Toraj Mohammadi.** *Effect of preparation variables on morphology and pure water permeation flux through asymmetric cellulose acetate membranes.* 2009, *Effect of preparation variables on morphology and pure water permeation flux through asymmetric cellulose acetate membranes.* *Journal of Membrane Science*, Vol. 326, pp. 627-634.

References

57. **Tai Shung Chung, Zhen Liang Xu, Wenhui Lin.** *Fundamental Understanding of the Effect of Air Gap Distance on the Fabrication of Hollow Fiber Membranes.* 1999, *Journal of Applied Polymer Science*, Vol. 72, pp. 379-395.
58. **Saeid Rajabzadeh, Tatsuo Maruyama, Tomohiro Sotani, Hideto Matsuyama.** *Preparation of PVDF hollow fiber membrane from a ternary polymer/solvent/nonsolvent system via thermally induced phase separation (TIPS) method.* 2008, *Separation and Purification Technology*, Vol. 63, pp. 415-423.
59. **Saeid Rajabzadeh, Tatsuo Maruyama, Tomohiro Sotani, Hideto Matsuyama.** *Microporous membranes based on poly(ether ether ketone) via thermally-induced phase separation.* x 1995, *Journal of Membrane Science*, Vol. 107, pp. 93-106.
60. **In Suk Cho, Jim Ho Kim, Sung Soo Kim.** *Thermal induced phase separation mechanism study for the preparation of semicrystalline polymeric membranes.* 1997, *Korea Polymer Journal*, Vol. 5, pp. 191-198.
61. **i Lv, Jing Zhou, Peng Xu, Qiangguo Du, Haitao Wang, Wei Zhong.** *Estimation of Phase Diagrams for Copolymer Diluent Systems in Thermally Induced Phase Separation.* 2007, *Journal of Applied Polymer Science*, Vol. 105, pp. 3513–3518 .
62. **Xun Yao Fua, Hideto Matsuyamaa, Masaaki Teramoto, Hideki Nagai.** *Preparation of polymer blend hollow fiber membrane via thermally induced phase separation.* 2006, *Separation and Purification Technology*, Vol. 52, pp. 363–371.

References

63. Rui Lv, Jing Zhou, Qiangguo Du, Haitao Wang, Wei Zhong. *Preparation and characterization of EVOH/PVP membranes via thermally induced phase separation*. 2006, Journal of Membrane Science, Vol. 281, pp. 700–706.
64. Dongmei Li a, William B. Krantz, Alan R. Greenberg, Robert L. Sani. *Membrane formation via thermally induced phase separation (TIPS): Model development and validation*. 2006, Journal of Membrane Science, Vol. 279, pp. 50-60.
65. Dong Bok Kim, Young Moo Lee, Wha Seop Lee, Seong Mu Jo, Byoung Chul Kim. *Double crystallization behavior in dry jet wet spinning of cellulose/N-methylmorpholine-N-oxide hydrate solutions*. 2002, European Polymer Journal, Vol. 38, pp. 109-119.
66. Ferguson, James. *Apparatus and method for spinning hollow polymeric fibres*. 6143411 United Kingdom, November 7, 2000.
67. H.A. Tsai, C.Y. Kuo, J.H. Lin, D.M. Wang, A. Deratani, C. Pochat-Bohatier, K.R. Lee, J.Y. Lai. *Morphology control of polysulfone hollow fiber membranes via water vapor induced phase separation*. 2006, Journal of Membrane Science , Vol. 278, pp. 390–400.
68. Yu Long, Ning Zhang, Yong Huang, Xuejun Wen. *Formation of Highly Aligned Grooves on Inner Surface of Semipermeable Hollow Fiber Membrane for Directional Axonal Outgrowth*. 2008, Journal of Manufacturing Science and Engineering, Vol. 130.
69. Seong Hyun Yoo, Jong Hak Kim, Jae Young Jho, Jongok Won, Yong Soo Kang. *Influence of the addition of PVP on the morphology of asymmetric polyimide phase inversion membranes: effect of PVP molecular weight*. 2004, Journal of Membrane Science, Vol. 236, pp. 203-207.

References

70. **Tai-Horng Young, Da-Ming Wang, Chih-Chen Hsieh, Leo-Wang Chen.** *The effect of the second phase inversion on microstructures in phase inversion EVAL membranes.* 1998, Journal of Membrane Science, Vol. 146, pp. 169-178.
71. **Loraine, Gregory A.** *Oxidation of Polyvinylpyrrolidone and an Ethoxylate Surfactant in Phase-Inversion Wastewater.* 2008, Water Environment Research, Vol. 80, pp. 373-379.
72. **Kim, Kwon Mahendran, Mailvaganam, Chen, Hua, Henshaw, Wayne Jerald.** *System and method for synthesizing a polymer membrane.* 20050142280 US, June 30, 2005.
73. **W. Albrecht, Th. Weigel, M. Schossig-Tiedemann, K. Kneifel, K.-V. Peinemann, D. Paul.** *Formation of hollow fiber membranes from poly(ether imide) at wet phase inversion using binary mixtures of solvents for the preparation of the dope.* 2001, Journal of Membrane Science, Vol. 192, pp. 217-230.
74. **Joel R. Fried, Polymer Science & Technology, 2nd ed. North Bergen, Book Mart and 335-337., 2007.** *Polymer Science & Technology.* 2nd Edition. New Jersey: Prentice Hall, 2007. pp. 335-337.
75. **X.Y. Fu, T. Sotani, H. Matsuyama.** *Effect of membrane preparation method on the outer surface roughness of cellulose acetate butyrate hollow fiber membrane.* 2008, Desalination, Vol. 233, pp. 10-18.
76. Cellulose acetate. *Wikipedia.* [Online] [Cited: October 30, 2009.] http://en.wikipedia.org/wiki/File:Cellulose_acetate_preparation.png.

References

77. **Muthusamy Sivakumar, Doraisamy Raju Mohan, Ramamoorthy Rangarajan.** *Studies on cellulose acetate polysulfone ultrafiltration membranes.* 2006, *Journal of Membrane Science*, Vol. 268, pp. 208–219.
78. **Lifeng Zhang, You-Lo Hsieh.** *Ultra-fine cellulose acetate/poly(ethylene oxide) bicomponent fibers.* 2008, *Carbohydrate Polymers*, Vol. 71, pp. 196–207.
79. **György Sza'mel, Attila Domja'n, Szilvia Kle'bert, Be'la Puka'nszky.** *Molecular structure and properties of cellulose acetate chemically modified with caprolactone.* 2008, *European Polymer Journal*, Vol. 44, pp. 357–365.
80. **Maria da Conceica C. Lucena, Ana Ellen V. de Alencar, Selma Elaine Mazzeto, Sandra de A. Soares.** *The effect of additives on thermal degradation of cellulose acetate.* 2003, *Polymer Degradation and Stability*, Vol. 80, pp. 149–155.
81. **G. Arthanareeswarana, P. Thanikaivelanb, K. Srinivasna, D and Rajendran, Mohan and M.** *Synthesis, characterization and thermal studies on cellulose acetate membranes with additive.* 2004, *European Polymer*, Vol. 40, pp. 2153-2159.
82. **Ji-hua Hao*, Hal-ping Dai, Pu-cheng Yang, Jian-min Wei, Zhen Wang.** *Cellulose acetate hollow fiber performance for ultra-low pressure reverse osmosis.* 1996, *Desalination*, Vol. 107, pp. 217-221.
83. **Chunxiu Liu, Renbi Bai.** *Preparation of chitosan/cellulose acetate blend hollow fibers for adsorptive performance.* 2005, *Journal of Membrane Science*, Vol. 267, pp. 68–77.

References

84. Jian-Jun Qin, Maung Htun Oo, Yi-Ming Cao, Leng-Siang Lee. *Development of a LCST membrane forming system for cellulose acetate ultrafiltration hollow fiber*. 2005, Separation and Purification Technology, Vol. 42, pp. 291–295.
85. Jian-Jun Qin a, Ying Li, Leng-Siang Lee, Hsiaowan Lee. *Cellulose acetate hollow fiber ultrafiltration membranes made from CA/PVP 360 K/NMP/water*. 2003, Journal of Membrane Science, Vol. 218, pp. 173–183.
86. Tai-Shung Chung, Zhen-Liang Xu, Wenhui Lin. *Fundamental Understanding of the Effect of Air-Gap Distance on the Fabrication of Hollow Fiber Membranes*. 1999, Journal of Applied Polymer Science, Vol. 72, pp. 379–395.
87. Tai-Shung Chung, Xudong Hu. *Effect of Air-Gap Distance on the Morphology and Thermal Properties of Polyethersulfone Hollow Fibers*. 1997, Journal of Applied Polymer Science, Vol. 66, pp. 1067–1077 .
88. M. Khayet a, M.C. García-Payoa, F.A. Qusayb, M.A. Zubaidyb. *Structural and performance studies of poly(vinyl chloride) hollow fiber membranes prepared at different air gap lengths*. 2009, Journal of Membrane Science, Vol. 330, pp. 30–39.
89. Khayet, M. *The effects of air gap length on the internal and external morphology of hollow fiber membranes*. 2003, Chemical Engineering Science, Vol. 58, pp. 3091-3104.
90. K.C. Khulbe, C.Y. Feng, F. Hamad, T. Matsuura, M. Khayet. *Structural and performance study of micro porous polyetherimide hollow fiber membranes prepared at different air-gap*. 2004, Journal of Membrane Science, Vol. 245, pp. 191–198.

References

91. **W.L. Chou, M-C. Yang.** *Effect of take-up speed on physical properties and permeation performance of cellulose acetate hollow fibers.* 2005, *Journal of Membrane Science*, Vol. 250, pp. 259–267.
92. **Jincai Su, Qian Yang, Joo Fuat Teo, Tai-Shung Chung.** *Cellulose acetate nanofiltration hollow fiber membranes for forward osmosis processes.* 2010, *Journal of Membrane Science*, Vol. 355, pp. 36–44.
93. **Kawanishi, H., Tsunashima, Y., Okada, S. and Horii, F.** *Change in chain stiffness in viscometric and ultracentrifugal fields: cellulose diacetate in N,Ndimethylacetamide dilute solution.* 1998, *Journal of Chemical Physics*, Vol. 108, pp. 6014-6025.
94. **Zhen-Liang Xu, F. Alsalhy Qusay.** *Polyethersulfone (PES) hollow fiber ultrafiltration membranes prepared by PES/non-solvent/NMP solution.* 2004, *Journal of Membrane Science*, Vol. 233, pp. 101-111.
95. **Katherine, G., et al.** *Rheology of Fiber-reinforced Cementations materials.* 2007, *Cement and Concrete Research*, Vol. 37, pp. 191–199.
96. **Huang, Y. and Band, L.** *Texture of Ethyl-Cyanoethyl Cellulose Mesophase.* 1999, *Chinese Journal of Polymer Science* , Vol. 9, pp. 86-93.
97. **I, Ani., et al.** *Rheology Assessment of Cellulose Acetate Spinning Solution and its Influence on Reverse Osmosis Hollow Fiber Membrane Performance.* 2003, *Polymer Testing* , Vol. 22, pp. 319–325.

References

98. **Christophe, A. and C., Steve.** *The Dam Break Problem for Herschel Bulkley Viscoplastic Fluids Down Steep Flumes*. 2009, *Journal of Non-Newtonian Fluid Mechanics* 2009, Vol. 158, pp. 18–35.
99. **Andreas, N., et al.** *Steady Herschel–Bulkley Fluid Flow in three-dimensional Expansions*. 2001, *Journal Non-Newtonian Fluid Mechanics*, Vol. 100, pp. 77–96.
100. **Kelessidis, V.C., Maglione, R., Tsamantaki, C. and Aspirtakis, Y.** *Optimal Determination of Rheological Parameters for Herschel–Bulkley Drilling Fluids and Impact on Pressure Drop, Velocity Profiles and Penetration Rates during Drilling*. 2006, *Journal of Petroleum Science and Engineering*, Vol. 53, pp. 203–224.
101. **Pierre, S.** *A new Elastoviscoplastic Model Based on the Herschel–Bulkley Viscoplastic Model*. 2009, *Journal of Non-Newtonian Fluid Mechanics*, Vol. 158, pp. 154–161.
102. **Diego, G. D. and Navaza, J. M.** *Rheology of Aqueous Solutions of Food Additives: Effect of Concentration, Temperature and Blending*. 2003, *Journal of Food Eng*, Vol. 56, pp. 387–392.
103. **Abu-Jdayil, B., Hazim, A. M. and Eassa, A.** *Rheology of Wheat Starch–Milk–Sugar Systems: Effect of Starch Concentration, Sugar Type and Concentration, and Milk Fat Content*. 2004, *Journal of Food Engineering*, Vol. 64, pp. 207–212.
104. **Zuoxiang, Z., et al.** *Relationship of Intrinsic Viscosity to Molecular Weight for Poly (1, 4-butylene adipate)*. 2010, *Polymer Testing*, Vol. 29, pp. 66–71.
105. **Braun, D., et al.** *Polymer Synthesis: Theory and Practice*. 4th Edition. Germany : Springer Verlag Berlin Heidelberg, 2005.

ملخص الأطروحة

إنتاج مياه الشرب الصالحة باستخدام تكنولوجيا المايكروفلتر والألترافلتر وقد أصبحت هذه التنقيبات مثيرة للاهتمام. وتنقية أو تصفية المياه باستخدام الأغشية المجوفة بدأت تجذب قدراً كبيراً من الاهتمام في جميع أنحاء العالم بسبب خصائصها الجيدة مثل قدرتها وكفاءتها العالية في إزالة الجسيمات الصلبة والفيروسات والجراثيم وقلة تكلفتها المادية. وهذه التقنية الجديدة أصبحت مفيدة في معالجة المياه الصناعية. وتقوم الدراسات الحالية في مجال تصنيع الأغشية البوليمرية المجوفة بمحاولة تحسين الخصائص الميكانيكية ومعدل تدفق الماء ونسبة إزالة الجسيمات الغير مرغوب بها من الماء.

في المشروع الحالي كان الهدف هو تصنيع الأغشية البوليمرية المجوفة التي حضرت من مادة السليوز أسيتات (cellulose acetate) ومادة ميثيلي أميند (N,N-Di-methyl-acetamind) كمذيب للبولمر واستخدام الماء كمختر خارجي للأغشية وبعض الأحيان استخدام الماء فقط أو خليط الإيثانول والماء كمختر داخلي للأغشية. تم تصنيع الأغشية المجوفة باستخدام تقنية (Non-Solvent Induced Phase Separation). وتم تقسيم هذا البحث إلى دراسة عدة متغيرات أثناء عملية التصنيع للأغشية المجوفة، وذلك لهدف توضيح والتوصل بوضوح إلى مدى معرفة المتغيرات والعوامل إلى تؤثر على كفاءة الأغشية الجوفة. وتم تقسيم البحث إلى عدة أقسام للدراسة وهي كالتالي:

- معرفة دراسة وحركة خليط السليوز أسيتات مع ميثيلي أميند عند تركيزات مختلفة للسليوز أسيتات (15% و 18% و 21% و 24%) وبالإضافة لذلك تغيير درجة حرارة الخليط عند درجات مختلفة (25 و 35 و 45 و 55 و 65 و 75 و 85) درجة سيليزية وذلك تحقق عند دراسة اللزوجة ودراسة (Hershed-Balkley (H-B) model) لمعرفة سلوك الخليط.
- دراسة تأثير تركيز مادة السليوز أسيتات (cellulose acetate) في خليط البوليمر عند عدة تركيزات للمادة السليوز أسيتات مع تغير سرعة معدل التدفق (6 و 7.5 و 9 و 10.5) سم³/دقيقة عند كل تركيز مع تثبيت باقي الظروف.

References

106. **Mustaffar, M. I., Ismail, A. F. and Illias, R.M.** *Study on the effect of polymer concentration on hollow fiber ultrafiltration membrane performance and morphology.* Johor : s.n., 2005. Regional Conference on Engineering Education RCEE.
107. **Darunee Bhongsuwan, Tripob Bhongsuwan.** *Preparation of cellulose acetate membranes for ultra-nano filtrations.* 2008, Kasetsart, Vol. 42, pp. 311-317.
108. **J. M. Valente, Alexandre Ya. Polishchuk, Victor M. M. Lobo, Hugh D. Burrows.** *Transport Properties of Concentrated Aqueous Sodium Dodecyl Sulfate Solutions in Polymer Membranes Derived from Cellulose Esters.* 2000, Langmuir, Vol. 16, pp. 6475–6479.
109. **Jianjun Qin, Tai Shung Chung.** *Effect of dope flow rate on the morphology, separation performance, thermal and mechanical properties of ultrafiltration hollow fiber membranes.* 1999, Journal of Membrane Science, Vol. 157, pp. 35-51.
110. **Tai-Shung Chung, Zhen-Liang Xu, Wenhui Lin.** *Fundamental Understanding of the Effect of Air-Gap Distance on the Fabrication of Hollow Fiber Membranes.* 1999, Journal of Applied Polymer Science, Vol. 72, pp. 379–395.
111. **M. Khayet, M.C. García-Payo, F.A. Qusayb, M.A. Zubaidy** *Structural and performance studies of poly(vinyl chloride) hollow fiber membranes prepared at different air gap lengths.* 2009, Journal of Membrane Science, Vol. 330, pp. 30–39.
112. **Alsahy, Qusay Fadhel.** *Effect of Ethanol Concentrations in Internal Coagulant on the Morphology and Separation Performance of Polyethersulfone (PES) Hollow Fiber UFMembranes Prepared by PES/Ethanol/NMP Solution.* 2007, Eng. & Technology, Vol. 25, pp. 253-265.

- دراسة مدى تغير خصائص وكفاءة الأغشية المجوفة عند تغير سرعة الماء الذي أعتبرناه مختر داخلي للأغشية أثناء عملية تصنيع الأغشية. وكانت سرعة تدفق المختر الداخلي هي 8 و 10 و 12 و 13 و 16 جرام لكل دقيقة.
- تغيير طول الفجوة بين (spinneret) والماء كمختر خارجي عند عدة مسافات لمعرفة تأثير طول الفجوة على البنية الداخلية والخارجية للأغشية وأداؤها. وقد تم دراسة تأثير الفجوة عند مسافة 5.5 و 7 و 9 و 10 سم.
- التأكد ومعرفة مدى تأثير المختر الداخلي على خصائص ومميزات الأغشية المجوفة ولتحقيق هذا الهدف تم إضافة الإيثانول في الماء بتركيز 50% و 35% و 25% و 18% مع تثبيت باقي المتغيرات أثناء عملية تصنيع الأغشية. وتم استنتاج ان استخدام الماء فقط كمختر داخلي يعطي أفضل الخصائص الميكانيكية ويزيد من كفاءة فصل المواد الصلبة التي قد توجد في المياه الملوثة. حيث كان معدل الفصل لمادة البروتين 12.10% وهذه النتيجة كانت الأفضل مقارنة بالعينات التي تم استخدام خليط الإيثانول كمختر داخلي للأغشية.